Bioinformatics in maize genome research

By

Ling Guo

A dissertation submitted to the graduate faculty

in partial fulfillment of the requirements for the degree of

DOCTOR OF PHILOSOPHY

Major: Bioinformatics and Computational Biolgy

Program of Study Committee:
Patrick S. Schnable, Co-Major Professor
Daniel A. Ashlock, Co-Major Professor
Hui-Hsien Chou
Heike Hofmann
Steven A. Whitham

Iowa State University

Ames, Iowa

2007

Copyright © Ling Guo, 2007. All rights reserved

UMI Number: 3274875

UMI®

UMI Microform 3274875

Copyright 2007 by ProQuest Information and Learning Company.
All rights reserved. This microform edition is protected against unauthorized copying under Title 17, United States Code.

ProQuest Information and Learning Company
300 North Zeeb Road
P.O. Box 1346
Ann Arbor, MI 48106-1346

TABLE OF CONTENTS

CHARPTER 1. GENERAL INTRODUCTION

Introduction

Maize (*Zea Mays L.*) is one of the most important crop plants in the world because of its important roles in both basic genetic research and agronomic economy. To improve and manipulate the economic important traits, scientists need to find all the genes, understand how they function and interactions. The traditional way of studying genes one-by-one makes the mission impossible. The recent evolutionary advances in biotechnology make it possible to study genes at large scale in an efficient way. Microarray is an example of those high-throughput technologies, which permits scientist to study the expression pattern of tens and thousands genes in a single microarray experiments. Genome sequencing is to put all the secrets about life in the hand of scientists. For maize, due to the size and complexity of maize genome, several maize genome projects had and have been generating a set of comprehensive and systemic resources to facilitate the sequencing of maize genome. There are over 1 million maize genomic sequences available, which include gene-enriched maize Genomic Survey Sequences (GSSs) (PALMER *et al.* 2003; WHITELAW *et al.* 2003) and BAC shotgun read generated by Consortium of Maize Genomics and random Whole Genome Shotgun (WGS) sequences generated by the Joint Genome Institute (JGI). there are over half million of maize expressed sequence tags (ESTs) in public database. The Maize Sequencing Consortium launched last year is targeting to sequence 1,900 BACs (http://www.maizegdb.org/MGSC2006Report.php). A high-resolution genetic map IBM2 with ~2,000 markers (COE *et al.* 2002; DAVIS *et al.* 1999; LEE *et al.* 2002; PALMER *et al.*

2003; SHAROPOVA *et al.* 2002) and three Bacterial Artificial Chromosome (BAC) libraries (TOMKINS *et al.* 2002; YIM *et al.* 2002) were constructed by Maize Mapping Project (MMP).

The biological information that scientists are interested in is buried in the enormous amount of biological data generated by the high-throughput technologies. Bioinfomatics is in the position to assist biologists to extract the interesting biology information buried in the data by using computational and statistical approach. In this dissertation, a new clustering algorithm is introduced to cluster microarray data, and a high-density genetic map ISU-IBM Map7 was constructed to integrate all the maize genomic resources to advance our understanding of maize genome.

Dissertation organization

This dissertation contains 2 manuscripts (Chapter 2-3) in preparation for journal publication and a general conclusion (Chapter 4). These papers are written by Ling Guo under Dr. Daniel A. Ashlock and Dr. Patrick S. Schnable's extensive guidance.

Chapter 2 is a manuscript in preparation for submission to Bioinformatics. In this manuscript we introduce a clustering method that can be use to cluster microarray data. Ling Guo developed and implemented the algorithm, conducted the analysis of parameter settings and the performance of the algorithm on synthetic microarray data sets.

Chapter 2 is a manuscript in preparation for submission to Genetics. In this manuscript we describe the construction of a high-density genetic map ISU-IBM Map7 and the utilization of

ISU-IBM Map7 to integrate all the genomic resource to advance our understand of maize genome. Ling Guo conducted most of the computational analysis and was the major contributor of the paper writing. Kai Ying did the PCR experiments for the calculation of genetic distance in F1BC population an analysis of integrate physical and genetic map. Karthik Viswanathan did the sequence confirmation of all IDP markers and maintenance the mapping project webpage. Karthik Viswanathan and Ling Guo constructed the primer design database. Olga Nikolova performance the analysis of distribution pattern of different gene expression groups. Dr. Tsui-Jung Wen, Hsin Chen, Ling Guo, and Dr. Daniel A. Ashlock assisted with the collection of mapping scores. Drs. Yefim I. Ronin and David Mester in Dr. Abraham Korol's group at University of Haifa implemented the MultiPoint mapping software packages.

References

COE, E., K. CONE, M. MCMULLEN, S. S. CHEN, G. DAVIS *et al.*, 2002 Access to the maize genome: an integrated physical and genetic map. Plant Physiol **128:** 9-12.

DAVIS, G. L., M. D. MCMULLEN, C. BAYSDORFER, T. MUSKET, D. GRANT *et al.*, 1999 A maize map standard with sequenced core markers, grass genome reference points and 932 expressed sequence tagged sites (ESTs) in a 1736-locus map. Genetics **152:** 1137-1172.

LEE, M., N. SHAROPOVA, W. D. BEAVIS, D. GRANT, M. KATT *et al.*, 2002 Expanding the genetic map of maize with the intermated B73 x Mo17 (IBM) population. Plant Mol Biol **48:** 453-461.

PALMER, L. E., P. D. RABINOWICZ, A. L. O'SHAUGHNESSY, V. S. BALIJA, L. U. NASCIMENTO *et al.*, 2003 Maize genome sequencing by methylation filtration. Science **302:** 2115-2117.

SHAROPOVA, N., M. D. MCMULLEN, L. SCHULTZ, S. SCHROEDER, H. SANCHEZ-VILLEDA *et al.*, 2002 Development and mapping of SSR markers for maize. Plant Mol Biol **48:** 463-481.

TOMKINS, J. P., G. DAVIS, D. MAIN, Y. S. YIM, N. DURU *et al.*, 2002 Construction and characterization of a deep-coverage bacterial artificial chromosome library for maize. Crop Sci. **42:** 928-933.

WHITELAW, C. A., W. B. BARBAZUK, G. PERTEA, A. P. CHAN, F. CHEUNG *et al.*, 2003 Enrichment of gene-coding sequences in maize by genome filtration. Science **302:** 2118-2120.

YIM, Y. S., G. L. DAVIS, N. A. DURU, T. A. MUSKET, E. W. LINTON *et al.*, 2002 Characterization of three maize bacterial artificial chromosome libraries toward anchoring of the physical map to the genetic map using high-density bacterial artificial chromosome filter hybridization. Plant Physiol **130:** 1686-1696.

CHAPTER 2. ADAPTATION OF MULTICLUSTERING TO THE ANALYSIS OF MICROARRAY EXPEREMENTS

Ling Guo, Patrick S. Schnable, Daniel A. Ashlock

A manuscript to be submitted to Bioinformatics

ABSTRACT

Motivation: Clustering has become an integral part of microarray data analysis and interpretation. It is helpful to reduce the scale of information generated by microarray experiment to the level that biologists can generate hypothesis. There is a danger that artifacts induced by clustering methods can cause misinterpretation of the data. Clustering method that can accurately capture the natural structure of the data would be a useful tool for biologists to discovery the biological meaning buried in the data. To this end, a new clustering algorithm, called K-means multiclustering, is introduced. The method can avoid the artifacts induced by distance or similarity metrics by amalgamating the results of many K-means clusterings.

Results: The multiclustering algorithm is a model-free clustering method. It is found to be reliable and consist in capturing the underlying data structure with high accuracy that is competitive with model based clustering and superior to other methods on synthetic micorarry data generated in a manner consistent with the hypothesis of model based clustering. The algorithm has a high level of immunity to artifacts introduced by the metric

used to measure the distance between data points. It can successfully cluster data sets which are designed to have different shapes and variation and cannot be correctly clustered by traditional clustering method. The cut plot computed by this method is a very simple and useful summary of the data structure. A detailed view of the formation of clustering can also be generated by the method to reveal the underlying hierarchical structure of data set.

Availability: The software was developed in C++. It is available from the third author upon request

Contact: dashlock@uoguelph.ca

Supplementary information: http://eldar.mathstat.uoguelph.ca/dashlock/MC/

1 INTRODUCTION

Microarray technology permits the analysis of expression pattern of thousands of genes simultaneously. In the last decade, this technology has been widely used in both biological and medical research with a wide range of applications, from basic cell processes in yeast to complex diseases in human. The enormous volume of biological data generated by microarrays, which contains complicated response of a living organism to particular stimuli at the transcriptional level, demands computational and statistical approaches to store, organize, analyze and interpret in order to reveal the underlying biological information. Clustering genes/samples based on the similarity of their gene expression profiles is one of the commonly used approaches in microarray analysis, and is used to predict the putative function of an unknown gene (Eisen, et al., 1998), identify genes involved in the same

metabolic pathway, and find common regulatory elements for a group of genes (DeRisi, et al., 1997). Clustering is also used to identify genes potentially related to poor response to standard cancer treatment and expression signatures for complex diseases. These information is useful for disease diagnosis, prognosis, personalized treatment and drug discovery.

Although there are many clustering algorithms, traditional clustering techniques such as hierarchical clustering, and K-means clustering (McQueen, 1967) are the predominant methods in microarray analysis (D'Haeseleer, 2005). Another effective and recently intensively studied method is mode-based clustering (Ghosh and Chinnaiyan, 2002; Yeung, et al., 2001). A detailed review of the literature about the clustering algorithms used in microarray analysis can be found in (Jiang, 2004).

Hierarchical clustering generates a binary tree that shows the relationship of the array profiles. Two approaches that are used in hierarchical clustering are agglomerative (bottom up) and divisive (top down) methods. The agglomerative algorithm was first used by Eisen et al. (Eisen, et al., 1998) to analyze gene expression data and has become the most commonly used clustering algorithm in microarray analysis. K-means clustering and SOM are the typical algorithms based on iterative relocation. Mode-based clustering methods assume that the entire data set is a mixture of component density functions, where each component represents one cluster.

Although there is no single clustering algorithm which can be used as a general tool for all clustering problems that have very different natural data structures, all methods are designed to identify certain properties of the data.

The clustering results of the first two types of clustering algorithms, hierarchical and K-means clustering, are sensitive to the methods used to measure the compactness or separation between data points. K-means clustering is also sensitive to its random initialization of initial cluster centers. Model based clustering suffers from a number of potential problems. There are a number of models that may fit a given set of data, but the correct model is seldom known *a-priori*. It is possible to envision data sets in which substantially different models are required for different portions of the data, yielding a difficult parameter estimation problem in which parts of the mixture of distribution are extreme or degenerate cases of the selected family of models. If the number of data points in each cluster is not large enough, the estimation of the parameters for the model will be difficult. Some scientists suggested to use multiple clustering methods and select a consensus of the clusters generated by them (Swift, et al., 2004; Wu, et al., 2002) When using amalgamation of different clustering methods, the outcome is highly variable, in part because of the degree to which different clustering methods are discovering compatible signals within the data. The process of finding consensus clusters can be done in a number of ways but none of which is clearly superior.

The method introduced there, K-means multiclustering, converges to a repeatable result, does not require the user to specify a statistical model of the data, and avoids introducing artifacts from the distance metric used to evaluate distances between points.

2 THE K-MEANS MULTICLUSTERING METHOD

2.1 *Background*

There are two major problems commonly faced by existing clustering methods. One is that there is no satisfactory method to identify the number of natural clusters in a data set. For hierarchical clustering, a subjective criterion is chosen to break the tree into clusters. A split will be made when it can generate clusters that make sense in biological view. Similarly in K-means clustering, the number of clusters is picked in advance demanding prior knowledge of data structure or K-means is run to generate many different numbers of clusters after which these different clusterings must be evaluated by the researcher. In many cases researchers do not have any information about the structure of the data set; instead they depend on clustering methods to help explore and understand the data. Even then, in order to use the existing clustering methods, they have to make expert guesses or randomly predict the approximate structure. Therefore, methods that can reveal the natural shape and cluster structure of the data will give scientists better chance of extracting useful biological information. Another issue is the selection of a distance measure. Different distance metrics "prefer'' different shapes for clusters. But the shape of data set and its natural clusters are typically unknown. Its discovery is a part of the mission of clustering.

In addition to the two common difficulties faced by all clustering methods, K-means algorithms suffers from randomness in initialization, i.e. different runs of the algorithm typically generate different results.

The key observation that leads to K-means multiclustering is that any one K-means clustering with an excessively large number of clusters yields useful information about which pairs of points should be tightly associated. Running K-means algorithm multiple times for a broad range of K yields potentially different information about which points should be associated and washes out the initialization effect of K-means algorithm. If we group information from Multiple K-means clustering we gain a better notion of which points should be associated. Intuitively, if two data points are very close to each other, they would be in one cluster more often that those who are not that close. The basic idea is to run K-means algorithm many times with different number of clusters, selected from a range, and then assign two data points to a cluster based on the number of times those two data points are placed together by the K-means algorithm. This procedure overcomes artifacts in the clustering induced by the intrinsic shape of a distance/similarity measure. This is because clusters are assembled only using short range information and overall cluster shapes are later reconstructed from only these short range interactions. The tendency of, for example, the Euclidian metric to prefer convex clusters, is lost; a long thin "river'' of data points that would make a very poor Euclidian cluster would still be a good cluster for multi-clustering because the individual points enjoy a transitive relationship of being close to some other cluster members. Another benefit of using multi-clustering is that the "natural" numbers of

clusters in a data set (if such a number exists) can be indicated by the cut plot as described subsequently.

2.2 *The K-means multiclustering algorithm*

Input:

1) A set S of r points in R^n

2) A number N of clusterings to perform

3) Distribution D of numbers of clusters

4) A weight cutoff C, $0 \leq C \leq 1$

Output:

A category function $Cat : S \rightarrow Z$

A cut plot $f : [0,1] \rightarrow Z$

Details:

Initialize an $r \times r$ *matrix M of pairwise connection strengths to contain all zeros*

Repeat N times

Select an integer d from D

K-means cluster S with d clusters

For each $\{i, j\} \in S \times S$ *with i, j in the same cluster*

Increment M[i][j]

Increment M[j][i]

end For

end Repeat

Normalize M[i][j] by dividing each entry of M[i][j] by N

Denote by W the graph on S with edge weights M[i][j]

For l equals 1 to N

Construct graph G with V(G) = S, E(G) pairs of points for which M[i][j] > l/N

Compute number of connected components c of C

Add the point (l/N, c) to the cut plot

end For

For x with l/N < x < (l+1)/N, f(x) = f(l/N)

Build a new graph on S with edges where M[i][j] > C

Enumerated the connected components of this graph

Cat[i] is the number of the connected component containing point i

Note: Z is the set of integer

Informally, the K-means multiclustering algorithm can be described as follows. Pick some number N of clusterings to perform (more is always better if you have the time). Pick a distribution D of possible numbers of clusters with a mean number of clusters larger than the largest number of clusters you would like to detect. Perform N clusterings, selecting the number of clusters in a given clustering from D. Initialize a set of pairwise connection strengths for each pair of points with an initial strength of zero. Whenever an individual K-means clustering places two points in a cluster together, increase their connection strength by 1. Finally choose a cutoff value C and retain only connections with that strength or greater. View the surviving clusters as edges of a graph that has the data items as vertices. The clusters are the connected components of this graph. The algorithm given above is given a cutoff value C but also generates the cut plot that permits the researcher to revise his notion about the desirable value of C. The cut plot is described in detail in Section 4.2;

briefly it is a graph of the number of clusters that would result as a function of the cutoff value C. Broad, flat spaces in the graph of this function – when they exist – correspond to natural numbers of clusters in the data.

3 CLUSTERING IDEALIZED DATA SETS

3.1 *Idealized data sets*

Three idealized, synthetic data sets with 2 or 3 designed clusters of different shapes were generated (Figure 1-3). The synthetic data sets were designed to defeat typical clustering algorithms except one in Figure 2 which was used as a control. Each data set contains 2000 points inside the unit square in R^2 with 2 or 3 natural clusters. We refer to these as the donut-and-ball (Figure 1, DR), horseshoe (Figure 2, U), and spiral (Figure 3, SP) data sets respectively. For each of these three types we also designed four different examples of varying difficulties (Ashlock, et al., 2005).

3.2 *Clustering parameters*

Euclidean distance is used to measure the distance between data points. There are 3 parameters that need to be defined for K-means multiclustering: the number of times to run K-means clustering (N), the distribution of the number of clusters for each run (D) and the cut off value for final clustering (C). Notice that C is in the range [0,1] due to the normalization; the number of times two points are together is divided by the number of clusterings performed to yield a connection strength that is always between 0 and 1 no matter how many clusterings are performed. For all the 3 sets of synthetic data, K means clustering

is run for 60 times, each time the number of clusters K is chosen to be the uniform distribution on [10,100], and the final clusters are determined by putting two data point in a cluster if they have been clustered for more than 20 times, that is the cutoff value of 0.33.

3.3 *Results*

As shown in Figure 1-3, K-means multiclustering algorithm successfully discovers the designed cluster structure of all the synthetic data, which is very hard for the traditional clustering algorithms. Different color means different clusters. This demonstrates that the algorithm can perform well on relatively idealized data that nevertheless are not well suited to direct partition using traditional clustering algorithm via Euclidian metric. As we know different distance metric prefers different shape of data, for example, Euclidian metric would be better for data with round shape and correlation coefficient for elongated data set. The designed data sets with different shapes, which are not preferred by Euclidian metric, can still be correctly clustered by K-means multiclustering with Euclidian metric. It indicates that the algorithm has a high level of immunity to artifacts introduced by the metric used to measure the distance between data points. This immunity is obtained by amalgamating the results of many k-means clusterings in a manner that builds the clusters from local information; most metric artifacts has their origin in point pairs in the same cluster that are not close to one another.

4 PROPERTIES AND PARAMETERS OF K-MEANS MULTICLUSTERING

4.1 *Selection of the range of D and the number of times to cluster*

The range of the distribution D and the number of clustering to perform vary with the structure of the data. In order to study how the selection of D and N affects the performance of K-means multiclustering algorithm, the multiclustering method was run with parameter sets consisting of different values of D and N on synthetic data sets with two clusters (the donut-and-ball data sets and the horseshoe data sets), three clusters (the spiral data set) and eighty-one clusters (the G81 data set, Figure 4). The donut-and-ball, horseshoe and spiral data sets are described in section 3.1. The G81 data set also contain 2000 data points inside the unit square and has 81 designed disk-shaped clusters arranged in a nine-by-nine grid.

The need for the distribution D is worth at least a brief discussion. If the number of clusters requested from the K-means algorithm is the same each time then the algorithm tends to find the same clusters more often, based on noise features of the data, which can generate artificial results. For the data used in this study, leaving the number of clusters computed the same across a K-means multiclustering resulted in spuriously high connection strengths between pairs of points near these repeating clusters. Changing the number of clusters requested from the K-means algorithm through a broad rang of values eliminated this effect.

The distributions of D for idealized synthetic data sets with 2 or 3 clusters used 3 different lower bound values for D (10, 60, 100) and 4 ranges with width (10, 40, 90, 190), while the number of clusterings N was set to 5 different values (30, 60, 100, 200, 300). For the

idealized synthetic data set with 81 clusters, the lower bounds of Ds were set at 10, 100 and 300, three ranges 100, 200, and 300 were used, and five values for N were tested: 50, 100, 200, 400, 500. The range of cut-off values at which the right number of clusters was detected, termed the *correct cut off region*, were calculated by running multiclustering algorithm on the synthetic data sets using the various sets of parameters given. The larger the correct cut off region is, the better the parameters selected is considered.

For the donut and ball (DR, Table 1), horse shoe (U, Table 2) and spiral (SP, Table 3) data sets with 2 or 3 designed clusters, the more difficult the clustering problem posed by the data, the narrower the correct cut off region. The SP data sets are more difficult than DR and U data sets, the correct cut off regions of SP are narrower than those of DR and U. The range of D with lower bound of 10 and medium widths [10, 50] and [10, 100] gave a larger correct cut off region in most of the tests. The narrow range that was obtained with lower bound of 10, such as [10, 20], will either perform the best for easy data (e.g. DR01, U01, U03) sets or the worst for hard data (e.g.: DR02, DR04, all SP). The wide range for the distribution D with lower bound of 10, [10, 200] always gave smaller correct cut off regions that the medium wide range with the same lower bound. Actually this is true for D with the higher lower bound of 60 and 100. In general, for data sets with 2 or 3 clusters, the range of D with lower bound of 10 and medium wideness are acceptable but the higher the lower bound, the wider the range, the worse the correct cut off region. For harder data, wider ranges yield better results than narrow ranges, but ranges that are too narrow or too wide perform poorly. The medium width of D tested in this study functions adequately. For some of the harder data sets (e.g. SP), a range for D with lower bound of 60 at narrow wideness yielding a range

of [60, 70] generates a better correct cut off region. If the range of D is fixed, varying the number N of times to cluster does not change the size of the correct cut off region dramatically, but for a wide range and high lower bound, larger N yield better results than can be generated by any narrow range of D. Therefore, the selection of appropriate D is more critical than the number of times the data are clustered. Considering the starting value of the correct cut off region, the higher the lower bound and the wider the range of D, the lower the start value becomes.

For the G81 data sets with 81 designed clusters (Table 3), the range of D of [10, 200] gave a better correct cut off region for all 4 data sets, even for the hardest one G81D04. When D is set to [100, 200] we obtain the best correct cut off region for G81D01. Choosing D with high lower bound and wide range always gave the worst size of correct cut off region. It is a surprise that the lower bound of D need not be larger than the real number of clusters. This is probably because a larger lower bound and wider range would yield a graph with a large number of moderate connection strengths that would not cut well. The cluster structure would include a large number of small, spurious clusters.

4.2 *The cut plot*

The cut plot is an important feature of K-means multiclustering, which displays the number of clusters across all possible cut weights. Once the algorithm has computed the connection weights for all pairs of points it then computes the number of clusters that would results for each value of C. Figure 5 shows the cut plot for donut-and-ball synthetic data set using

parameters defined in section 3.2 with D [10,100] and N = 60. The designed number of clusters for this data set is two. Notice that all four cut plots have broad, flat regions which give many values of C for which the number of cluster is two. The easiest data in Figure 1 DR01 gives two clusters at a cut value of zero which means that points in the donut and the ball were never grouped together. The hardest data set in Figure 1 DR04 has the narrowest region where the number of cluster is two, and the only one with a nontrivial flat region where the number of clusters is more than two. The similar results of cut plot are also obtained for horseshoe (Figure 6) and spiral (Figure 7) data sets. The results from our synthetic data indicate that the cut plot gives guidance as to estimating strength of different number of clusters, in the form of the broadness of the area of the cut plot that yields a give number of clusters. A large flat area on the cut plot is a strong signal indicating the strength of an estimate that the data contains a certain number of clusters, in essence it indicates that the gap between clusters is much larger than the distance among nearest neighbors within those clusters. The gap between clusters indicated by a flat region at the low cut off value in a cut plot is larger than that between clusters with flat region at high cut off value. Examples of data sets that has large distinguishable gap between clusters are the synthetic data sets shown in Figure 1-3. When data has this character, the cut plot can give advice as to the correct number of clusters. The cut plot also yields the information that there is no obvious natural clusters if this is the case, that is there will be no significant flat area on the cut plot. Therefore, the cut plot is a way to visualize the hierarchical structure of a data set.

A simple data set was generated to show how the cut plot can indicate the hierarchical data structure. The data set has 25 data points with designed structure as shown in Figure 8. The cut plot generated by K-means multiclustering algorithm with D [2, 7] and N 100 is shown in

Figure 8. This simple data set is designed to have 1, 2, 3 or 4 clusters depending on the definition of clusters. The cut plot generated by K-means multiclustering can indicates this kind of structure by showing the flat regions at 1, 2, 3, and 4 clusters. The gap between red and blue clusters are more clear that that between the black and green clusters, which can be reflected in the cut plot as a large flat region at 3 clusters.

Different runs of multiclustering algorithm can produce different cut plots, especially at high cut off value, but the overall shape of the cut off plot remains the same. The variation of the cut plot at high cut off value indicates the random factor effect on the clustering results; on the other hand, the consistent part indicates the real data structure which can not be affected by the random factor. Also different selections of multiclustering parameters can generate different cut plots for a given data set, never the less the significant structure in the data stays the same. The sort of simple summary of aspects of the structure of the data given by the cut plot is potentially useful.

4.3 *Hierarchical structure produced by K-means Multiclustering*

In addition to the cut plot which can provide a simple summary of the data structure by, K-means multiclustering can also provide a detailed view of the clusters formed to reveal the underlying structure of the data with a hierarchical tree. The hierarchical tree built from multiclustering algorithm shows how the data are merged into a cluster at different cut off values, which is also an indicator of the hierarchical structure of the clusters of data points.

The data structure used to build the tree is shown in Figure 9. All the internal nodes are linked by cluster_links (blue) to a specific cut off box. Those internal nodes are clusters at specific cut off value. All the leaf nodes in a subtree of an internal node are all the data points that belong to that cluster (internal node). Therefore, by traversing the subtree of an internal node down to the leaves, we can find all the members of that cluster. A bottom-up approach will be used to construct the tree where the end leaf nodes are individual data points. The tree is initialized at a cut off of 100%, placing the data point in a cluster that were invariably together. Data points in a cluster at a cut off 100% are linked by sibling_link (green), and an internal cluster node will be generated, which is linked to cut off array box at cut off 100%. The first data point node is linked to its cluster node by a childred_link (red), and the rest of the data point leaf nodes are linked to their cluster node by parent_links (black). As the cut off decreases, the existing internal nodes (clusters) at previous cut off level would merge to form new internal nodes with larger number of leaf nodes under them (more data elements in a cluster).

This cluster formation is basically the reflection of the connection strength between the data points or the lower level clusters. K-means multiclustering algorithm can generate the tree in text format which can be used to draw a tree with standard tree drawing software. A graphic view of the resulting hierarchical tree can be presented as a dendrogram by tree drawing software like Rainbow (http://genome.cs.iastate.edu/Rainbow/manual/). Figure 10 shows the detailed tree view drawn by Rainbow of the hierarchical data structure of data set described in section 4.2 (Figure 8).

5 RUNING K-MEANS MULTICLUSTERING ON SYNTHETIC MICROARRAY DATA SETS

5.1 *Synthetic microarry time series data sets*

Because of a lack of unambiguous clusters for real biological microarry data set, it is difficult to evaluate the performance of clustering methods on biological microarray data. A collection of sixty simplified microarray time series data sets with six time points are generated for this study. The sixty data sets are divided into 6 groups, each group consists of 10 data sets with the same number of designed clusters. The number of clusters in this study are 5, 10, 15, 20, 25, 30. For each data set, the number of members in each cluster is picked randomly from [10, 200]. Therefore, the data sets contain 500, 1,000, 1,500. 2,000, 2,500, 3000 data points for the 6 groups respectively. The pattern of fold change along 6 time points of each cluster in a data set is expressed by a string like "012210", which means "down–no change-up-up-no change-down". Strings designating the patterns are also selected randomly, and the variance in fold change within each cluster is also randomly picked from [0.05, 0.2]. These data sets are intended to simulate the microarray data which, after statistical preprocessing including nomalization, standardization and significance testing, have an idealized form. After preproccessing of biological data, clustering methods are run on the genes already known to have statistically significant gene expression activity. For this reason, no noise data (statistically non-significant data points) are simulated.

5.2 *Clustering methods*

In order to evaluate the relative performance of K-means multiclustering, three typical clustering methods, Model-based clustering, hierarchical clustering and standard K-means clustering, are used to cluster the 60 synthetic microarray data sets. Model-based clustering was selected because the way we generate our synthetic data set fits the assumption of model-based clustering method, which is that the data set is a finite Gaussian mixture, and each cluster is represented by a Gaussian probability distribution. Therefore, Model-based clustering can serve as a positive control. The hierarchical clustering method was selected because K-means multiclustering can find the hierarchical structure of data sets. Comparing the accuracy of the hierarchical structure generated by our method to the traditional hierarchical clustering method is desirable. The model-based clustering we used in this study is from the "Mclust" function implemented in an add-on R package "mclust", and hierarchical clustering and K-means clustering are from functions "hclust" and "kmean" in R library "stats".

5.3 *Adjusted Rand Index*

The Rand index (Rand, 1971) is a method to calculate the number of pair-wise agreement and disagreement in two clustering results. Given two partitions into sets U and V, for all possible pairs of data points i and j, there are four outcomes: a pair is together in both partitions, in only the first, in only the second, or in neither. Let a be the number of pairs that i and j are in same cluster in U and V; b is the number of pairs that i and j are in same cluster in U, but not in V; c is number of pairs that i and j are in same cluster in V, but not in U; d is

the number of pairs that i and j are not in a cluster in both U and V. Hence, a and d describe the agreement, b and c describe the disagreement. The Rand Index is then defined as:

$$R(U,V) = \frac{(a+d)}{(a+b+c+d)}$$

The adjusted Rand Index (Hubert and Arabie, 1985; Yeung, et al., 2001) is calculated base on the contingency table defined by U and V, where the value n_{ij} represents the number of objects that are in the i th cluster in U and j th cluster in V. The adjusted Rand Index is given as:

$$\frac{\sum_{ij}\binom{n_{ij}}{2} - \left[\sum_{i}\binom{n_{i.}}{2}\sum_{j}\binom{n_{.j}}{2}\right] / \binom{n}{2}}{\frac{1}{2}\left[\sum_{i}\binom{n_{i.}}{2} + \sum_{j}\binom{n_{.j}}{2}\right] - \left[\sum_{i}\binom{n_{i.}}{2}\sum_{j}\binom{n_{.j}}{2}\right] / \binom{n}{2}}$$

The maximum values of the adjusted Rand Index is 1 when two partitions are the same. Its expected value in the case of random clustering is 0. And the higher the adjusted Rand Index, the higher the agreement between two partitions. Since the adjusted Rand Index is more sensitive than Rand Index, we use adjusted Rand Index to compare the clustering results from four clustering methods to the designed truth.

5.4 *Comparison methods*

There are two ways to compare different clustering results to the designed truth. The first way is to pick a clustering result that gives the correct number of clusters. For our clustering methods, we select the clustering results that give exactly the correct number of clusters or the one that gives the number of clusters very close to the correct number if there is no

clustering result with the correct number of clusters. For the model-based and K-means clustering methods, we give the correct number of clusters to the methods; for hierarchical clustering we cut the tree at a joining strength chosen so as to generate clustering results with the correct number of clusters.

The second comparison method is to find the clustering results that are closest to the truth, which is in our case the clustering results that give the largest adjusted Rand Index. This method will give us an idea about the ability of a method to reveal the designed data structure under ideal circumstances. To find the clustering results with the best predicted data structure revealed by our multiclustering algorithm, we calculate the adjusted Rand Index for all clusterings with different number of clusters along the cut plot. For Model-based clustering we give a wider range of number of clusters to the function; a wide range of different cut value and number of clusters are fed to hierarchical clustering and K-means methods respectively.

5.5 *Consistency analysis*

The multiclustering method is stochastic, and so different runs of the algorithm may generate different clustering results. In order to study the performance consistency of K-means multiclustering methods, five runs of K-means multiclustering are conducted on all 60 synthetic microarry time series data sets. The distribution of D in this study is uniform on [10,100] and run 500 times.

From Figure 12, we can see that the 5 different runs have the very similar best adjusted Rand Index (the second comparison method) on the 60 synthetic microarry data sets. The standard deviations for the adjusted Rand Indices of 5 runs on all the synthetic data sets tested are all less than 0.02; the average best adjusted Rand Indices are above 0.95 (Table 6). The consistently high vale of the best Rand Indices for all data sets indicate that multiclustering method is reliable in finding the designed clusters.

The adjusted Rand Indices of the five runs based on the clustering results with the best guess as to the number of cluster, i.e. the first comparison method, fluctuate more than those with the best Rand Index (Figure 11). Of the 60 data sets, the five runs on eleven of them have standard deviations of above 0.03 (Table 5). The group of synthetic data sets with 30 clusters has the lowest average adjusted Rand Index of 0.86, and the rest sets with less than 30 clusters have the average adjusted Rand Index above 0.93.

The more the clusters in a data set, the smaller the gap between clusters. This, in turn, means that the data set is more difficult to cluster correctly at cut values that yield more clusters. A consistent result from the two different comparison methods is that muticlustering has better performance (i.e. higher adjusted RandIndex value) on data sets with fewer clusters than those with more clusters. For almost all data sets except one in groups with 5 clusters, multiclustering algorithm can find the perfect clustering results. Comparing with the adjusted Rand Indices of the second comparison method, the adjusted RandIndices of the first comparison method are not as stable. The data sets with fluctuating adjusted Rand Indices from different runs are not only in groups with more clusters. Almost all groups

except the group with 10 clusters have data sets with fluctuating adjusted Rand Index. This suggests that the number of clusters is not the major reason for instability of the multiclustering results. We guess the reason might be the big variation within the clusters or very similar the fold change patterns among clusters. For those data sets that exhibit slightly different results in different runs, the variation may also reflect the random factors in the operation of the clustering algorithm. The variation between runs may thus be useful for determining which clusters the data actually support. The results from the two methods are very close for data set with fewer clusters, which indicates that multiclutering algorithm can find both the right number of clusters and right structure for data sets with fewer clusters, but not the right number of clusters for data sets with more clusters. The stable best adjusted RandIndex and fluctuated Rand Index of the first method among 5 runs suggest that the most accurate clustering results generated by K-means multiclustering are very stable, even though the number of clusters may change, or stray from the designed structure. This shows the consistency in the ability to identify the designed data structure.

5.6 *The effect of parameter settings*

Based on our experience from our synthetic data set, that is the distribution of D [10,100] works fine when the number of clusters is less than 100, three distributions for D are used: uniform on each of [10,100], [10, 50], and [50, 100].

Using the first comparison method, we can see that different Ds seem have less impact on performance for the synthetic data sets with the numbers of clusters less than 20 (Figure 13).

The most different adjusted RandIndices (first method) from different Ds can be found in the data sets with 30 clusters. For data sets with over 20 clusters, there is no a single distribution of D that would get the best performance for all the data sets. This may be because for data sets with fewer numbers of clusters the complexity of the data sets is less, therefore for hard data set, to get the right number of clusters and right structure the selection of D is very important.

When we use the second comparison method, different distributions of D give very similar best adjusted Rand Index values (Figure 14) for all the data sets with different number of clusters; in this case the selection of parameters does not affect the ability of the algorithm to find the designed data structure.

5.7 *Performance comparison among clustering methods*

The average of adjusted Rand Indices from the five runs of K-means multiclustering (as described in section 5.5) is used as the clustering result of multiclustering algorithm for the performance comparison to the other three clustering methods.

For the first comparison method (Figure 15, Table 7), multiclustering finds the perfect clustering results with adjusted Rand Indices of 1.0 for 9 data sets out of 10 with 5 clusters; Model-based clustering performs poorly on 3 out those 10 data sets. For the forty data sets with 10 – 25 clusters, K-means multiclustering has the similar adjusted RandIndices as Model-based clustering methods except 3 data sets. Model-based clustering method shows

the best performance for the 10 data sets with 30 clusters; in general multiclustering is the second best. The performance of hierarchical clustering and K-means clustering varies greatly from data sets to data sets, while multiclustering has up and down in the adjusted RandIndices only in data sets with 30 clusters. Except one data set with 15 clusters, multiclustering method shows superior or similar clustering compared to hierarchial clustering method. As we expected, multiclusering performs better than K-means clutering, but it is interesting to find that K-means is slightly better than multiclustering on two data sets with 30 clusters. We use the same distribution of D on all the data sets for this study, as we mentioned before there is no universal parameters that fit to all data sets, different distribution of D may help to find the right number of clusters and right structure at the same time. In general, when we consider the ability of clustering methods to find the right number and right structure of clusters, multiclustering method is similar to the positive control method, i.e. Model-based clustering, on data sets with fewer clusters and better than the two other traditional clustering methods – hierarchical clustering and K-means clustering.

In comparison to other methods, the results from the second comparison method (Figure 16, Table 8) show that for almost all the 60 data sets, multiclustering is the method with the highest best adjusted Rand Index, which means that it can find the clustering closest to the truth. The best adjusted Rand Indices of the multiclustering algorithm for all data sets are above 0.9. For some data sets multiclustering has higher best adjusted Rand Indices than the positive control method – Model-based clustering. Not like the adjusted Rand Indices computed by the first method, the best adjusted Rand Indices of multiclustering do not vary from data sets to data sets, which show the ability of multiclusetering to consistently find the

right data structure for different data sets with high accuracy. Combining the results from section 5.5 and 5.6, we can see that the ability of multiclustering algorithm to discover the real data structure, which is measured by the adjusted Rand Index by the second comparison method, is stable from different runs, different distribution of D, and different data sets. This indicates the strong ability of multiclustering to capture the natural shape of data sets.

The ultimate goal of clustering is to explore the data set and divided the data points into groups based on their relationship. In most cases, the nature dividing of the data is not clear, the number of clusters is really depending on the definition of clusters. The internal relationship among data points, which is helpful to interpret the underlying meaning carried by the data, is the most important thing for scientist. Therefore, a good clustering method should be able to reveal the underlying data structure. As we show above multiclustering has the ability of capturing the designed data structure of synthetic microarray data sets with high accuracy, it would be a useful tool for biologist to explore microarray data.

6 DISCUSSION AND CONCLUSIONS

This manuscript introduces, defines, and tests multiclustering. It is found to be reliable and consist in capturing the underlying data structure, and competitive with model based clustering and superior to other methods on data generated in a manner consistent with the hypothesis of model based clustering. Data which are poorly conditioned relative to the assumptions of model based clustering may be a domain where the ability of multiclustering to function without a model will yield clearly superior performance. The ability of multiclustering to reduce artifacts due to the choice of metric used to compare data points

and to function without a model for the distribution of the data reduce the number of assumptions that must be made. This study demonstrates that multiclustering is relatively robust to the parameter choices to find the right number of clusters and the right structure that must be made and gives some rules of thumb for choosing those parameters. The selection of the distribution of D is more critical than that of N, the number of cluterings to perform. High lower bounds (too far away from the real number of clusters) and wide ranges for D are not favored by our testing data sets with 2, 3 and 81 clusters. For the same type of data, wider ranges for D would be helpful to data sets with smaller gaps between clusters.

A difficulty in interpreting microarry clustering results is the fact that, given a data set, a clustering method can always generate clusters for it. In some cases different clustering methods will produce very different clusters. People may misinterpret the data by examining improperly clustered data; the use of clustering thus puts a larger burden on the researcher to make careful interpretations. The distance or similarity metric chosen, the computational preparation of the data prior to clustering, and the choice of which data to disregard are all possible sources of algorithmic artifacts in clustering. Careful examination is required to check if the clusters are natural clusters instead of artifacts of the algorithm. Another difficulty in clustering microarray data is that there is no clear definition of cluster. The clustering results are often based on the relative distance among data points. A single clustering result will not reflect the overall relationship among the data points. Therefore, the hierarchical tree generated by multiclustering is a better way to show the underlying data structure. Instead of giving a clustering result, the multiclustering algorithm produces a hierarchical tree which gives the whole picture of the relative relationship among data points.

This provides biologists a more complete view of the whole data set, which would help them to discover and interpret the underlying biological meaning. Therefore, the multiclustering algorithm that can consistently identify the data structure with high accuracy that is comparable to that of model-based clustering on data sets that are designed to follow the assumption of Model-based clustering, and display the over all data structure using a hierarchical tree is helpful tool for biology to explore the relationship among genes in which they are interested.

In spite of the shortcomings of clustering, it is still a powerful tool for microarray analysis. Since the scale of information generated by a microarray experiment is far beyond the level that can be handled by human without some form of computational assistance. The major purpose of clustering in microarray analysis is to reduce the data to the level that biologist can generate hypothesis, or explain the relations between genes and phenotypes. Therefore, the relationships between clusters of genes and phenotypes predicted on clustering based analysis are tentative. Keeping this in mind and along with the intensive research effort to more accurate clustering method, we can avoid, or at least minimize misunderstandings. Finally, the accuracy of the clustering methods also depends on the quality of the microarray data and the statistical approach used to preprocess the raw data.

ACKNOWLEDGEMENTS

We thank Duhong Chen for providing “RainBow” tree drawing software. This project was supported by competitive grants from the National Science Foundation Plant Genome Program (DBI-9975868 and DBI-0321711).

REFERENCES

Ashlock, D., Kim, E.Y. and Guo, L. (2005) Multi-clustering: Avoiding The Natural Shape of Underlying Metrics, *ANNIE 2005*.

D'Haeseleer, P. (2005) How does gene expression clustering work?, *Nat Biotechnol*, **23**, 1499-1501.

DeRisi, J.L., Iyer, V.R. and Brown, P.O. (1997) Exploring the metabolic and genetic control of gene expression on a genomic scale, *Science*, **278**, 680-686.

Eisen, M.B., Spellman, P.T., Brown, P.O. and Botstein, D. (1998) Cluster analysis and display of genome-wide expression patterns, *Proc Natl Acad Sci U S A*, **95**, 14863-14868.

Ghosh, D. and Chinnaiyan, A.M. (2002) Mixture modelling of gene expression data from microarray experiments, *Bioinformatics*, **18**, 275-286.

Hubert, L. and Arabie, P. (1985) Comparing partitions *Journal of Classification*, 193-218.

Jiang, D.T., C. Zhang, A. (2004) Cluster analysis for gene expression data: a survey, *IEEE Transactions on knowledge and Data Engineering*, **16**, 1370-1386.

McQueen, J.B. (1967) Some methods for classification and analysis of multivariate observations. , **1**, 281-297.

Rand, W. (1971) Objective criteria for the evaluation of clustering methods, *Journal of the American Statistical Association*, **66**, 846-850.

Swift, S., Tucker, A., Vinciotti, V., Martin, N., Orengo, C., Liu, X. and Kellam, P. (2004) Consensus clustering and functional interpretation of gene-expression data, *Genome Biol*, **5**, R94.

Wu, L.F., Hughes, T.R., Davierwala, A.P., Robinson, M.D., Stoughton, R. and Altschuler, S.J. (2002) Large-scale prediction of Saccharomyces cerevisiae gene function using overlapping transcriptional clusters, *Nat Genet*, **31**, 255-265.

Yeung, K.Y., Fraley, C., Murua, A., Raftery, A.E. and Ruzzo, W.L. (2001) Model-based clustering and data transformations for gene expression data, *Bioinformatics*, **17**, 977-987.

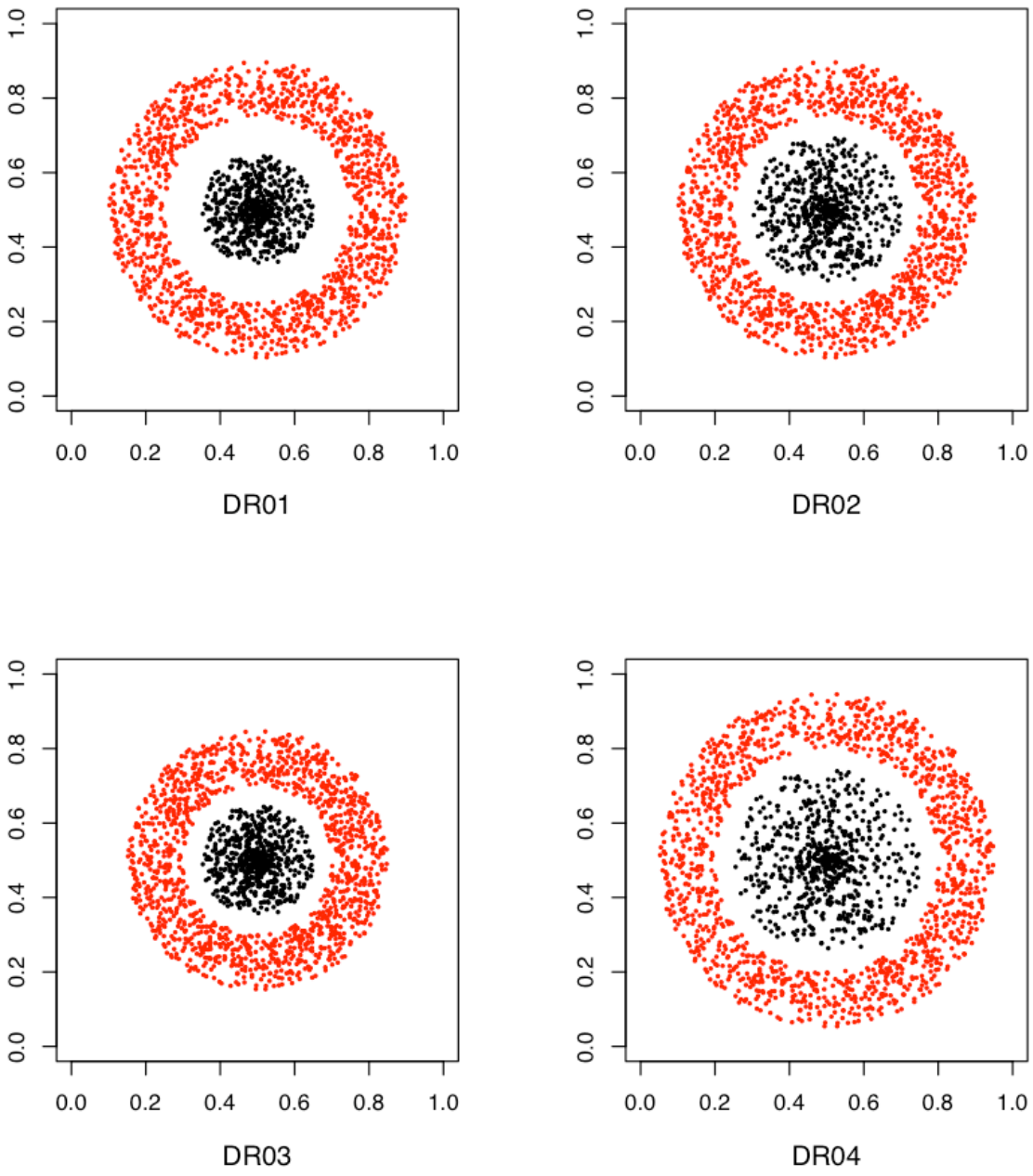

Figure 1. Partition of the four donut-and-ball data sets (DR) by multi-K means clustering with the distribution of D on [10,100], N=60 and a cut threshold C=0.33. Different colors mean different clusters.

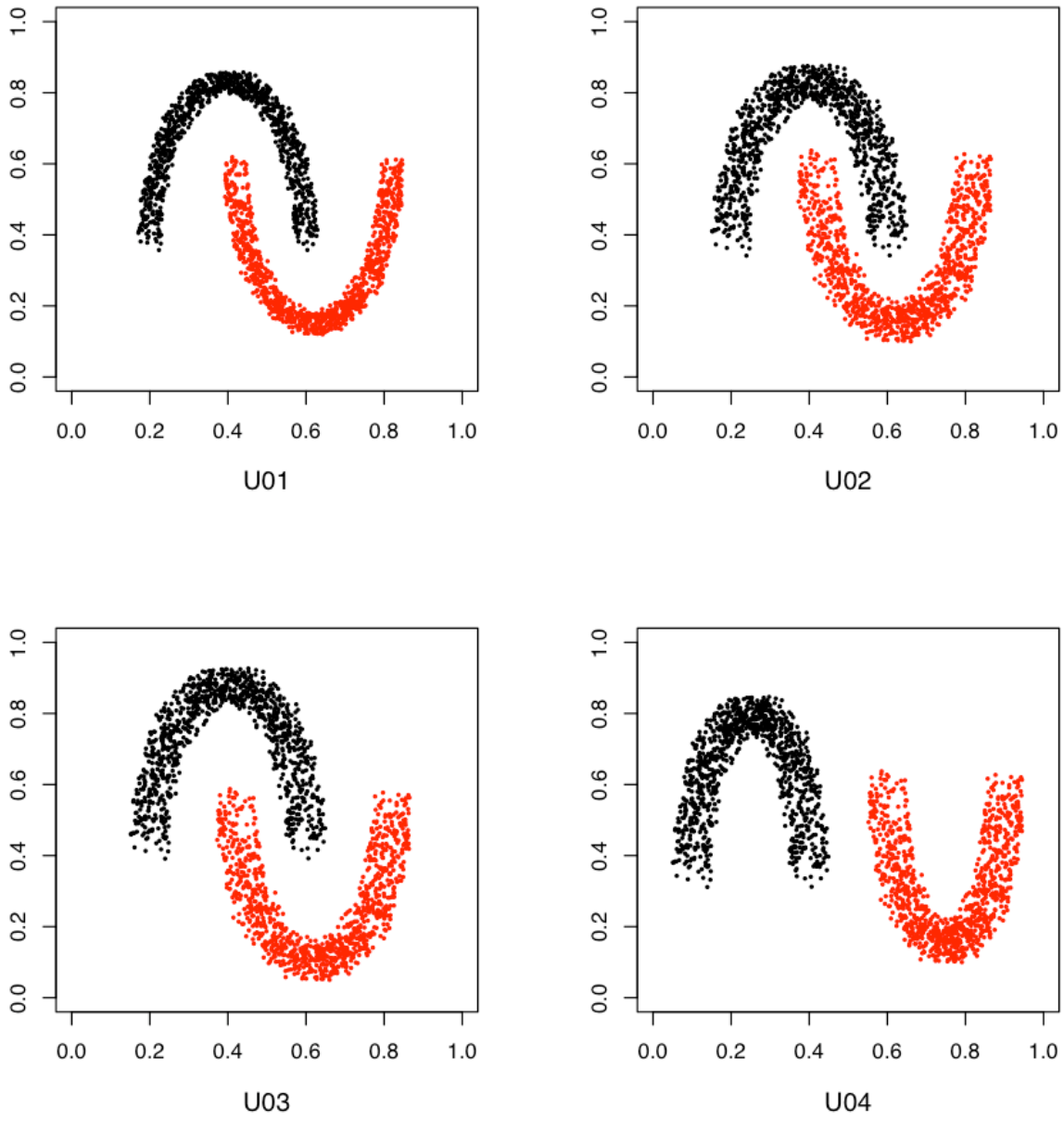

Figure 2. Partition of the four horseshoe data sets (U) by multi-K means clustering with the distribution of D on [10,100], N=60 and a cut threshold C=0.33. Note that the fourth data set can be correctly clustered with standard K-means clustering.

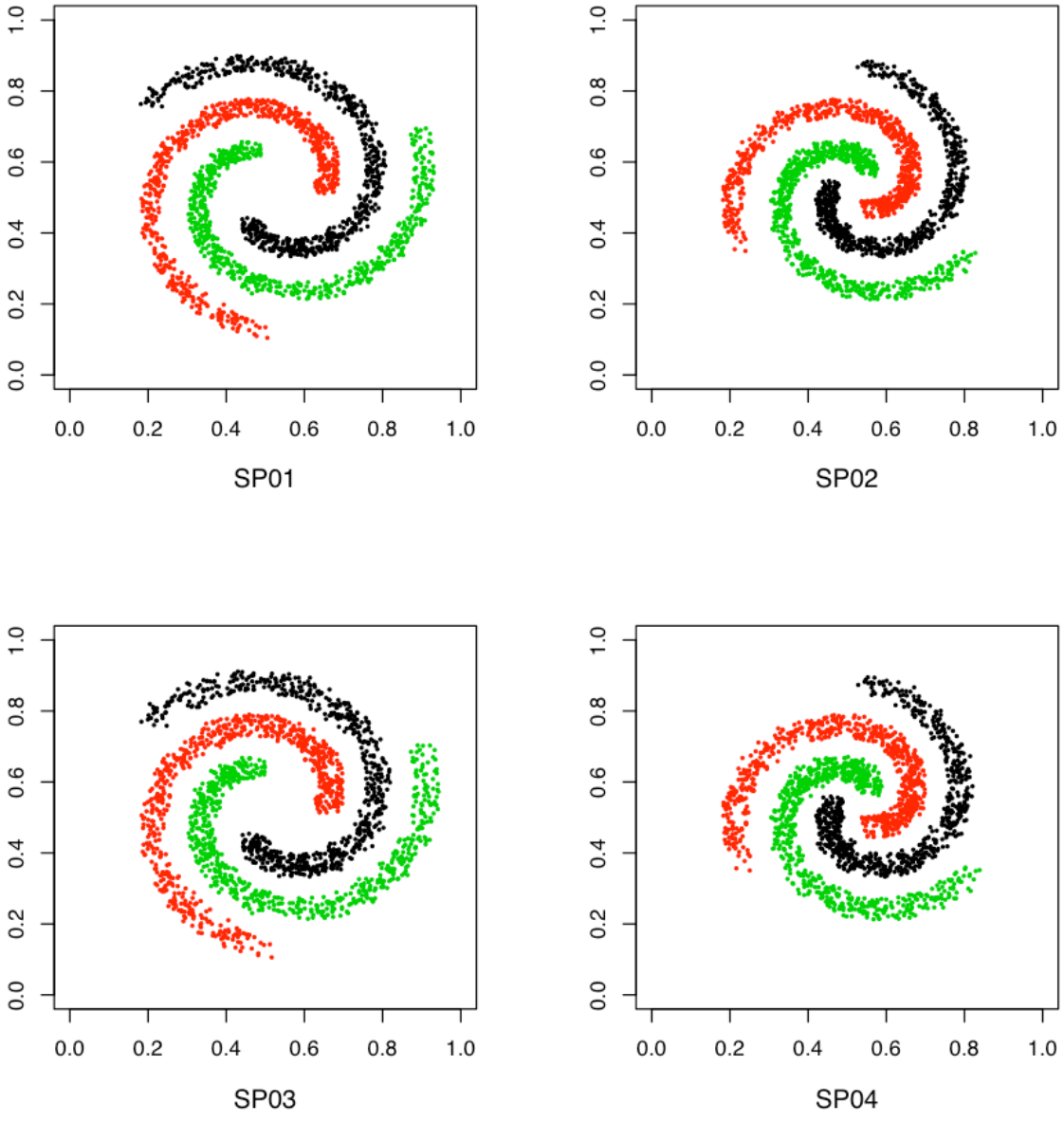

Figure 3. Partition of the four spiral data sets (SP) by K-means multiclustering with the distribution of D on [10,100], N=60 and a cut threshold C=0.33.

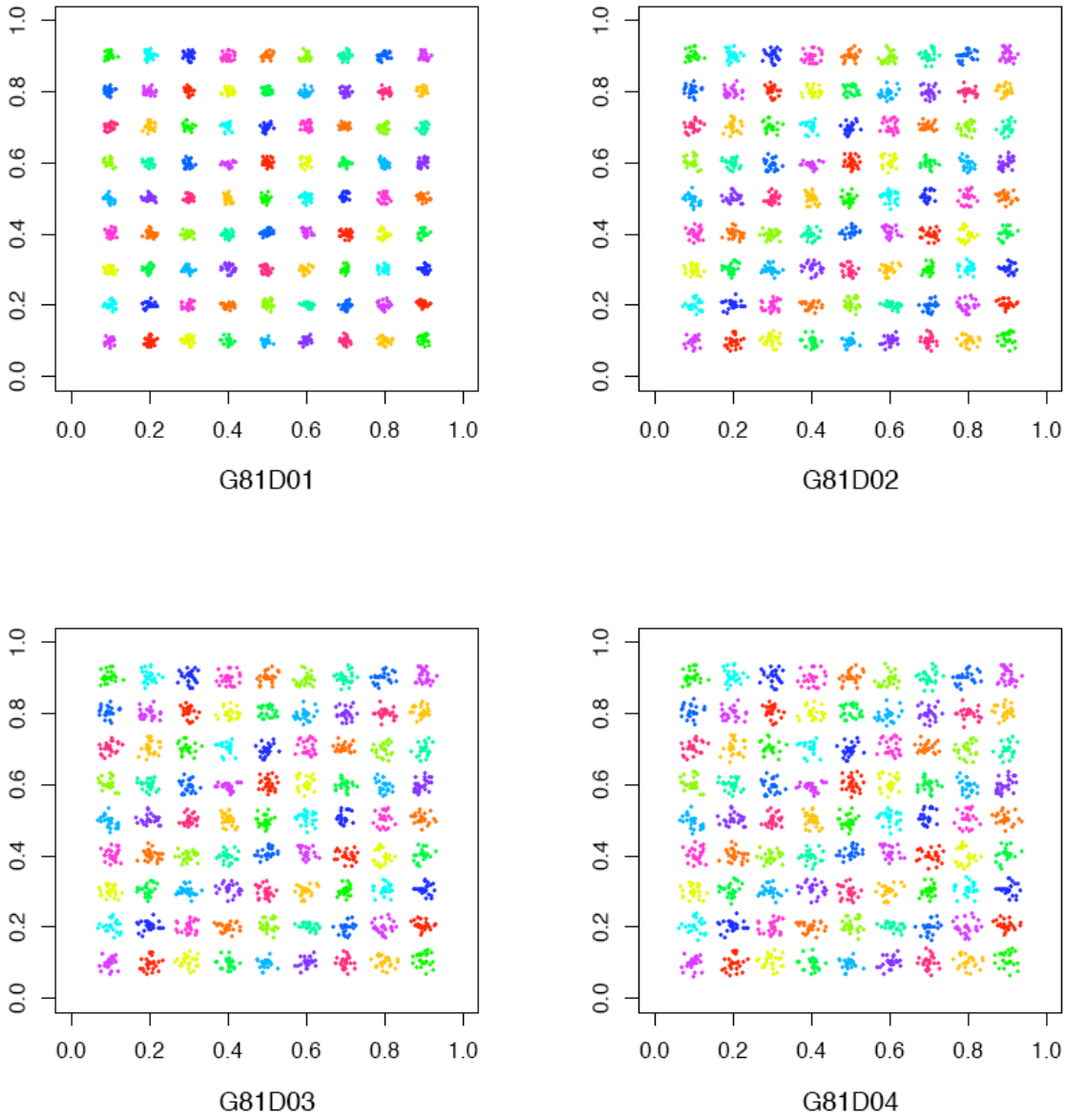

Figure 4. Partition of the four G81 data sets by K-means multiclustering with the distribution of D on [10,200], N=60 and a cut threshold C=0.56.

Table 1. The best and worst10 parameter settings for all four DR sets

Data sets	The best				The worst			
	Parameters		Cut off		Parameters		Cut off	
	D[1]	N[2]	Start[3]	Width[4]	D[1]	N[2]	Start[3]	Width[4]
DR01	[10,20]	60	2	84	[100,290]	300	2	33
	[10,20]	30	3	83	[100,140]	200	2	30
	[10,20]	200	2	81	[100,140]	300	2	30
	[10,20]	300	2	81	[100,190]	100	2	30
	[10,20]	100	2	80	[100,140]	60	2	27
	[10,50]	30	3	79	[100,190]	60	2	27
	[10,50]	60	2	74	[100,140]	30	3	26
	[10,50]	100	2	74	[100,190]	30	3	26
	[10,50]	200	2	73	[100,290]	30	3	26
	[10,50]	300	2	72	[100,140]	100	2	25
DR02	[10,50]	60	22	51	[100,290]	30	7	30
	[10,50]	100	21	50	[100,290]	60	3	30
	[10,100]	200	17	49	[100,110]	100	4	28
	[10,50]	300	25	48	[100,110]	60	3	27
	[10,100]	300	18	48	[100,110]	30	7	23
	[10,50]	200	25	47	[10,20]	300	61	15
	[10,100]	30	27	46	[10,20]	100	64	13
	[10,100]	100	19	46	[10,20]	200	64	11
	[60,70]	60	13	44	[10,20]	30	67	10
	[10,50]	30	30	43	[10,20]	60	72	1
DR03	[10,50]	200	8	67	[100,110]	100	2	37
	[10,50]	100	8	66	[100,190]	100	2	37
	[10,50]	300	9	66	[100,290]	200	2	37
	[10,50]	60	8	65	[100,190]	60	2	35
	[10,50]	30	13	60	[100,290]	300	2	35
	[10,20]	200	25	56	[100,110]	30	3	34
	[10,20]	300	26	56	[100,290]	30	3	34
	[10,100]	60	10	55	[100,190]	200	2	33
	[10,100]	100	7	53	[100,190]	300	2	32
	[10,100]	200	6	53	[100,290]	60	2	31

[1] D is the distribution of the number of clusters for each run
[2] N is the number of times to run K-means clustering
[3] The lowest cut off value at which the correct number of clusters is found
[4] The width correct cut off

Table 1. (continued)

Data sets	The best				The worst			
	Parameters		Cut off		Parameters		Cut off	
	D[1]	N[2]	Start[3]	Width[4]	D[1]	N[2]	Start[3]	Width[4]
DR04	[10,100]	300	22	41	[100,110]	60	12	20
	[10,100]	200	23	39	[100,190]	200	10	20
	[10,100]	100	26	36	[100,290]	30	17	20
	[10,200]	300	14	36	[100,190]	30	23	17
	[10,100]	60	27	35	[100,110]	30	20	13
	[10,200]	60	18	35	[10,20]	30	70	7
	[10,200]	200	16	35	[10,20]	60	75	2
	[60,70]	300	21	35	[10,20]	100	72	2
	[60,150]	200	11	35	[10,20]	300	72	2
	[60,150]	300	10	35	[10,20]	200	72	1

Table 2. The best and worst10 parameter settings for all four U data sets

Data sets	The best				The worst			
	Parameters		Cut off		Parameters		Cut off	
	D	N	Start	Width	D	N	Start	Width
U01	[10,20]	60	10	70	[100,190]	30	3	34
	[10,20]	100	10	68	[100,190]	200	2	34
	[10,20]	200	12	68	[100,190]	300	2	34
	[10,50]	60	3	67	[60,250]	60	2	30
	[10,20]	30	17	66	[100,290]	100	2	27
	[10,20]	300	11	66	[100,290]	300	2	27
	[10,50]	300	3	64	[100,290]	200	2	26
	[10,100]	60	3	64	[60,250]	30	3	20
	[10,50]	30	7	63	[100,290]	30	3	20
	[10,50]	200	3	63	[100,290]	60	2	18
U02	[10,50]	30	10	67	[60,250]	300	2	35
	[10,100]	60	3	64	[100,190]	60	2	35
	[10,100]	100	4	64	[60,250]	100	2	34
	[10,50]	200	13	63	[60,250]	200	2	34
	[10,50]	300	12	63	[60,250]	60	3	32
	[10,100]	200	6	63	[100,290]	60	2	31
	[10,100]	300	8	63	[100,290]	100	2	29
	[10,50]	60	13	62	[100,290]	200	2	28
	[10,50]	100	12	61	[100,290]	300	2	25
	[10,100]	30	7	60	[100,290]	30	3	24
U03	[10,20]	60	13	72	[100,190]	60	2	36
	[10,50]	100	3	72	[100,190]	100	2	36
	[10,50]	300	4	72	[100,140]	60	2	35
	[10,20]	200	13	71	[100,190]	200	2	35
	[10,50]	200	4	71	[60,250]	100	2	34
	[10,20]	300	13	70	[100,290]	60	2	31
	[10,20]	100	12	69	[100,290]	30	3	27
	[10,100]	60	5	68	[100,290]	300	2	27
	[10,50]	60	3	67	[100,290]	200	2	26
	[10,100]	30	3	67	[100,290]	100	2	25
U04	[10,50]	60	2	75	[60,250]	30	3	34
	[10,50]	30	3	74	[100,140]	100	2	34
	[10,50]	100	2	72	[100,190]	200	2	34
	[10,50]	300	2	72	[100,190]	300	2	34
	[10,50]	200	2	71	[100,290]	30	3	34
	[10,20]	30	10	70	[100,140]	200	2	33
	[10,20]	60	8	69	[100,290]	60	2	28
	[10,20]	300	6	67	[100,290]	100	2	27
	[10,100]	30	3	67	[100,290]	300	2	25
	[10,100]	300	2	67	[100,290]	200	2	24

Table 3. The best and worst10 parameter settings for all four SP data sets

Data sets	The best				The worst			
	Parameters		Cut off		Parameters		Cut off	
	D	N	Start	Width	D	N	Start	Width
SP01	[10,50]	100	29	38	[60,250]	30	3	7
	[10,50]	60	33	35	[100,290]	100	2	7
	[10,50]	200	32	32	[100,290]	200	2	7
	[10,50]	300	29	32	[60,250]	100	2	6
	[60,70]	200	2	28	[100,290]	300	2	6
	[10,50]	30	40	27	[10,20]	30	73	4
	[60,70]	30	3	27	[10,20]	60	78	4
	[60,70]	100	2	27	[10,20]	100	77	2
	[60,70]	300	2	27	[10,20]	200	79	2
	[60,100]	30	3	27	[10,20]	300	0	0
SP02	[60,70]	100	2	49	[60,250]	60	2	25
	[10,50]	100	25	47	[100,290]	100	2	25
	[60,70]	60	2	46	[60,250]	30	3	24
	[10,50]	300	26	45	[60,250]	100	2	23
	[60,100]	60	2	45	[100,290]	60	2	23
	[10,50]	200	27	44	[10,20]	60	63	10
	[10,100]	300	10	44	[10,20]	100	66	9
	[60,70]	30	3	44	[10,20]	30	67	6
	[60,70]	300	2	44	[10,20]	300	70	4
	[60,100]	30	3	44	[10,20]	200	71	2
SP03	[60,70]	200	2	43	[100,290]	30	3	14
	[60,70]	300	2	42	[100,290]	60	3	14
	[10,100]	300	13	39	[60,250]	30	7	13
	[60,100]	200	2	38	[100,290]	300	3	13
	[10,100]	30	20	37	[10,50]	30	37	6
	[10,100]	100	12	37	[10,20]	60	78	4
	[10,100]	200	13	37	[10,20]	100	78	1
	[60,70]	60	3	37	[10,20]	200	78	1
	[60,100]	30	3	37	[10,20]	30	0	0
	[60,70]	100	2	36	[10,20]	300	0	0
SP04	[10,50]	200	30	44	[100,140]	30	10	23
	[10,100]	30	13	44	[100,290]	200	5	23
	[60,70]	100	5	44	[60,250]	60	8	22
	[60,70]	200	5	44	[100,290]	30	3	20
	[10,50]	100	33	43	[100,290]	60	3	19
	[10,50]	300	30	42	[10,20]	30	77	3
	[10,100]	60	13	42	[10,20]	60	77	1
	[10,100]	200	14	42	[10,20]	200	78	1
	[10,100]	300	13	42	[10,20]	100	0	0
	[10,100]	100	13	40	[10,20]	300	0	0

Table 4. The best and worst10 parameter settings for all four G81 data sets

Data sets	The best 10				The worst			
	Parameters		Cut off		Parameters		Cut off	
	D	N	Start	Width	D	N	Start	Width
G81D01	[100,200]	100	37	27	[300,500]	500	2	6
	[10,200]	50	56	22	[300,400]	50	2	6
	[100,200]	200	42	19	[10,100]	100	84	6
	[100,400]	50	12	18	[300,600]	400	2	5
	[100,300]	50	18	18	[300,600]	50	2	4
	[100,200]	50	38	18	[300,600]	200	2	4
	[100,400]	100	14	16	[300,600]	500	2	4
	[10,200]	100	62	16	[300,500]	50	2	4
	[100,300]	200	26	15	[300,500]	200	2	4
	[100,400]	400	18	14	[300,600]	100	2	3
G81D02	[10,200]	50	46	30	[100,200]	50	32	8
	[10,100]	100	63	24	[300,400]	400	3	8
	[10,100]	200	67	23	[300,500]	50	2	8
	[10,100]	50	66	22	[300,500]	100	2	7
	[10,300]	100	36	22	[300,500]	200	2	7
	[100,300]	50	18	22	[300,600]	100	2	6
	[100,400]	50	12	22	[300,600]	200	2	6
	[10,200]	100	56	20	[300,600]	400	2	6
	[10,300]	50	32	20	[300,600]	500	2	5
	[10,100]	400	72	18	[300,600]	50	4	4
G81D03	[10,200]	50	46	28	[300,500]	500	5	2
	[100,300]	50	18	28	[300,600]	100	3	2
	[10,300]	100	37	26	[300,600]	400	4	2
	[10,100]	200	60	24	[300,600]	500	4	2
	[100,200]	50	30	24	[300,500]	100	4	1
	[100,400]	50	12	24	[300,500]	200	6	1
	[10,200]	100	52	22	[300,600]	200	4	1
	[10,300]	50	36	22	[300,400]	100	0	0
	[100,400]	100	13	22	[300,500]	50	0	0
	[10,100]	400	64	21	[300,600]	50	0	0
G81D04	[10,200]	400	46	20	[100,300]	400	0	0
	[10,100]	400	59	19	[100,300]	500	0	0
	[10,200]	200	46	19	[300,400]	100	0	0
	[10,200]	500	46	19	[300,400]	400	0	0
	[10,100]	500	61	17	[300,400]	500	0	0
	[10,100]	200	65	13	[300,500]	50	0	0
	[100,200]	200	38	13	[300,500]	200	0	0
	[100,200]	500	39	13	[300,500]	500	0	0
	[10,200]	100	51	12	[300,600]	50	0	0
	[10,300]	50	40	12	[300,600]	400	0	0

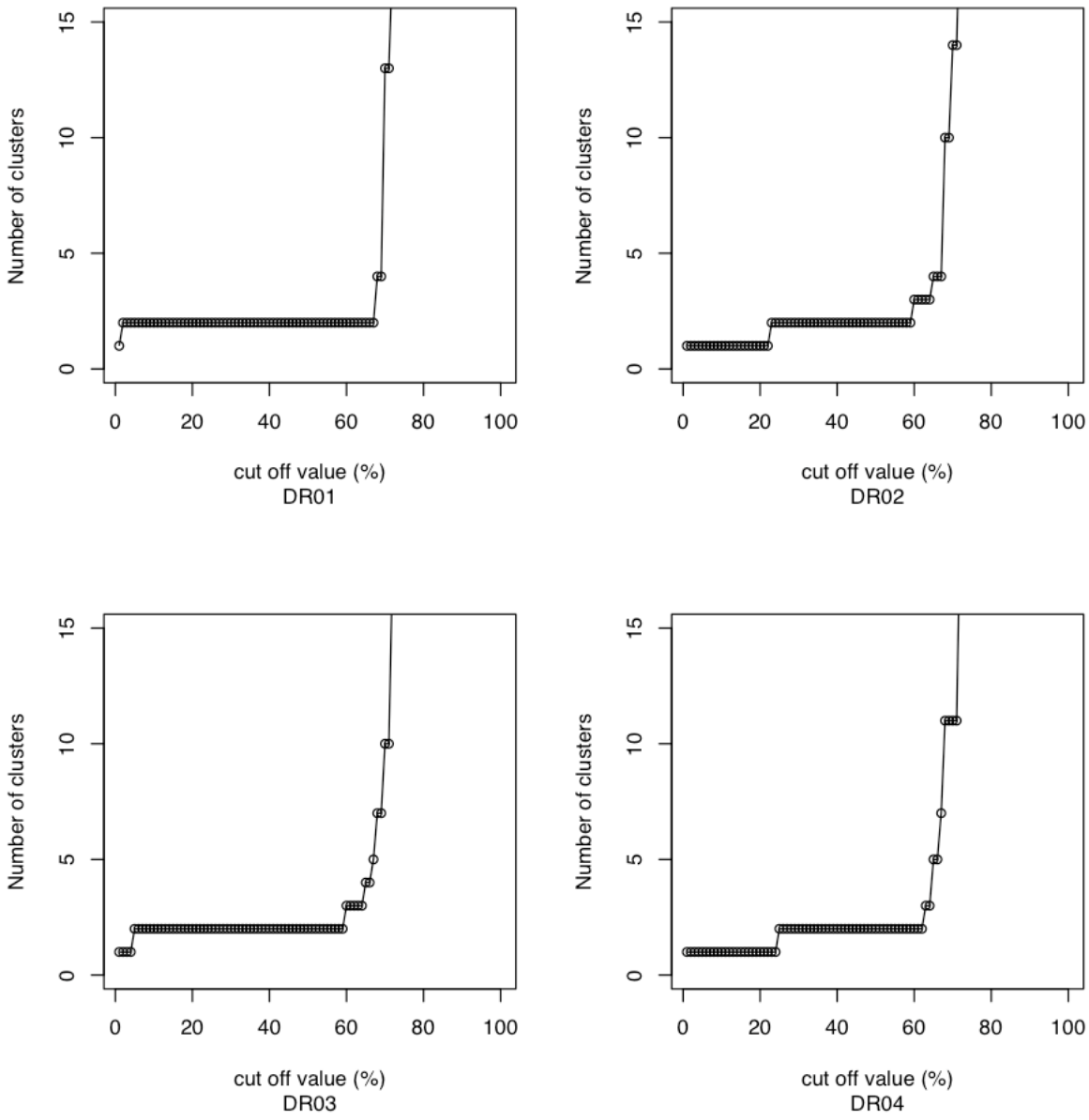

Figure 5. The cut plots for the four dount-and-ball data sets (DR) produced by the K-means multiclustering method with the distribution of D [10,100] and N=60.

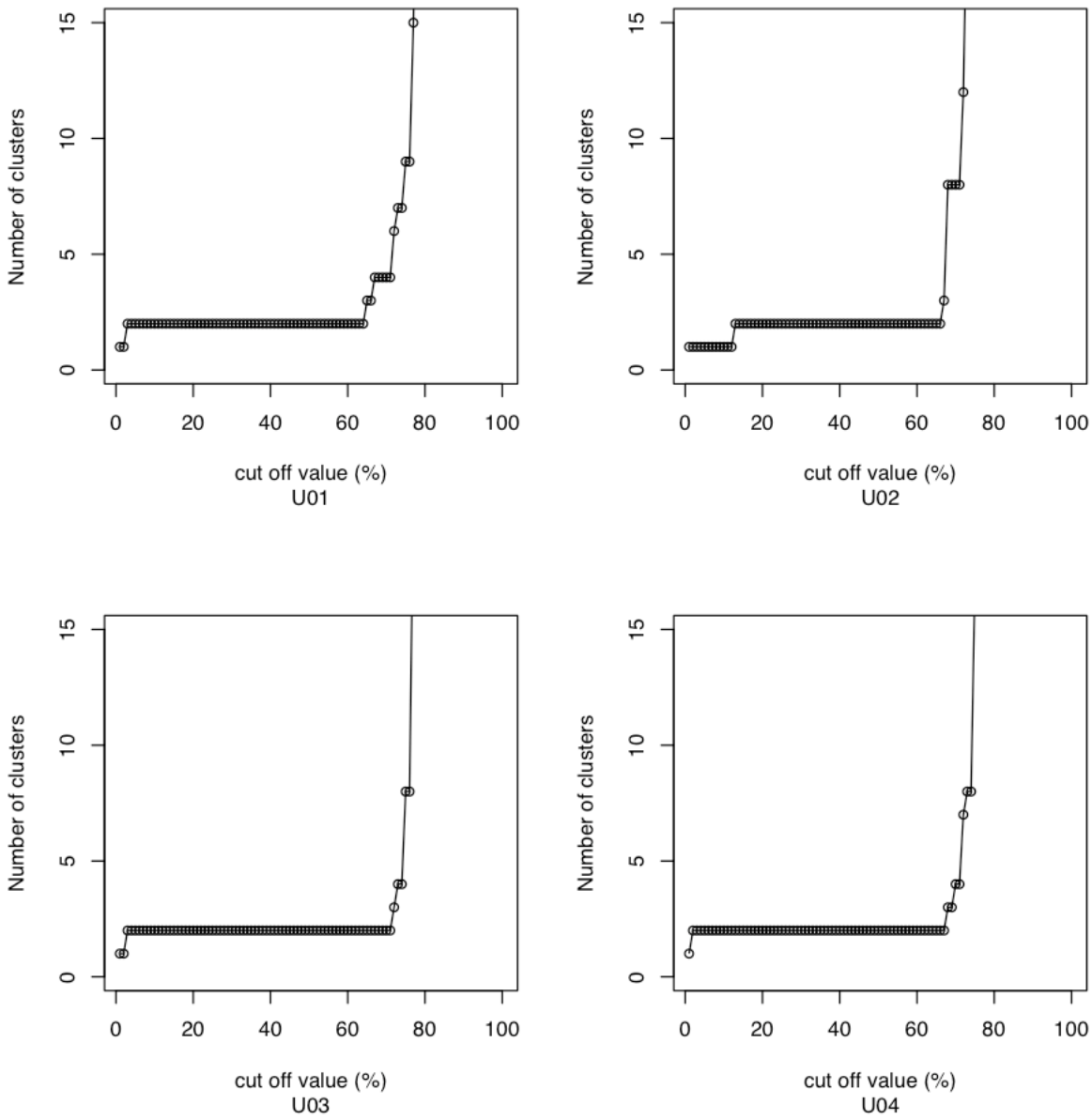

Figure 6. The cut plots for the four horseshoe data sets (U) produced by the K-means multiclustering method with the distribution of D [10,100] and N=60.

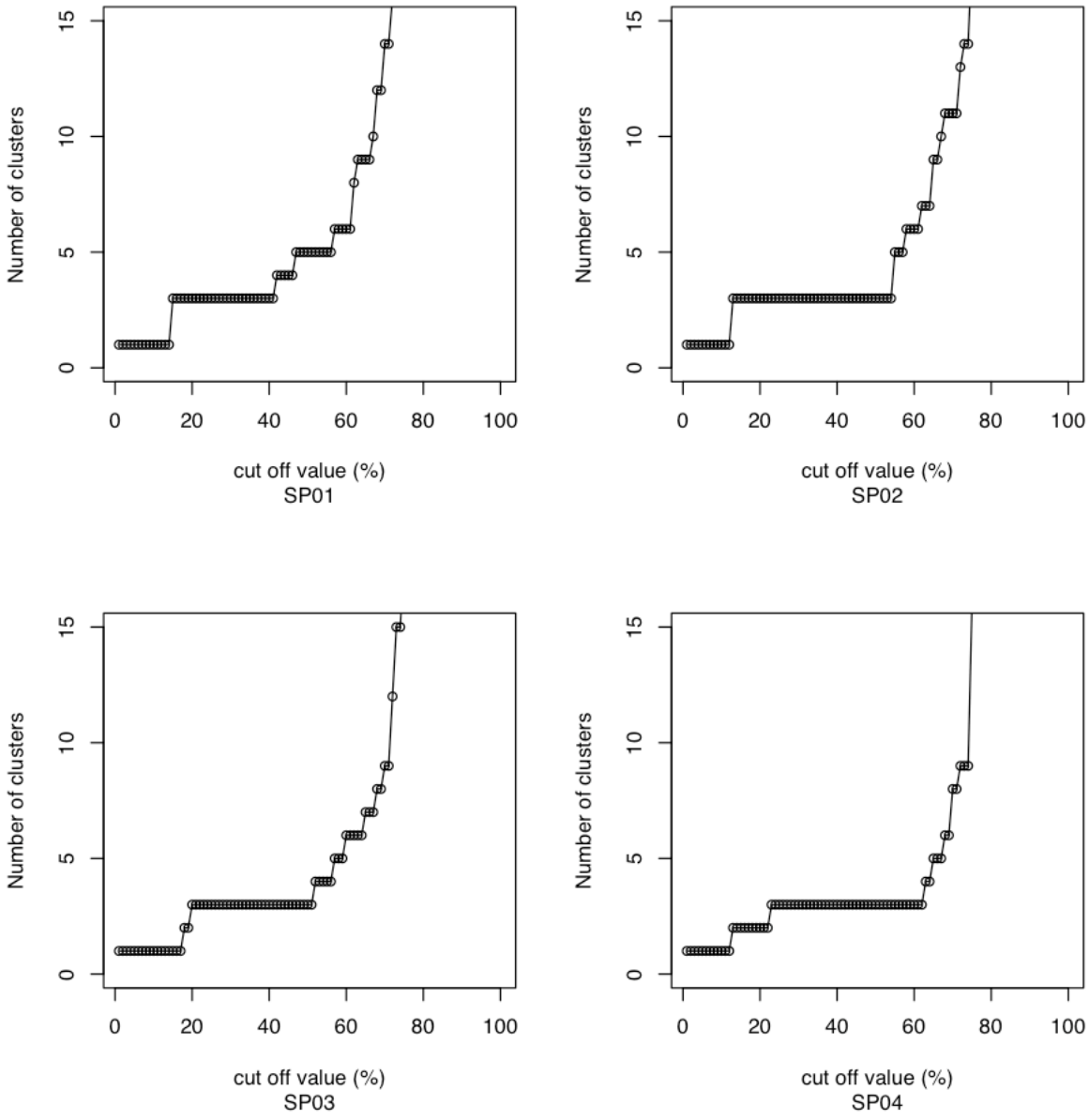

Figure 7. The cut plots for the four spiral data sets (SP) produced by the K-means multiclustering method with the distribution of D [10,100] and N=60.

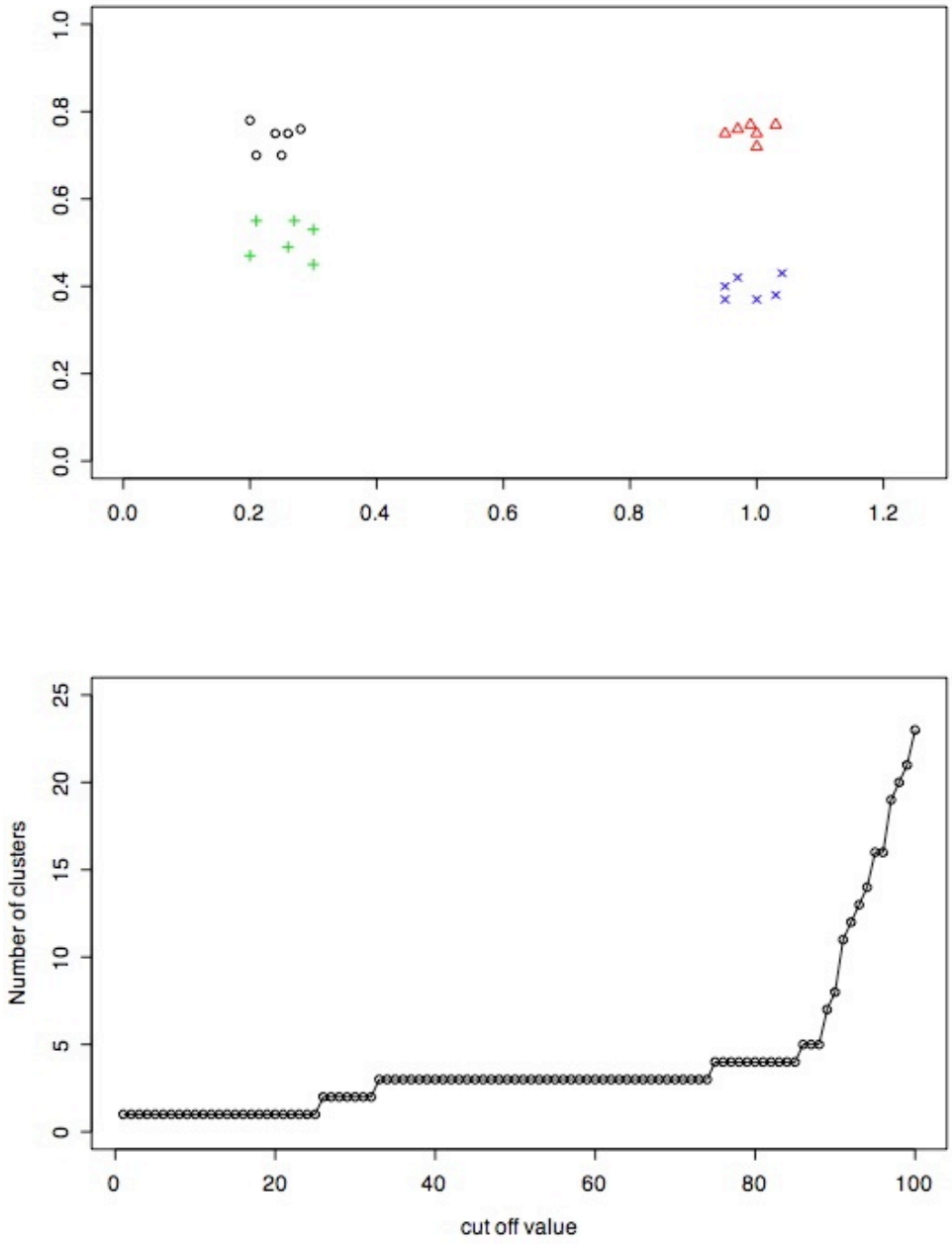

Figure 8. The data set with 25 data points and designed structure of 2, 3, and 4 clusters (upper panel) and its cut plot computed by K-means multiclustering with D [2,7], N=100.

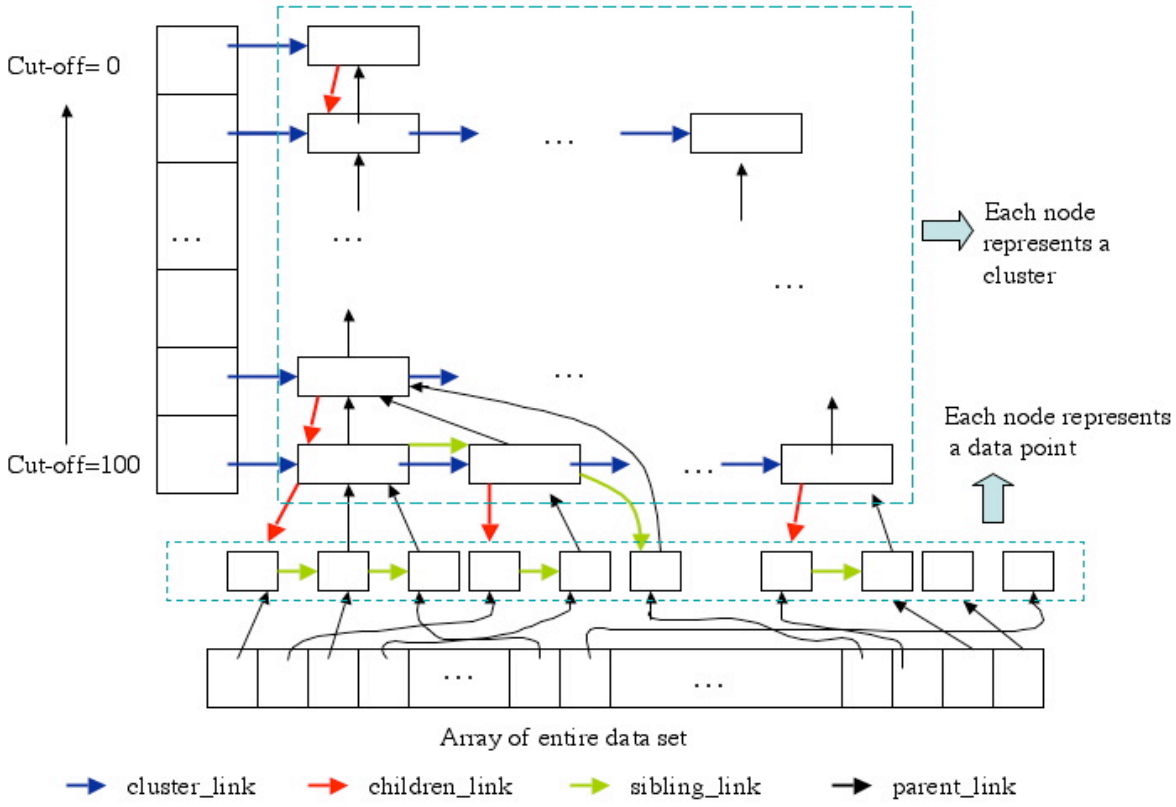

Figure 9. Detailed data structure for building hierarchical tree of clusters generated by K-means multiclustering means algorithm

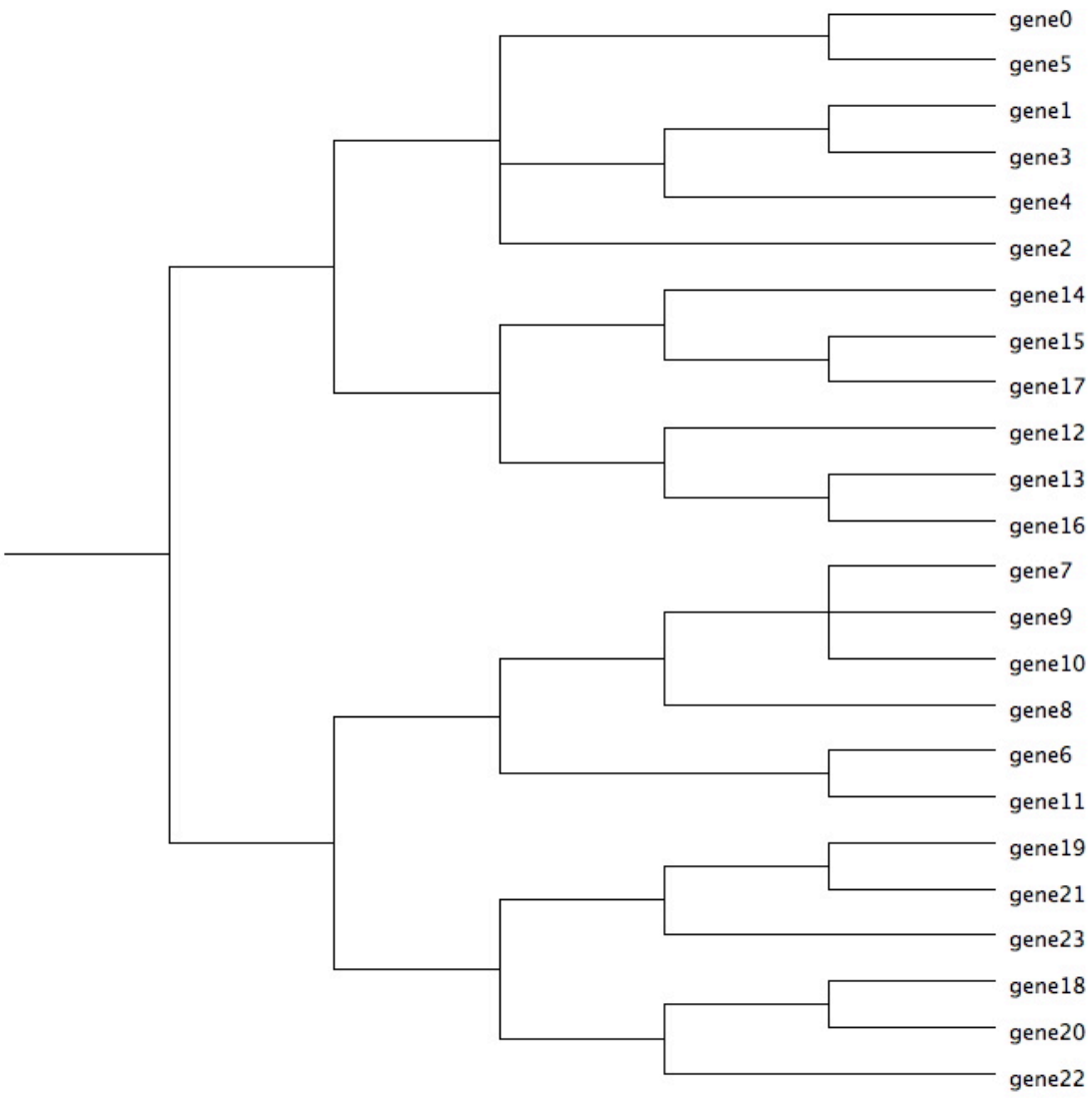

Figure 10. The detailed hierarchical tree view of the synthetic data set with 25 data points in Figure 8.

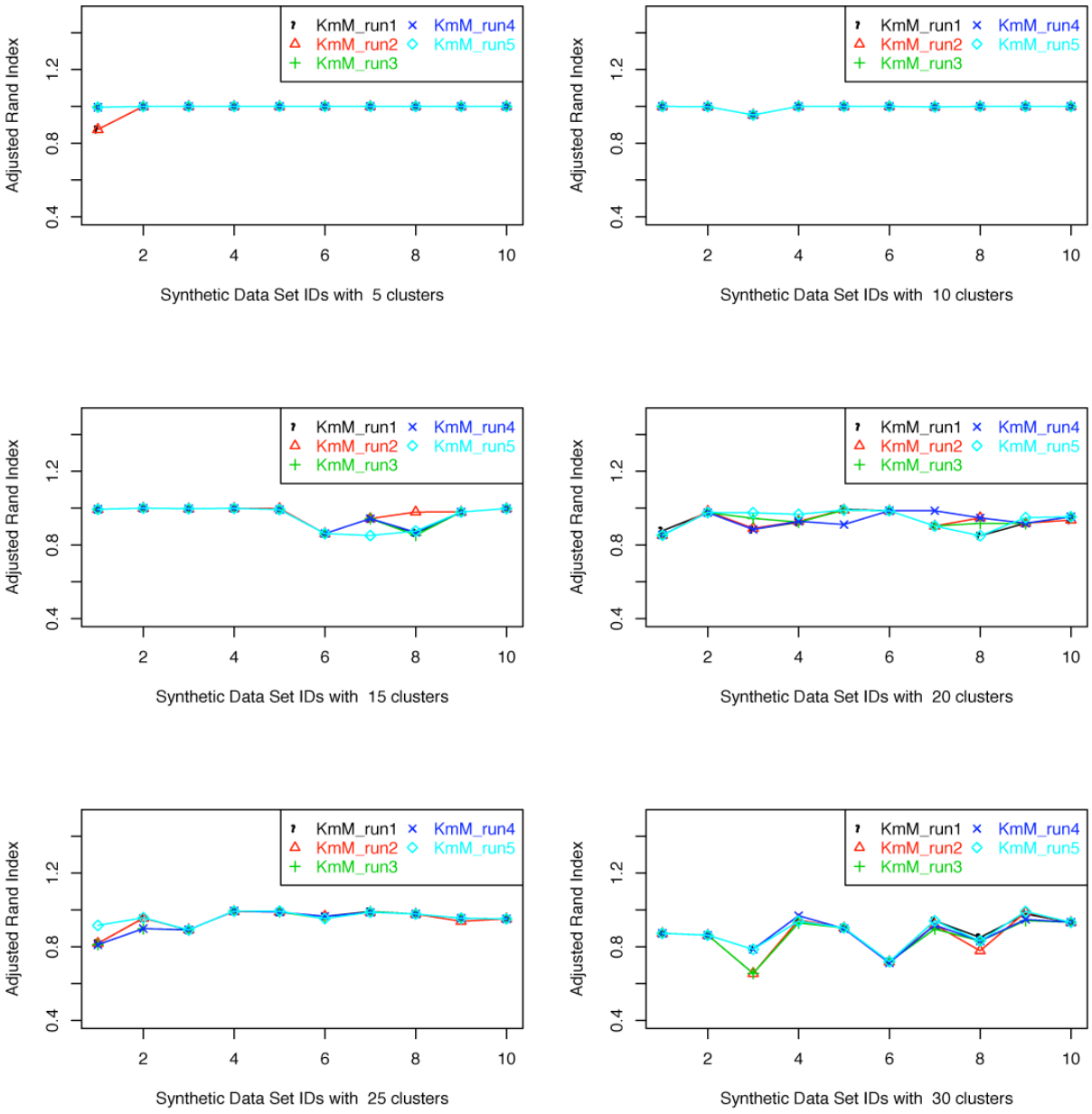

Figure 11. The adjusted Rand Indices (first comparison method) of 5 runs of K-means multiclustering with D [10,100], N=500 on 60 synthetic microarray data sets

Table 5. The average and standard deviation of adjusted Rand Indices (first method) from 5 runs of K-means multiclustering (D [10,100], N=500) on 60 synthetic microarray data sets

Data sets ID	No. of clusters in data sets					
	5	10	15	20	25	30
1	0.947±0.066	1.000±0.000	0.994±0.000	0.858±0.011	0.835±0.045	0.873±0.000
2	1.000±0.000	0.998±0.000	1.000±0.000	0.977±0.003	0.933±0.032	0.863±0.000
3	1.000±0.000	0.954±0.000	0.997±0.000	0.916±0.042	0.892±0.000	0.734±0.071
4	1.000±0.000	1.000±0.000	0.999±0.000	0.934±0.018	0.993±0.001	0.944±0.015
5	1.000±0.000	1.000±0.000	0.993±0.003	0.975±0.036	0.989±0.002	0.902±0.002
6	1.000±0.000	1.000±0.000	0.862±0.000	0.986±0.000	0.960±0.007	0.718±0.003
7	1.000±0.000	0.997±0.000	0.925±0.041	0.920±0.037	0.989±0.002	0.923±0.019
8	1.000±0.000	1.000±0.000	0.888±0.051	0.902±0.049	0.978±0.000	0.825±0.027
9	1.000±0.000	1.000±0.000	0.979±0.000	0.924±0.014	0.952±0.008	0.969±0.023
10	1.000±0.000	1.000±0.000	0.998±0.000	0.946±0.010	0.951±0.000	0.933±0.000

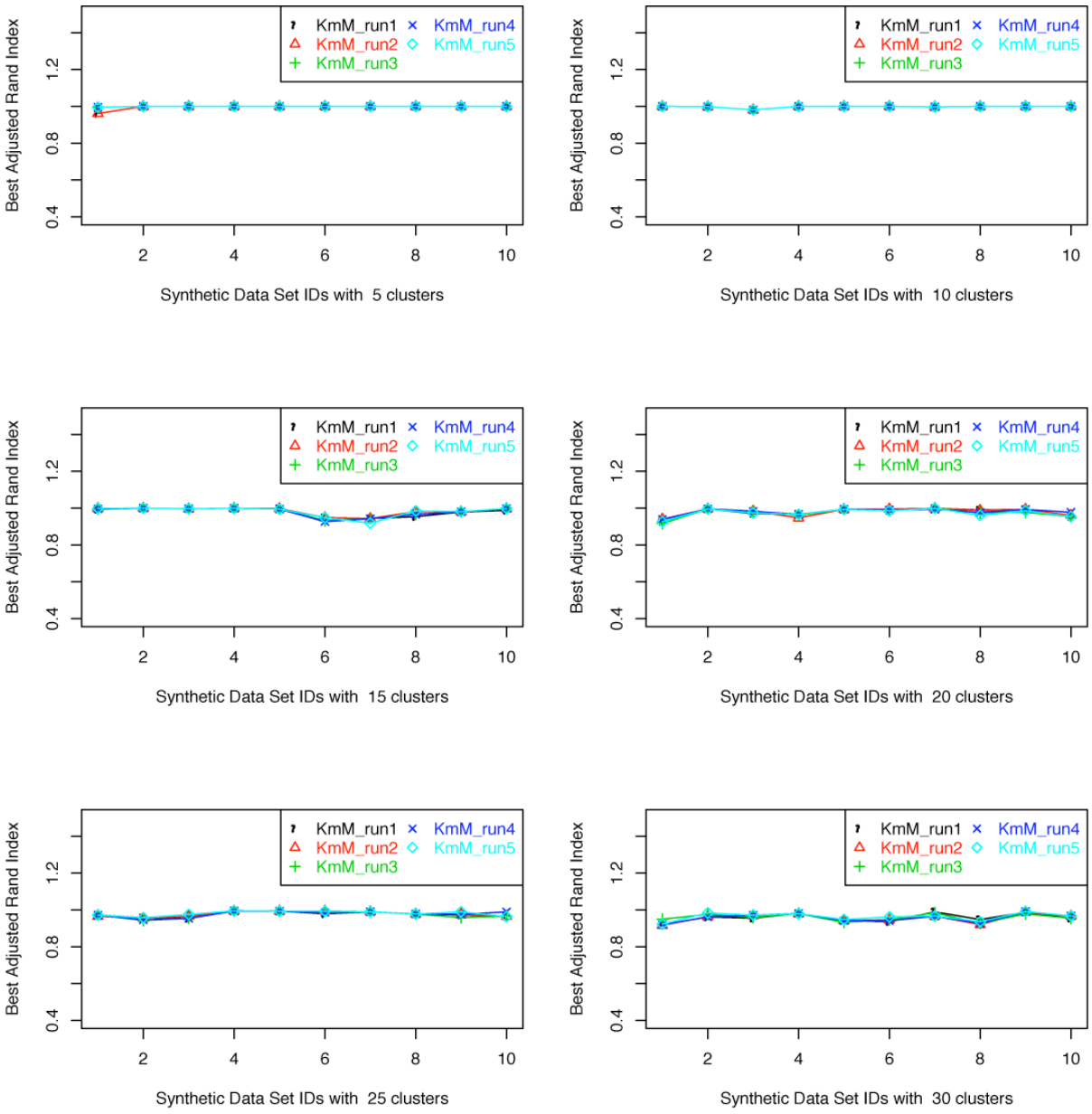

Figure 12. The best adjusted Rand Indices (second comparison method) of 5 runs of K-means multiclustering with D [10,100] N=500 on 60 synthetic micoarray data sets

Table 6. The average and standard deviation of best adjusted Rand Indices (second method) from 5 runs of K-means multiclustering (D [10,100], N=500) on 60 synthetic microarray data sets

Data sets ID	No. of clusters in data sets					
	5	10	15	20	25	30
1	0.982±0.019	1.000±0.000	0.996±0.003	0.930±0.010	0.971±0.003	0.925±0.014
2	1.000±0.000	0.998±0.000	1.000±0.000	0.996±0.000	0.952±0.007	0.969±0.010
3	1.000±0.000	0.981±0.000	0.997±0.000	0.979±0.006	0.961±0.010	0.965±0.007
4	1.000±0.000	1.000±0.000	0.999±0.000	0.962±0.009	0.995±0.001	0.980±0.001
5	1.000±0.000	1.000±0.000	0.996±0.002	0.994±0.000	0.994±0.000	0.941±0.006
6	1.000±0.000	1.000±0.000	0.941±0.010	0.989±0.004	0.989±0.006	0.946±0.010
7	1.000±0.000	0.997±0.000	0.939±0.011	0.998±0.002	0.990±0.000	0.975±0.011
8	1.000±0.000	1.000±0.000	0.971±0.013	0.978±0.011	0.978±0.000	0.932±0.011
9	1.000±0.000	1.000±0.000	0.980±0.001	0.988±0.007	0.974±0.011	0.987±0.005
10	1.000±0.000	1.000±0.000	0.996±0.004	0.960±0.010	0.970±0.011	0.962±0.007

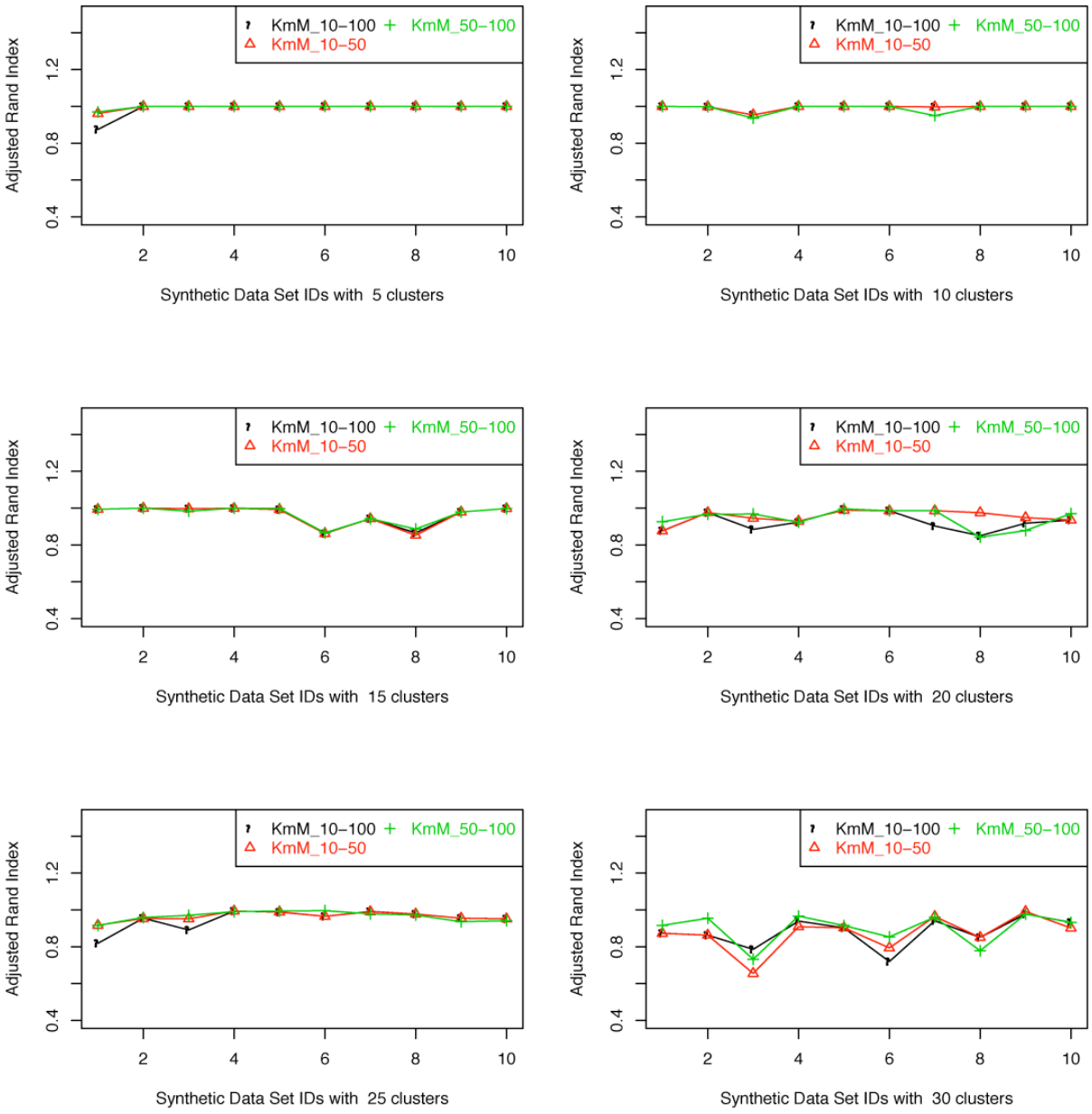

Figure 13. The comparison of adjusted Rand Indices (first method) from K-means multiclustering results with different distribution of D. KmM_10-100 with D [10,100], KmM_10-50 with D [10,50], KmM_50-100 with D [50,100].

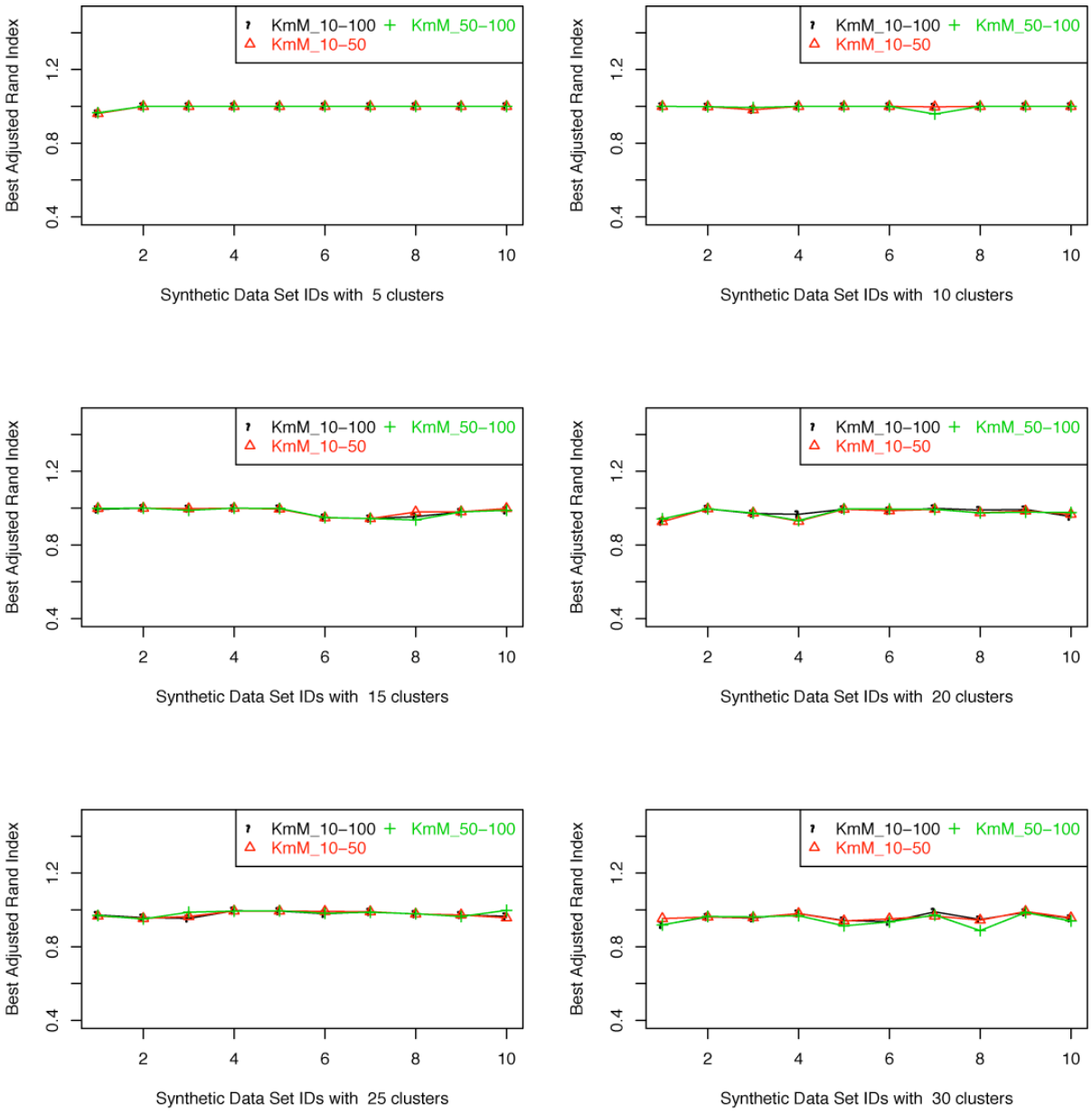

Figure 14. The comparison of best adjusted Rand Indices (second method) from K-means multiclustering results wtih different distributions of D. KmM_10-100 with D [10,100], KmM_10-50 with D [10,50], KmM_50-100 with D [50,100].

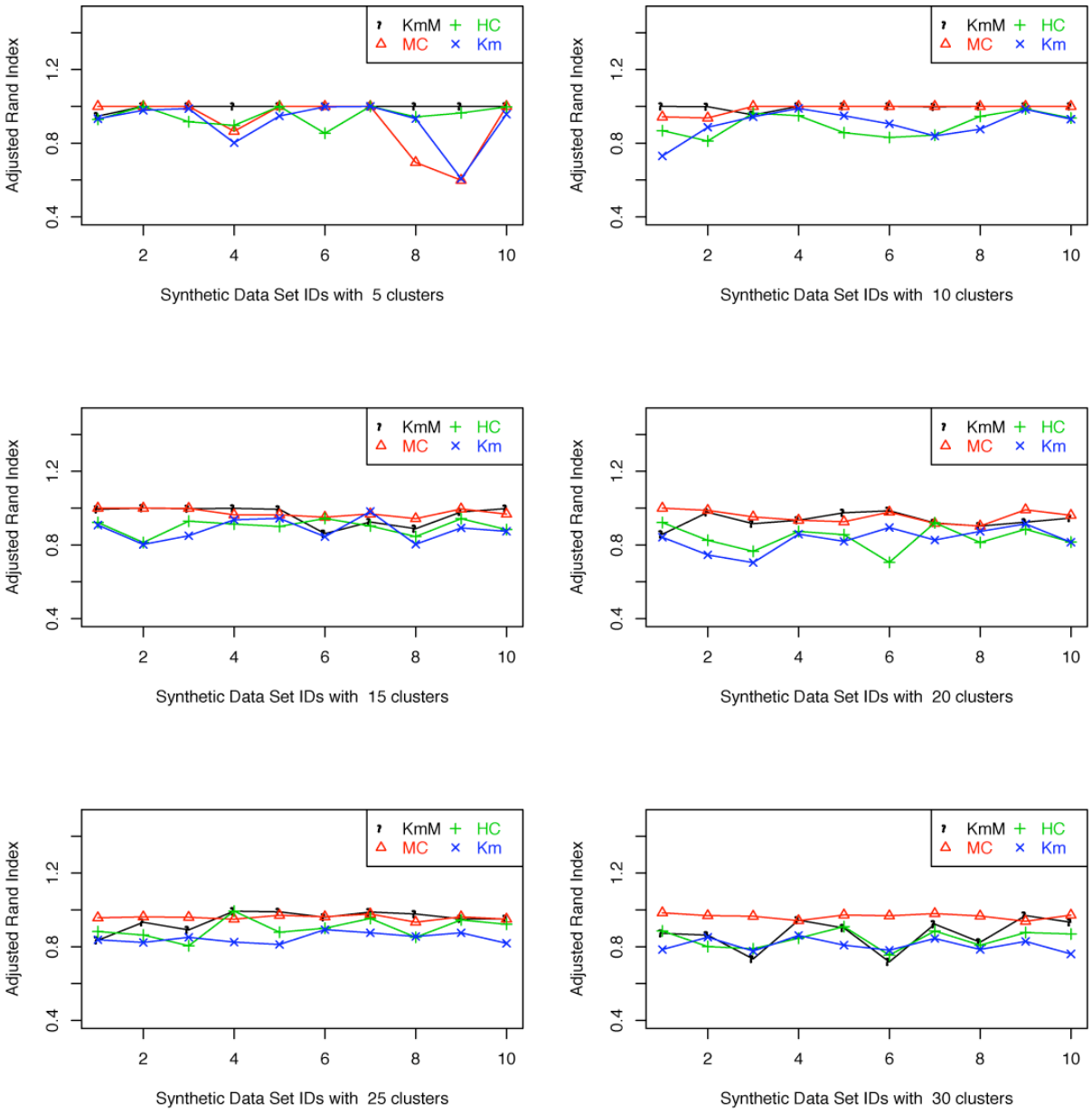

Figure 15. The comparison of performance (first method) of four clustering algorithms. KmM: K-means Multiclustering, MC: Mode-based Clustering, HC: Hierarchical Clustering, Km: K-means Clustering

Table 7. The adjusted Rand Indices (first method) of 60 microarray synthetic data sets from four clustering algorithm

Data sets		K-means multiclustering	Model-based clustering	Hierarchical clustering	K-means clustering
No. of clusters	Data sets IDs				
5	1	0.947	1	0.93	0.933
	2	1	1	1	0.979
	3	1	1	0.916	0.988
	4	1	0.865	0.897	0.802
	5	1	1	1	0.948
	6	1	1	0.854	0.997
	7	1	1	1	1
	8	1	0.696	0.943	0.933
	9	1	0.599	0.964	0.608
	10	1	1	0.997	0.957
10	1	1	0.943	0.868	0.731
	2	0.998	0.937	0.812	0.886
	3	0.954	1	0.963	0.943
	4	1	1	0.949	0.989
	5	1	1	0.857	0.949
	6	1	1	0.831	0.905
	7	0.997	1	0.844	0.839
	8	1	1	0.946	0.877
	9	1	1	0.986	0.984
	10	1	1	0.937	0.931
15	1	0.994	1	0.922	0.908
	2	1	1	0.814	0.803
	3	0.997	0.999	0.929	0.85
	4	0.999	0.964	0.913	0.937
	5	0.993	0.964	0.901	0.944
	6	0.862	0.951	0.944	0.845
	7	0.925	0.969	0.903	0.982
	8	0.888	0.943	0.846	0.804
	9	0.979	0.996	0.943	0.893
	10	0.998	0.968	0.884	0.874
20	1	0.858	1	0.922	0.842
	2	0.977	0.988	0.825	0.746
	3	0.916	0.953	0.766	0.704
	4	0.934	0.935	0.874	0.859
	5	0.975	0.926	0.856	0.82
	6	0.986	0.979	0.706	0.895

Table 7. (continued)

Data sets		K-means multiclustering	Model-based clustering	Hierarchical clustering	K-means clustering
No. of clusters	Data sets IDs				
	7	0.92	0.917	0.921	0.827
	8	0.902	0.903	0.814	0.874
	9	0.924	0.991	0.886	0.914
	10	0.946	0.961	0.816	0.815
25	1	0.835	0.957	0.882	0.838
	2	0.933	0.962	0.864	0.823
	3	0.892	0.96	0.805	0.851
	4	0.993	0.95	0.993	0.825
	5	0.989	0.971	0.879	0.812
	6	0.96	0.963	0.901	0.893
	7	0.989	0.978	0.954	0.876
	8	0.978	0.933	0.852	0.856
	9	0.952	0.963	0.946	0.876
	10	0.951	0.95	0.922	0.819
30	1	0.873	0.984	0.886	0.785
	2	0.863	0.969	0.801	0.852
	3	0.734	0.966	0.789	0.776
	4	0.944	0.942	0.846	0.862
	5	0.902	0.973	0.909	0.809
	6	0.718	0.968	0.754	0.781
	7	0.923	0.98	0.885	0.845
	8	0.825	0.967	0.808	0.785
	9	0.969	0.938	0.877	0.829
	10	0.933	0.972	0.869	0.761

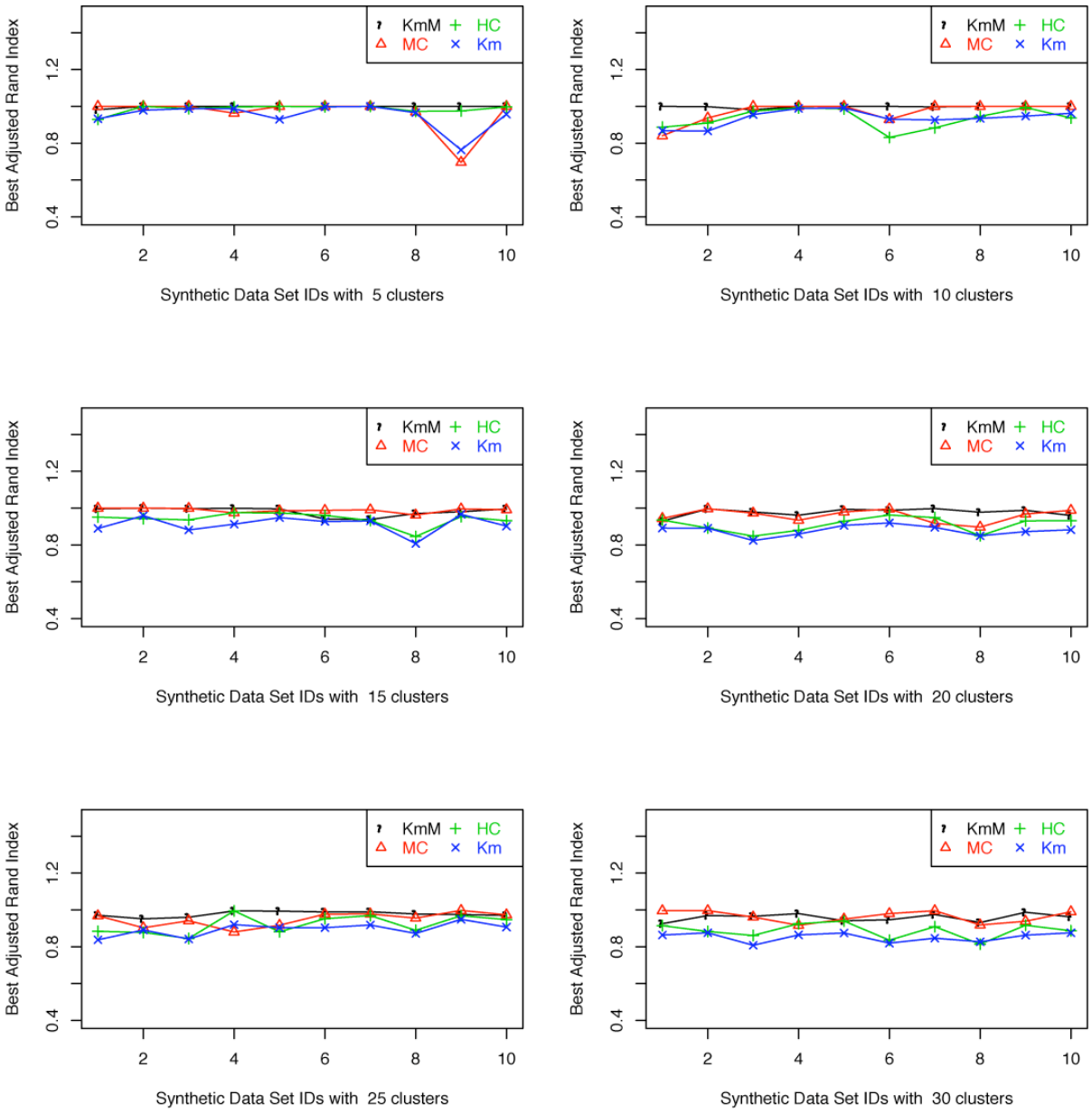

Figure 16. The comparison of performance (second method) of four clustering algorithms. KmM: K-means Multiclustering, MC: Mode-based Clustering, HC: Hierarchical Clustering, Km: K-means Clustering

Table 8. The best adjusted Rand Indices (second method) of 60 microarray synthetic data sets from four clustering algorithms

Data sets		K-means multiclustering	Model-based clustering	Hierarchical clustering	K-means clustering
No. of clusters	Data sets IDs				
5	1	0.982	1	0.93	0.933
	2	1	1	1	0.979
	3	1	1	0.988	0.988
	4	1	0.963	0.997	0.987
	5	1	1	1	0.93
	6	1	1	0.998	0.997
	7	1	1	1	1
	8	1	0.97	0.973	0.966
	9	1	0.696	0.975	0.764
	10	1	1	0.997	0.957
10	1	1	0.841	0.887	0.868
	2	0.998	0.937	0.91	0.866
	3	0.981	1	0.974	0.955
	4	1	1	0.992	0.989
	5	1	1	0.986	0.992
	6	1	0.929	0.831	0.93
	7	0.997	1	0.884	0.927
	8	1	1	0.946	0.935
	9	1	1	0.994	0.947
	10	1	1	0.937	0.963
15	1	0.996	1	0.952	0.89
	2	1	1	0.943	0.959
	3	0.997	0.999	0.936	0.882
	4	0.999	0.974	0.975	0.913
	5	0.996	0.986	0.974	0.949
	6	0.941	0.988	0.96	0.928
	7	0.939	0.991	0.933	0.93
	8	0.971	0.963	0.846	0.808
	9	0.98	0.996	0.954	0.966
	10	0.996	0.992	0.932	0.902
20	1	0.93	0.944	0.935	0.892
	2	0.996	0.997	0.892	0.891
	3	0.979	0.973	0.848	0.824
	4	0.962	0.935	0.88	0.859
	5	0.994	0.979	0.929	0.906
	6	0.989	0.995	0.962	0.92

Table 8. (continued)

Data sets		K-means multiclustering	Model-based clustering	Hierarchical clustering	K-means clustering
No. of clusters	Data sets IDs				
	7	0.998	0.917	0.949	0.896
	8	0.978	0.897	0.85	0.85
	9	0.988	0.968	0.931	0.873
	10	0.96	0.988	0.932	0.883
25	1	0.971	0.968	0.884	0.838
	2	0.952	0.903	0.878	0.891
	3	0.961	0.941	0.845	0.842
	4	0.995	0.88	0.995	0.92
	5	0.994	0.917	0.881	0.904
	6	0.989	0.977	0.952	0.904
	7	0.99	0.978	0.969	0.918
	8	0.978	0.956	0.889	0.872
	9	0.974	0.997	0.969	0.949
	10	0.97	0.973	0.947	0.907
30	1	0.925	0.996	0.915	0.864
	2	0.969	0.996	0.883	0.876
	3	0.965	0.961	0.861	0.808
	4	0.98	0.916	0.925	0.864
	5	0.941	0.95	0.94	0.875
	6	0.946	0.98	0.836	0.819
	7	0.975	0.996	0.909	0.846
	8	0.932	0.918	0.814	0.827
	9	0.987	0.938	0.917	0.863

CHAPTER 3. A NEW INTEGRATED GENETIC AND PHYSICAL MAP OF MAIZE REVEALS CHROMOSOME LEVEL ORGANIZATION OF GENE EXPRESSION PATTERNS

Ling Guo, Hsin D. Chen, Kai Ying, Karthik Viswanathan, Tsui-Jung Wen, Olga Nikolova, Natalja Zazubovits, Scott J. Emrich, Daniel A. Ashlock, Patrick S. Schnable

A manuscript to be submitted to Genetics

ABSTRACT

A high-density genetic map, ISU-IBM Map7, of maize was constructed by integrating ~3,300 existing markers and 4,700 new InDel Polymorphism (IDP) markers derived from genes and predicted genes. Over 1,800 of these IDPs are codominant markers that can be detected via Temperature Gradient Capillary Electrophoresis (TGCE). Because IDP markers are sequence based, they can be used to integrate the genetic and physical maps using sequence similarity rather than hybridization-based approaches. As of February 2007 the maize physical map created by the Arizona Genome Institute (AGI) contained 292,502 BACs grouped into 721 finger print contigs (FPCs) and singletons. As of 2/2/2007 ~6,430 of these had been at least partially sequenced by the maize genome sequencing project. The sequences of 418 FPCs match at least one marker from ISU-IBM Map7 and 322 FPCs match at least two closely linked markers. Sixty-nine of these 322 FPCs had not previously been anchored by hybridization-based approaches. Using this integrated genetic/physical map it was possible to position 2,146 genes from the maize cDNA microarray SAM1.0 on the map.

Analysis of microarray data revealed statistically significant differences in the distribution of strongly and weakly expressed genes across multiple chromosomes. This finding demonstrates the existence of chromosome level regulation of gene expression. All project data are available at: http://maize-mapping.plantgenomics.iastate.edu/.

INTRODUCTION

An integrated high-density genetic/physical map provides a foundation for both basic and applied research in maize (*Zea mays L.*), which is both an important crop plant and a model for genetic studies. Due to the inclusion of four generations of random mating, the B73 × Mo17 (IBM) collection of intermated recombinant inbred lines (IRILs) provides 17 times more mapping resolution than do previous populations (COE *et al*. 2002; LEE *et al*. 2002). Using 302 IBM IRILs the Maize Mapping Project (MMP) constructed a linkage map (IBM2) that contains approximately 2,000 markers (DAVIS *et al*. 1999; SHAROPOVA *et al*. 2002). About 57% of these markers are sequence based (FU *et al*. 2006). More recently (FU *et al*. 2006) produced a genetic map based on 91 IBM IRILs that contains 2,029 of the MMP markers plus 1,329 additional PCR-based, InDel Polymorphism (IDP) markers. All of the IDP markers are based on sequenced genes or gene models.

Three Bacterial Artificial Chromosome (BAC) libraries have been constructed from the maize inbred line B73 (TOMKINS *et al*. 2002; YIM *et al*. 2002), which represents about 27-fold coverage of maize genome. These BACs were assembled into contigs using FPC software (SODERLUND *et al*. 2000). The University of Arizona's July 2005 release of the physical map contained 721 FingerPrint Contigs (FPCs)

(http://www.genome.arizona.edu/fpc/maize/). To integrate the genetic and physical maps, ~10,600 overgo probes designed from EST unigene contigs were hybridized to BACs (GARDINER *et al*. 2004). Although 12% of these overgos hybridized to more BACs than expected for single-copy probes, it was possible to use this strategy to anchor 56% (400/711) of the FPCs to chromosomes.

During the fall of 2005, The Maize Sequencing Consortium began sequencing a dynamically defined minimum tiling path of these BACs. As of Feb. 2007, the sequences of ~6,400 BACs had been deposited into GenBank; ultimately, ~19,000 BACs will be sequenced. Previously, over 1 million maize genomic sequences of maize, including gene-enriched maize Genomic Survey Sequences (GSSs) (PALMER *et al*. 2003; WHITELAW *et al*. 2003) and BAC shotgun reads generated by Consortium of Maize Genomics and random Whole Genome Shotgun (WGS) sequences generated by the Joint Genome Institute (JGI) had been deposited into Genbank. Theses genomic sequences were assembled into Maize Assembled Genomic Islands (MAGIs) with at least 98% of accuracy (EMRICH *et al*. 2004; FU *et al*. 2005). Additionally, over half million of maize expressed sequence tags (ESTs) have been deposited into Genbank.

Using PCR-based approaches we identified gene-associated InDels in these GSSs, MAGIs, and ESTs. These InDels were converted into InDel Polymorphism (IDP) markers which were used to gentoype a panel of 91 IBM IRILs and thereby generate a genetic map of maize that contains >8,000 markers. Because most of these markers are based on defined gene sequences, it was possible to use this map to anchor hundreds of the sequenced BACs and

their FPCs to chromosomes. Using the resulting integrated genetic/physical map it was possible to position 2,146 genes from the maize cDNA array SAM1.0 on the map. Analysis of microarray data revealed statistically significant differences in distributions of strongly and weakly expressed genes across multiple maize chromosomes, suggesting the existence of chromosome level regulation of gene expression patterns.

MATERIALS AND METHODS

The maize lines used in this study are identical to those used by (FU *et al.* 2006)

Sequence sources and batch primer design of ISU IDP markers

A total of 39,490 pairs of PCR primers were designed to amplify genic regions of the maize genome using repeat-masked ESTs, GSSs, MAGIs genomic contigs, or BAC ends sequences (Table 1). All source sequences are available from NCBI GenBank (ESTs, cDNAs, GSSs and BAC ends) or the MAGI webpage.

Primer pairs were designed in a batch mode. The batch primer design pipeline was built around Primer3 (ROZEN and SKALETSKY 2000). A wrapper written in AWK/C++ formats the data to be compatible for Primer3 input and selects primer pairs generated by Primer3 based on different primer design strategies. Primer pairs designed based on ESTs were designed in 3' UTRs, which we defined as 300 bp upstream of the polyA sites. For primers designed based on genomic sequences, gene structures were first determined by aligning the genomic sequences to ESTs using the splice-alignment software GeneSeqer (BRENDEL *et al.* 2004). If no EST alignment was available the *ab initio* gene prediction software FGENESH (http://www.softberry.com), which we had shown to be the most accurate for maize (YAO *et*

al. 2005), was used to predict gene structures. Primers were then designed to amplify introns. Different types of intron-spanning primers were designed to study their effects on rates of PCR success and ability to detect different types of polymorphisms (Table 2).

Special marker design strategies

Synteny between the maize and rice genomes was used to identify markers that could potentially fill gaps in the ISU-IBM Map4 maize genetic map (FU *et al*. 2006). Rice syntenic blocks were identified by using sequences from 3,044 mapped IDP markers that were available at the time of this experiment to query the 61,250 rice protein sequences obtained from The Institute for Genomic Research's (TIGR's) release 3.0 of the rice genome (http://www.tigr.org/tdb/e2k1/osa1/pseudomolecules). For these queries, the original maize sequences used for the design of the 3,044 primer pairs were used, with the exception of 2.31 MAGIs for which updated 3.1 MAGIs were used if available. Matches (BLASTX; e-value <= 1e-10) were filtered against the TIGR GFF annotations such that only annotated gene models were used to query the IDP markers (TBLASTN; e-value <= 1e-10); reciprocal mutual best hits were then used as the basis for further analysis.

As a first step towards filling gaps in the genetic map, the largest gap on each chromosome of the ISU-IBM Map4 was identified. A minimum of four gap flanking markers (two on each side of the gap) were used to define the syntenic region in rice. In a few cases higher identity alignments within putative syntenic regions were used to support proposed syntenic relationships.

To facilitate the integration of the genetic and physical maps, we designed markers that could be linked to unanchored FPC BAC contigs through overgo probes. The FPC contigs and overgo probes were downloaded from http://www.genome.arizona.edu/fpc/maize/ and MaizeGDB and http://www.maizegdb.org/cgi-bin/overgoreports.cgi?id=1 respectively. About 7,246 "low copy overgo probes" (i.e., those that hybridized to ≤ 25 BACs) were used in this study. This process identified 501 MAGI 3.1 sequences that had not previously been used for primer design and that were at least 95% identical (at most 2 mismatches) to low copy overgo sequences which hybridized to BAC(s) from unanchored BAC contigs. Intron-spanning PCR primers were designed from each of these MAGIs.

To include genes that are not identified via methylation filtration (MF) and High C_ot (HC)-based gene enrichment techniques another version of MAGIs, MAGI4, which include random Whole Genome Shotgun (WGS) sequenced by the Joint Geneome Institute (JGI) in addition to GSSs, were used to detect IDP markers for JGI only contigs. About 3,000 primer pairs were designed from those JGI only MAGIs; 220 were found polymorphic.

Agarose gel electrophoresis and TGCE genotyping

Primer pairs were used to amplify B73 and Mo17 genome DNA using our standard PCR conditions (FU *et al.* 2006). PCR products were analyzed via agarose gel electrophoresis to identify polymorphisms between B73 and Mo17 as described by (FU *et al.* 2006). Primer pairs that generated amplicons from both B73 and Mo17 that could not be distinguished based on size via agarose gel electrophoresis were subjected to Temperature Gradient Capillary Electrophoresis (TGCE) (HSIA *et al.* 2005) in an effort to detect SNPs and small

InDel polymorphisms between B73 and Mo17. The accuracy and efficiency of TGCE was improved by use of the GRAMA software (MAHER *et al*. 2006), which automates the analysis of TGCE-derived genotyping data. All markers were used to genotype the same 91 IBM IRILs as analyzed by Fu et al. 2006. The resulting polymorphism and mapping data are available at the project webpage (http://maize-mapping.plantgenomics.iastate.edu/).

Construction of ISU-IBM Map7

Genotyping scores for 8,076 markers were available from the 91 IBM IRILs. Of these, 2,046 (25%) that had been generated by MMP were downloaded from MaizeGDB (http://www.maizegdb.org/map.php). The remaining 6,030 (75%) markers were generated by the ISU maize genetic mapping project (http://maize-mapping.plantgenomics.iastate.edu/) as described above and by Fu et al., 2006. Sixty of the MMP markers were removed because genotyping data were missing for over 20 of the 91 IRILs. An additional 117 ISU/MMP markers that had B73/Mo17 segregation ratio over 2.75 were also excluded from this study. To simplify map construction, 2,288 markers that had the same genotyping score as other markers were temporarily removed during map construction, but subsequently re-incorporated into the final map.

The genotyping scores for the 91 IBM IRILs of the remaining 5,611 markers were analyzed using the Multi-Point mapping software package (http://www.multiqtl.com, (FU *et al*. 2006; MESTER *et al*. 2003; MESTER *et al*. 2004). To construct ISU-IBM Map7, the ISU-IBM Map4 was used as a framework. There are two types of markers on ISU-IBM Map7: skeleton and muscle markers. Skeleton markers had stable orders based on 1,000 jackknife runs. In

contrast, muscle markers had unstable local ordering, but their approximate positions relative to skeleton markers are correct with a high level of certainty (Fu et al. 2006).

The estimation of centromere positions and the calculations of genetic distances in centimorgans are as for ISU-IBM Map4 (FU *et al.* 2006). The 441 ISU/MMP markers that could not be placed into any of the 10 large linkage groups using the Multi-Point mapping software package and 1,590 additional markers from FALQUE *et al.* 2005 were linked to markers on ISU-IBM Map7 using U-Map-It, a software tool that links a new marker to existing markers on a genetic map by comparing sets of genotyping scores (FU *et al.* 2006).

Calculation of genetic distances in an F_1BC population

The genetic distances that separate a pair of randomly selected codominant markers that based on Map7 are separated by distance of 4-10 cM on for each chromosome were determined in an F_1 backcross population (F_1BC). This F_1BC population was produced by backcrossing an F_1 derived from the cross of the inbred line B73 (Schnable lab accession #660) and Mo17 (Schnable lab accession #3532) to Mo17. These inbred lines were originally obtained from Donald Robertson (Iowa State University) and Paul Scott (USDA-ARS/Iowa State University), respectively. DNA was extracted from 372 F_1BC seedlings. PCR reactions were conducted to analyze the genotypes of the 10 pairs of markers in the F_1BC seedlings; the resulting amplicons were analyzed via agarose gel electrophoresis. The recombination rate associated with each pair of markers was obtained and the genetic distance computed using the Haldane function (HALDANE 1919). DNA extraction, PCR extraction and genotyping were conducted as described previously (FU *et al.* 2006).

Confirmation of the sequence sources of ISU markers using e-PCR

Because of the possibility of non-specific amplification, it is important to confirm that the sequences that had been mapped are the genes used for PCR primer design. It was also desirable to link the mapped genes to maize genomic sequences and ESTs. Two versions of the assembled maize GSSs MAGI3.1 (EMRICH *et al*. 2004; FU *et al*. 2005) and MAGI4 and assembled maize EST sequences MEC98 (http://magi.plantgenomics.iastate.edu/downloadall.html) were used for this purpose. All genomic and EST assemblies and assembly criteria are available online (http://magi.plantgenomics.iastate.edu/downloadall.html).

To be confident about the links between PCR-based markers and target sequences, the sequences of the PCR primers should match the target sequences in correct orientation and the observed product sizes should match the size expected based on the target sequence (ePCR). Primer sequence matches were conducted by aligning the sequences of PCR primer pairs to a target sequence. Based on the degree of sequence identity required for PCR primers to amplify a template, the criteria for primer sequence matches were: 1) the first 3 bp at the 5' end of primer sequences were ignored; 2) the 3 bp at the 3' end of primer sequence were required to perfectly match the target sequence; and 3) at most 2 mismatches were allowed in the remainder of the primer. A sequence was considered as a match for a pair of PCR primers if the forward and reverse primer sequences aligned to the target sequence satisfying the criteria and in the right orientation. Product match was to check if the observed product size of the mapped polymorphic band of the gene matched the predicted product size obtained based on the position of the PCR primer of a gene on a target sequence. The observed product sizes of the mapped ISU IDP markers were collected from PCR gel

electrophoresis. The predicted product size was computed based on the alignment positions of forward and reverse primer sequences on a target sequence.

A MAGI3.1/MAGI4 sequence was considered as the confirmed sequence source of a marker if the difference between predicted and observed sizes of the PCR product was less than 10% of the observed product size. If a MEC sequence could be aligned by GenSeqer to a MAGI3.1/MAGI4 that was a confirmed source of a marker, and if the primer pair sequences of that marker could be found in the MEC by the sequence match criteria explained above, then this MEC was considered as the expressed sequence source of that marker.

If a confirmed MAGI3.1/MAGI4 source could not be identified via the approach described above for a mapped ISU marker that had a B73 PCR product, the original primer design source was checked. In the case of markers for which the original design source was an EST sequence, the existence of introns make it difficult to accurately predict the size of the genomic PCR product using alignment of the primer pair to the EST sequence. An acceptable criteria used was that expected size should less than or equal to observed size plus 15% of observed size; or the original primer design source was of the genomic origin (like BAC Ends, GSS, some well studied genes, and MAGI2.31), the same criteria as above were used. If the predicted size matched the observed size then the original design sequence was considered as the confirmed sequence source of the marker. If an EST sequence was the confirmed sequence source of a marker, then the MEC in which this EST was a member was also considered as the confirmed expressed sequence source of that marker.

Link sequenced BACs to markers on ISU-IBM Map7

As of Feb 2nd 2007, 6,430 BAC sequences were downloaded from NCBI. The same e-PCR criteria as above were used to link BACs to 6,030 ISU markers. To link BACs to MMP markers on ISU-IBM Map7 at sequence level, the original sequences of 785 MMP markers were found and downloaded from MaizGDB and MMP project webpage (http://www.maizemap.org/bioinformatics.htm). GMAP (http://www.gene.com/share/gmap/) was used to align BACs sequences and the sequences from which the MMP markers derived. If the sequence alignments were at or above 95% of identity with over 80% of coverage of the MMP marker sequences, the BACs were linked to the corresponding MMP markers.

Link microarray information to genetic map

There is a set of 3 SAM cDNA microarray chips (SAM1.1, SAM2.0, SAM3.0) made by ISU Plant Science Institute, Center for Plant Genomics Microarray Facility (http://schnablelab.plantgenomics.iastate.edu:8080/madi/home.do). The EST sequences on those chips were resequenced to confirm. To link the mapped markers on ISU-IBM Map7 to those spots on chips, the confirmed genomic sequences of markers were aligned to the EST sequences on chips by GMap. If the alignments have 95% in similarity and cover over 80% of EST sequences, the connections between microarray spots to mapped markers were accepted. Markers with EST sources were linked to spots if both of the source EST sequences were in the same MEC p95 contig.

Gene expression patterns along the chromosome

The 13,999 informative spots on SAM 1.1 (GPL 2613) maize cDNA array chip (SWANSON-

WAGNER *et al*. 2006) were analyzed. Nine biological replications in a loop design, including all pair-wise comparisons among three genotypes (B73, Mo17, and F_1: B73xMo17) and two dye channels (Cy3 and Cy5) resulted in 18 expression values per informative spot. The quantile normalization method was applied to the background corrected raw signal for every spot on the chip. Genes were sorted by the average value after normalization and divided into two groups - the bottom 25% and top 25% genes that were termed weakly and strongly expressed genes, respectively. Those genes that could be linked to the ISU-IBM Map7 from the weakly and strongly expressed gene sets were extracted. The Kolmogorov-Smirnov (K-S) test (SMIRNOV 1939) was used to compare the distributions along each chromosome of the weakly and strongly expressed gene sets.

Data management, presentation and sharing

ISU-IBM Map7 was made available for public use via the MAGI website. A graphical view of Map7 is available using CMap (http://www.gmod.org/CMap). The MAGI website also permits users to browse and search Map7 markers by chromosome or polymorphism type and to view each marker's PCR primer and design details. Users can search for mapped sequences based on MAGI or MEC sequence IDs, or alternatively can blast against markers design source sequences and related sequences to determine if their query sequence has been mapped. Internally, a relational database was used to organize, store and manage these and related project data. This database includes marker information such as PCR primers, primer design strategy, gel electrophoresis and TGCE-based PCR survey results, genotyping results, and markers relation to other original design sequences. This database was also used to

easily identify target sequences for primer design strategies and prevent designing duplicate primers from same source.

RESULTS

Identification of codominant markers with small indels using TGCE technology

Bhattramakki et al. reported that 53% of 502 investigated loci contained indel polymorphisms between B73 and Mo17. Over 80% of these indels had lengths of ≤ 3 bp that can not be detected by agarose gel electrophoresis. To identify and add more markers to our genetic map, a new technology, TGCE, was utilized. TGCE is a sensitive and reliable technology that is able to identify a single SNP in amplicons of > 800 bp and 1 bp indels in amplicons of ~ 500 bp (HSIA *et al*. 2005). Not all primers were subjected to the TGCE survey, but of those that did, only those that exhibited a single peak for both B73 and Mo17 samples and multiple peaks for the mixed sample of B73 and Mo17 were select for genotyping. Hence, all TGCE markers are codominant. Codominant markers are more informative than dominant markers, because they can distinguish heterozygotes. On average for every 100 primer pairs surveyed via agrarose gel electrophoresis, only identified 3.2 exhibited size polymorphisms, while TGCE technology discovered 7.2 more codominant polymorphisms that can not be detected by gel electrophoresis. This adds about 1.5 times more valuable codominant markers and amounts to about one-third of all the polymorphisms found in this study (Table 1). The 2.2-fold higher rate of codominant polymorphisms detected by TGCE than agrarose gel electrophoresis may reflect that the polymorphism fragments that could be amplified from both B73 and Mo17 were relatively conservative

between B73 and Mo17, therefore they are more likely to have small variation that can be detected by TGCE than large variation that can be detected by gel electrophoresis.

Different intron spanning primer design methods

For intron spanning primers, five different types of primers (Table 2) were designed based on the different positions of the primers on gene structures. The types of primer pairs were defined by two letters that indicated the positions of the forward and reverse primers on the gene structure. If a primer was on an exon, that primer was called an E primer; if on an exon-intron boundary, it was a B primer; if it was on a region without any evidence of exon, which means no EST or FGENESH support, it was an O primer. EB primer pairs mean that one primer was on exon and another primer on exon-intron boundary. The EE primer pairs had the highest TGCE based polymorphism rate (10.9%), and OO primer pairs had the highest gel based polymorphism rate (29.1%). The reason for the high gel base polymorphism rate of OO primer pairs was not clear, it could due to the small sample size. It is also interesting to observe that the primer pairs with at least one O primer had a higher rate of gel based B73 presence/Mo17 absence polymorphism than those without O primer pairs. For primer pairs with at least one primer on an exon, both the gel based and TGCE base polymorphism rates of EB primers were lower than that of EE and EO primers. The primer pairs with one B primer always had lower gel based size polymorphism than primer pairs without B primer. Based on this analysis, PCR primer pairs with primers on exon-intron boundary could lower the chance to find size polymorphism.

MITEs and codominant markers

Our previous analysis of 15 codominant markers that could be detected via agarose gel electrophoresis whose PCR product of B73 and Mo17 differed in size at least 100 bp indicated that 80% (12/15) were associated with annotated or predicted miniature inverted-repeat transposable elements (MITEs) (FU *et al.* 2006). We therefore hypothesized that designing primers flanking MITEs would increase the frequency of codominant markers. To test this hypothesis, the original sequences from which all of the 39,343 primers designed by the project were aligned to 816 MITEs downloaded from The Institute for Genome Research (TIGR) maize repeat database v4.0 (http://maize.tigr.org/repeat_db.shtml). A total of 94 primers were found to flank MITEs. Twenty-six of these 94 primers detected polymorphisms (27.6%) that could be detected via agarose gel electrophoresis, of which 10 (10.6%) were size codominant polymorphisms and 16 (17%) were presence/absence dominant polymorphisms. As compared to the overall rate of gel-based polymorphisms (Table 1), the MITEs flanking primers have 2.7 times more (27.6% vs. 9.8%) size polymorphisms and 3.3 more (10.6% vs. 3.3%). Hence, as predicted by Fu et al. (2006) designing primers that flank MITEs substantially increases the probability of finding polymorphisms, that can be detected via agrarose gel electrophoresis.

A refined maize genetic map

Our high throughput maize genetic mapping project generated 6,030 IDP markers based on sequences with evidence of being genes, most of which are PCR based IDP markers. Along with the 2,046 MMP markers, we are able to build a high density genetic map. 177 (2%) markers were removed due to the large numbers of missing values in the data (≥ 20) or

extreme segregation ratios (≥ 2.75) A total of 7,458 (92%) markers were mapped on ISU-IBM map7 (Table 3).

441 (5.5%) markers could not be placed into any of the 10 large linkage groups by MutiPoint mapping software package. 334 of these markers could be linked to markers on the ISU-IBM Map7 using U-Map-It software (methods) to identify their approximate positions on Map7. Falque et almapped 1,056 candidate gene loci using the IBM IRILs. Along with other markers, there are 1,590 IBM markers with mapping scores. Since RFLP was mostly used, which used 81 or 85 IRILs for genotyping (FALQUE *et al*. 2005), these markers that are considered as containing too many missing values when compared to ISU genotyping data with 91 IRILs would have difficulty in finding accurate position and were not included in the construction of the primary genetic map using MultiPoint mapping software. Out of the 1,590 markers, U-Map-It was able to link 1,527 markers to markers on ISU-IBM Map7 to estimate their approximate position on Map7.

Comparing to the earlier released ISU-IBM Map4, the current ISU-IBM Map7 has over twice as many total markers (7,458 vs. 3,358) and landmarks (1,648 vs. 857). Of the total markers, 77% (5,719) are ISU IDP markers and 23% are MMP markers (1,738).

The total chromosome length of Map7 is 92 cM longer than that of Map4 (1,883 cM vs 1,788 cM, Table 4). The average interval between markers on Map7 is shorter (1.1 cM on Map7 vs. 2 cM on Map4) and the largest interval between markers on each of 9 chromosomes of Map7 is also smaller than those of Map4 (Table 4).

In an effort to identify how much Map7 was extended on both ends of each chromosome as compared to Map4, the 20 terminal markers shared by Map7 and Map4 at both ends of each of the 10 chromosomes were identified. The genetic distances from the shared terminal markers to their corresponding chromosome ends were calculated and compared (Table 4). For the short arm ends, Map7 is 24.5 cM longer than Map4 and chromosome 6 of Map7 is extended by 8.4 cM. The long arm end of chromosome 5 on Map7 is 35.7 cM shorter than that on Map4. Also note that the total chromosome length of chromosome 5 on Map7 is 38 cM shorter than that of Map4.

Of the 1,427 ISU markers on ISU-IBM Map4, 1,327 (93%) were also included in Map7. The orders of these shared markers are generally quite consistent between the two maps. Most of the markers (73/100) that were included in Map4 but were not used for the construction of Map7 were excluded due to quality check failure, the removal of internal quality control markers from Map4, and the exclusion of markers with segregation ratios over 2.75. 15 out of the remaining 27 (56%) markers that could not be placed on Map7 were located on the long arm end of chromosome 5 of Map4 that is missing on Map7.

Confirmation of the genomic and EST sequence sources of ISU markers on ISU-IBM Map7

Currently the maize genome sequencing projects are generating hundreds and thousands of sequences from B73 inbred lines. Linking the ISU IDP markers to these sequences would be of great use to maize community. To identify the sequence source of ISU mapped markers, we selected 5,442 mapped markers (95% of total) that had B73 products to verify the related

B73 genomic sequences and ESTs, which were markers with Size, B73+/Mo17- and TGCE polymorphic type, i.e., only markers with B73-/Mo17+ polymorphisms were excluded. There are 4,916 (81.5% of all the mapped markers) markers that were able to identify sequences that had predicted a product size match observed product size as prescribed in material and methods. A web interface was built to allow user to BLAST the confirmed sequence sources of all the markers to discover if the genes of interest have been mapped, and if so, their map positions, and other information about the corresponding markers.

Filling genetic map gaps using rice synteny to derive maize markers

Among 3,044 maize IDP markers, 1,278 had a significant match to at least one non-transposon protein of rice that was deemed orthologous with maize using a reciprocal best hit criterion (materials and methods). Using this information it was possible to identify clear syntenic blocks corresponding to the largest gap on each of four of the ten maize chromosomes (Table 5). Using the two maize markers flanking each gap, a total of 769 rice protein sequences were extracted, of which 325 had maize orthologous MAGIs determined using reciprocal best hits.

Twenty-five markers derived from those 325 MAGIs were successfully mapped on ISU-IBM Map7 using gel-based methodology (Table 5). Six are within the predicted region, two per chromosome except chromosome 5. Interestingly, there were 11 markers designed based on the largest gap on chromosome 5, seven of those were mapped to a contiguous interval of 7.8 cM on chromosome 4. e-PCR successfully matched six those markers to BACs from FPC BAC contig 182 which was anchored to chromosome 4 (Table 5). All evidence indicates that

the gap filling markers designed based on chromosome 5 on ISU-IBM Map4 actually map to chromosome 4. A similar interesting case was found on chromosome 9. There are six rice-based maize markers are predicted to be on chromosome 9, 2 markers were mapped to the expected position, the remaining four mapped to a very short interval on chromosome 1 and one of those 4 markers could be matched to FPC BAC contig on chromosome 1 by e-PCR. This suggests that either that region has been translocated or that these orthologous genes have been lost during recent diploidization of the maize genome. Failure of mapping those chromosomes 5 gap filling markers to chromosome 5 may partially due to the fact that the gap position on ISU-IBM Map4 that is close to the long arm telomere which is missing from chromosome 5.

Genetic distances in F_1BC and IBM populations

The genetic distances between 10 pairs of markers (one pair per chromosome) were determined in the F_1BC (Methods). Although the genetic distances of these 10 pairs of markers differ in the F_1BC and the IRILs, the correlation between the distances from the two populations is statistically significant ($r=0.675$; p-value = 0.03). Genetic distances between the same genes vary in different genetic backgrounds (YANDEAU-NELSON *et al*. 2006; YAO and SCHNABLE 2005).

Utility for QTL mapping

To test the utility of the high density ISU-IBM Map7 in QTL mapping, 13 QTL regions previously associated with variance in the cell wall composition in the IBM population using MMP data (HAZEN *et al*. 2003) were positioned on ISU-IBM Map7 using flanking markers.

The numbers of markers within the QTL intervals on Map7 were compared to those within the corresponding intervals of the IBM2 map (Table 6). The ISU-IBM Map7 has 2 to 20 fold more markers within each QTL interval as compared to the IBM2 map. In addition, using the sequence-based ISU markers it was possible to link 4 to 28 sequenced BACs to each QTL interval. These additional sequence-based markers and linkages to sequenced BACs will facilitate the identification of causative QTLs.

An integrated genetic and physical map of the maize genome

Previously, overgo probes derived from 10,600 unigenes were used to hybridize to high-density BAC filters (GARDINER *et al*. 2004) containing clones from three BAC libraries which provide a theoretical 2- fold coverage of maize genome (COE *et al*. 2002; CONE *et al*. 2002; TOMKINS *et al*. 2002; YIM *et al*. 2002). Overgo hybridization data were download from the MMP website. Of the 16,316 overgo probes, 15,123 hybridized to one or more BACs. This indicates that about 7.3% (1,193/16,316) of overgo did not hit a BAC, i.e., about 7.3% of genes were not covered by BAC libraries. The overgo probes that hit ≤ 25 BACs were termed low copy overgo probes. The hybridizations of low copy overgo probes to BACs were considered to be real hybridization. There are 12,871 low copy overgo probes, of which 12,421 hit BACs and 450 hit BACs that failed to assemble into FPC contigs. So about 3.6% (450/12,421) of low copy overgo hit BACs that are not in FPC contigs, and about 2.7% of BACs that have good fingerprints but are not in FPC contigs.

Of the 6,430 sequenced BACs downloaded from NCBI as of Feb. 2007, 1,969 BACs were hit by 2,208 ISU IDP markers and 367 MMP markers. There are 1,570 BACs hit only by ISU

markers, 131 hit only by MMP markers and 236 BAC hit by both. These BACs were from 418 FPC contigs of which 50 were not anchored before. Supplementary table 1 shows the detailed anchoring information of all 418 BAC contigs. About 80% (334/418) of the BAC contigs were hit by two or more markers. If a BAC was hit by multiple closely linked markers whose genetic distances were less than 30 cM, the BAC was considered be anchored by those closely linked markers. There are total of 322 BAC contigs (77%) can be anchored, of which 18 were not anchored before and one BACs could be anchored by combining our anchoring information with that from MMP. For the 304 BAC contigs that were anchored by Maize Mapping Project, 16 BAC contigs were anchored to different positions than before. Out of the 16 BACs, 6 were hit by multiple markers of which some markers were not consistent with the majority closely linked markers by our procedure, but consistent with the anchored positions by MMP; 2 BACs were anchored to positions that were consistent with the minority of the MMP anchoring evidence. For the 31 BAC contigs that couldn't be anchored before and in our study the markers we found that could be linked to those BAC contigs would be valuable information for further anchoring of those BACs.

Genetic map and functional genome

By linking markers on ISU-IBM Map7 to spots on the ISU spotted cDNA microarrays, it was possible to study the distribution of gene expression patterns along chromosomes. The microarray expression data used for this study came from an analysis of the inbred line B73, Mo17 and their F_1 hybrid (SWANSON-WAGNER *et al*. 2006). Genes were sorted based on their expression values in these microarray experiments. High- and low-expression genes were defined as the top 25% and bottom 25% of genes. Statistically significant differences were

observed in the distributions of the high- and low-expression genes along chromosome 1,2, 3, 4, 6, 7 and 10 (Table 8). These differences were consistent across the three genotypes (Figure 2).

DISCUSSION

ISU-IBM Map7 - A high-density genetic map of genes

The IBM population with approximately 17 times the resolution power of previous maize mapping populations due to random mating at F_2 (COE *et al*. 2002; LEE *et al*. 2002; SHAROPOVA *et al*. 2002; WINKLER *et al*. 2003) provides the mapping resource for the construction of high-resolution genetic maps. The first IBM genetic map constructed by the MMP contained ~2,000 markers of which less than 60% were sequence defined (COE *et al*. 2002; CONE *et al*. 2002). The ISU-IBM Map7 reported here contains 7,458 markers, (9,319, if one includes markers mapped by U-Map-It); over 70% of the 5,719 markers developed by the ISU mapping project were derived from genes or predicted genes with confirmed sequence sources. Compared to the ISU-IBM Map4, ISU-IBM Map7 has about a three-fold increase in the number of skeleton markers (3,612 vs. 1,274), about a two-fold increase in the number of landmarks (1,648 vs. 851). In addition, the average interval between landmarks decreased from 2 cM to 1 cM. This high-resolution genetic map populated with genic markers provides a powerful resource for the QTL analyses. For the cell wall data set (Table 7), ISU-IBM Map7 has many more markers within almost all QTL intervals than IBM2. The integration of the genetic and physical map allows sequenced BACs to be linked to QTL intervals, which will facilitate the identification of the genes controlling agronomically important traits.

TGCE technology for genetic mapping

It has been reported that over 80% of maize indels have lengths of ≤ 3 bps (BHATTRAMAKKI *et al*. 2002). Such a small indels cannot be identified by agarose gel electrophoresis. Using TGCE technology (LI *et al*. 2002) it is possible to detect a SNP or 1-bp indel in an 800-bp fragment (HSIA *et al*. 2005). A significant advantage of using TGCE for genotyping is that SNP or small indel polymorphisms can be identified without sequencing the polymorphic alleles. This report demonstrates that TGCE technology can be used to identify SNPs and small InDels that could not be identified by gel electrophoresis. Importantly, TGCE markers doubled the recovery of codominant markers, which are more informative than presence/absence dominant markers.

To identify IDP markers we screened ~40,000 primer pairs. Approximately 14.5% of the screened primer pairs display a polymorphism between inbred lines B73 and Mo17, using agarose gel electrophoresis or TGCE. This estimate of the rate of polymorphisms between B73 and Mo17 is an underestimate because not all the primer pairs were subjected to analysis via TGCE (Table 1). Of all the polymorphisms detected in this study, 54% (3,114 / 5,719) are size codominant. About 60% of the codominant polymorphisms were found by TGCE. Our results also suggested that MITEs spanning primer pairs can increase the chance to find codominant markers by 3 times for all other types of primer pairs. The overall presence/absence polymorphism rate is about 7% (Table 1) in this study which is lower that the previous reported rate 30% (BRUNNER *et al*. 2005).

Problems with using rice synteny to derive maize markers

To fill in the largest gaps on ISU-IBM map4 and also investigate the possibility of using rice synteny to map maize genes, 25 markers from 4 chromosomes designed from MAGIs that were identified from their rice syntenies. Six markers from 3 chromosomes were successfully mapped to expected positions. While 7 out 11 markers from chromosome 5 were mapped to chromosome 4, which is consistent with report of shuffling of genes in syntenic regions of rice and maize. That paper shows that genes from regions on chromosome 4 and chromosome 5 in maize have the same synteny region on chromosome 2 in rice. The complication and overlap existed between maize and rice synteny makes the task of using rice synteny to derive maize markers difficult.

Integration of physical and genetic map

Of the 721 FPCs released in July 2005, 300 could not be anchored to maize chromosomes. And our analysis of the hybridization of BACs and overgo probes indicates that about 7.3% of genes were not covered by BACs, plus 3.6% of genes hit BACs that were not in FPCs. The unanchored FPCs and the incomplete coverage of maize genome by FPCs are the issues we have to deal with during the maize whole genome sequencing effort. ISU-IBM Map7 with around 9,319 markers would be a powerful resource for the anchoring of unanchored FPCs and the development of strategies to sequence FPCs uncovered fragments. As of Feb.2007, one third of the BACs that will be sequenced by The Maize Sequencing Consortium were downloaded and used to align to markers on ISU-IBM Map7. About one third of the ISU markers hit one or more BACs. The proportion of BACs and markers are consistent. Using these data it was possible to anchor 322 FPCs, of which 18 FPCs had not

been previously anchored. In addition there are 31 unanchored FPCs that had hit one of ISU IDP markers. Although these FPCs cannot be mapped now, but those markers reveal some information about those unanchored BACs, and help us to develop strategies to anchor those difficult FPCs. For example, the confirmed sequences of these ISU markers can be used to discover more sequence sources for probe designing to identify more BACs by using BAC pooling strategy for anchoring (YIM *et al*. 2007). About 5.2% (16/304) of FPCs anchored by both MMP and ISU were inconsistent. After these FPCs are sequenced it is critical to carefully reanalyze their anchoring relative to the genetic map.

Chromosome-level regulation of gene expression

We observed that strongly and weakly expressed genes are differentially distributed along maize chromosomes. This phenomenon was observed in all three analyzed genotypes. This observation indicates that gene expression can be regulated at the level of chromosome organization. Analyses of expression data using chromosome tiling microarrays (JIAO *et al*. 2005; LI *et al*. 2005) indicated that rice genes located in euchromatic regions are more actively transcribed than those located in heterochromatic regions, and increased transcription activity in heterochromatin region was observed under stress. Similarly, in maize it has been shown that ESTs (which are enriched for highly expressed genes) are clustered in euchromatic regions (ANDERSON *et al*. 2006). We therefore hypothesize that the differences in the distributions of strongly and weakly expressed genes along maize chromosomes reflect the differential localization of these genes in euchromatic and heterochromatic regions.

ACKNOWLEDGEMENTS

We thank Fusheng Wei of the Arizona Genome Institute for information about FPCs, Cheng-Ting "Eddy" Yeh for computational support, Josh Shendelman, Yi-Yin “Rita” Chen, Elizabeth Hahn, and Sarah Hargreaves for collecting mapping data. This project was supported by competitive grants from the National Science Foundation Plant Genome Program (DBI-9975868 and DBI-0321711).

REFERENCES

ANDERSON, L. K., A. LAI, S. M. STACK, C. RIZZON and B. S. GAUT, 2006 Uneven distribution of expressed sequence tag loci on maize pachytene chromosomes. Genome Res **16:** 115-122.

BHATTRAMAKKI, D., M. DOLAN, M. HANAFEY, R. WINELAND, D. VASKE *et al.*, 2002 Insertion-deletion polymorphisms in 3' regions of maize genes occur frequently and can be used as highly informative genetic markers. Plant Mol Biol **48:** 539-547.

BRENDEL, V., L. XING and W. ZHU, 2004 Gene structure prediction from consensus spliced alignment of multiple ESTs matching the same genomic locus. Bioinformatics **20:** 1157-1169.

BRUNNER, S., K. FENGLER, M. MORGANTE, S. TINGEY and A. RAFALSKI, 2005 Evolution of DNA sequence nonhomologies among maize inbreds. Plant Cell **17:** 343-360.

COE, E., K. CONE, M. MCMULLEN, S. S. CHEN, G. DAVIS *et al.*, 2002 Access to the maize genome: an integrated physical and genetic map. Plant Physiol **128:** 9-12.

CONE, K. C., M. D. MCMULLEN, I. V. BI, G. L. DAVIS, Y. S. YIM *et al.*, 2002 Genetic, physical, and informatics resources for maize. On the road to an integrated map. Plant Physiol **130:** 1598-1605.

DAVIS, G. L., M. D. MCMULLEN, C. BAYSDORFER, T. MUSKET, D. GRANT *et al.*, 1999 A maize map standard with sequenced core markers, grass genome reference points and 932 expressed sequence tagged sites (ESTs) in a 1736-locus map. Genetics **152:** 1137-1172.

DOONER, H. K., 1986 Genetic Fine Structure of the BRONZE Locus in Maize. Genetics **113:** 1021-1036.

EMRICH, S. J., S. ALURU, Y. FU, T. J. WEN, M. NARAYANAN *et al.*, 2004 A strategy for assembling the maize (Zea mays L.) genome. Bioinformatics **20:** 140-147.

FALQUE, M., L. DECOUSSET, D. DERVINS, A. M. JACOB, J. JOETS *et al.*, 2005 Linkage mapping of 1454 new maize candidate gene Loci. Genetics **170:** 1957-1966.

FU, H., and H. K. DOONER, 2002 Intraspecific violation of genetic colinearity and its implications in maize. Proc Natl Acad Sci U S A **99:** 9573-9578.

FU, Y., S. J. EMRICH, L. GUO, T. J. WEN, D. A. ASHLOCK *et al.*, 2005 Quality assessment of maize assembled genomic islands (MAGIs) and large-scale experimental verification of predicted genes. Proc Natl Acad Sci U S A **102:** 12282-12287.

FU, Y., T. J. WEN, Y. I. RONIN, H. D. CHEN, L. GUO *et al.*, 2006 Genetic dissection of intermated recombinant inbred lines using a new genetic map of maize. Genetics **174:** 1671-1683.

GARDINER, J., S. SCHROEDER, M. L. POLACCO, H. SANCHEZ-VILLEDA, Z. FANG *et al.*, 2004 Anchoring 9,371 maize expressed sequence tagged unigenes to the bacterial artificial chromosome contig map by two-dimensional overgo hybridization. Plant Physiol **134:** 1317-1326.

HALDANE, J. B. S., 1919 The combination of linkage values and the calculation of distances between the loci of linked factors. J. Genet. **8:** 299-309.

HAZEN, S. P., R. M. HAWLEY, G. L. DAVIS, B. HENRISSAT and J. D. WALTON, 2003 Quantitative trait loci and comparative genomics of cereal cell wall composition. Plant Physiol **132:** 263-271.

HSIA, A. P., T. J. WEN, H. D. CHEN, Z. LIU, M. D. YANDEAU-NELSON *et al.*, 2005 Temperature gradient capillary electrophoresis (TGCE)--a tool for the high-throughput discovery and mapping of SNPs and IDPs. Theor Appl Genet **111:** 218-225.

JIAO, Y., P. JIA, X. WANG, N. SU, S. YU *et al.*, 2005 A tiling microarray expression analysis of rice chromosome 4 suggests a chromosome-level regulation of transcription. Plant Cell **17:** 1641-1657.

LEE, M., N. SHAROPOVA, W. D. BEAVIS, D. GRANT, M. KATT *et al.*, 2002 Expanding the genetic map of maize with the intermated B73 x Mo17 (IBM) population. Plant Mol Biol **48:** 453-461.

LI, L., X. WANG, M. XIA, V. STOLC, N. SU *et al.*, 2005 Tiling microarray analysis of rice chromosome 10 to identify the transcriptome and relate its expression to chromosomal architecture. Genome Biol **6:** R52.

LI, Q., Z. LIU, H. MONROE and C. T. CULIAT, 2002 Integrated platform for detection of DNA sequence variants using capillary array electrophoresis. Electrophoresis **23:** 1499-1511.

MAHER, P. M., H. H. CHOU, E. HAHN, T. J. WEN and P. S. SCHNABLE, 2006 GRAMA: genetic mapping analysis of temperature gradient capillary electrophoresis data. Theor Appl Genet **113:** 156-162.

MESTER, D., Y. RONIN, D. MINKOV, E. NEVO and A. KOROL, 2003 Constructing large-scale genetic maps using an evolutionary strategy algorithm. Genetics **165:** 2269-2282.

MESTER, D. I., Y. I. RONIN, E. NEVO and A. B. KOROL, 2004 Fast and high precision algorithms for optimization in large-scale genomic problems. Comput Biol Chem **28:** 281-290.

MEYERS, B. C., S. V. TINGEY and M. MORGANTE, 2001 Abundance, distribution, and transcriptional activity of repetitive elements in the maize genome. Genome Res **11:** 1660-1676.

PALMER, L. E., P. D. RABINOWICZ, A. L. O'SHAUGHNESSY, V. S. BALIJA, L. U. NASCIMENTO *et al.*, 2003 Maize genome sequencing by methylation filtration. Science **302:** 2115-2117.

ROZEN, S., and H. SKALETSKY, 2000 Primer3 on the WWW for general users and for biologist programmers. Methods Mol Biol **132:** 365-386.

SHAROPOVA, N., M. D. MCMULLEN, L. SCHULTZ, S. SCHROEDER, H. SANCHEZ-VILLEDA *et al.*, 2002 Development and mapping of SSR markers for maize. Plant Mol Biol **48:** 463-481.

SMIRNOV, N. V., 1939 Estimate of deviation between empirical distribution functions in two independent samples. Bulletin Moscow University **2:** 3-16.

SODERLUND, C., S. HUMPHRAY, A. DUNHAM and L. FRENCH, 2000 Contigs built with fingerprints, markers, and FPC V4.7. Genome Res **10:** 1772-1787.

SWANSON-WAGNER, R. A., Y. JIA, R. DECOOK, L. A. BORSUK, D. NETTLETON *et al.*, 2006 All possible modes of gene action are observed in a global comparison of gene expression in a maize F1 hybrid and its inbred parents. Proc Natl Acad Sci U S A **103:** 6805-6810.

TOMKINS, J. P., G. DAVIS, D. MAIN, Y. S. YIM, N. DURU *et al.*, 2002 Construction and characterization of a deep-coverage bacterial artificial chromosome library for maize. Crop Sci. **42:** 928-933.

WHITELAW, C. A., W. B. BARBAZUK, G. PERTEA, A. P. CHAN, F. CHEUNG *et al.*, 2003 Enrichment of gene-coding sequences in maize by genome filtration. Science **302:** 2118-2120.

WINKLER, C. R., N. M. JENSEN, M. COOPER, D. W. PODLICH and O. S. SMITH, 2003 On the determination of recombination rates in intermated recombinant inbred populations. Genetics **164:** 741-745.

YANDEAU-NELSON, M. D., B. J. NIKOLAU and P. S. SCHNABLE, 2006 Effects of trans-acting genetic modifiers on meiotic recombination across the a1-sh2 interval of maize. Genetics **174:** 101-112.

YAO, H., L. GUO, Y. FU, L. A. BORSUK, T. J. WEN *et al.*, 2005 Evaluation of five ab initio gene prediction programs for the discovery of maize genes. Plant Mol Biol **57:** 445-460.

YAO, H., and P. S. SCHNABLE, 2005 Cis-effects on meiotic recombination across distinct a1-sh2 intervals in a common Zea genetic background. Genetics **170:** 1929-1944.

YAO, H., Q. ZHOU, J. LI, H. SMITH, M. YANDEAU *et al.*, 2002 Molecular characterization of meiotic recombination across the 140-kb multigenic a1-sh2 interval of maize. Proc Natl Acad Sci U S A **99:** 6157-6162.

YIM, Y. S., G. L. DAVIS, N. A. DURU, T. A. MUSKET, E. W. LINTON *et al.*, 2002 Characterization of three maize bacterial artificial chromosome libraries toward anchoring of the physical map to the genetic map using high-density bacterial artificial chromosome filter hybridization. Plant Physiol **130:** 1686-1696.

YIM, Y. S., P. MOAK, H. SANCHEZ-VILLEDA, T. A. MUSKET, P. CLOSE *et al.*, 2007 A BAC pooling strategy combined with PCR-based screenings in a large, highly repetitive genome enables integration of the maize genetic and physical maps. BMC Genomics **8:** 47.

Table 1. Sequence sources and polymorphsim types of all ISU IDP markers on ISU-IBM Map7

Primer design method	Sequence source[1]	Gel detected polymorphisms					TGCE detected polymorphisms		Total No. polymorphisms
		No. primers[2]	Size[3]	B+/M-[4]	B-/M+[5]	Subtotal	No. primers[2]	Polymorphisms[5]	
3' UTRs	EST[6]	12,227	300 (2.5%[12])	613 (5.0%)	109 (0.9%)	1,022 (8.4%)	12,227	754 (6.2%)	1,776 (14.5%)
Intron spanning	GSS[7]	1,289	43 (3.3%)	37 (2.9%)	12 (0.9%)	92 (7.1%)	1,289	150 (11.6%)	242 (18.8%)
	MAGI2.31[8]	1,463	67 (4.6%)	51 (3.5%)	14 (1.0%)	132 (9.0%)	1,463	188 (12.9%)	320 (21.9%)
	MAGI3.1[8]	20,747	755 (3.6%)	1,417 (6.8%)	95 (0.5%)	2,267 (10.9%)	9,942	694 (7.0%)	2,961 (14.3%)

[1] Number of primer pairs subjected to surveys for polymorphism via the indicated method
[2] Number of primer pairs that detected (codominant) size polymorphisms between B73 and Mo17
[3] Number of primer pairs that detected B73 presence and Mo17 absence (dominant) polymorphism
[4] Number of primer pairs that detected B73 absence and Mo17 presence (dominant) polymorphism
[5] Number of polymorphism identified by TGCE method only, those that can be identified by gel electrophoresis are not included.
[6] Expressed Sequence Tag.
[7] Gene-enriched maize Genome Survey Sequences generated by the Consortium for Maize Genomics.
[8] Maize Assembled Genomic Islands version 2.31/3.1/4.0 (http://magi.plantgenomics.iastate.edu/).
[9] BAC end sequences.
[10] Structure Known Genes.
[11] Includes several genes of particular interest to members of the Schnable Lab, genes nominated by the research community for mapping, and Nearly Identical NIPs (Emrich et al., 2006).
[12] Number of primer pairs that detect polymorphisms per 100 primer pairs surveyed
[13] Seven markers for which polymorphism data are not available not included in this table

Table 1. (continued)

Primer design method	Sequence source	Gel detected polymorphisms					TGCE detected polymorphisms		Total No. polymorphisms
		No. primers	Size	B+/M-	B-/M+	Subtotal	No. primers	Polymorphisms	
	MAGI4.0[8]	2,880	89 (3.1%)	124 (4.3%)	7 (0.2%)	220 (7.6%)	0	0 (0.0%)	220 (7.6%)
	BEs[9]	546	2 (0.4%)	20 (3.7%)	3 (0.5%)	25 (4.6%)	546	41 (7.5%)	66 (12.1%)
	SKGs[10]	191	4 (2.1%)	4 (2.1%)	11 (5.8%)	19 (9.9%)	191	2 (1.0%)	21 (11.0%)
	Subtotal	27,116	960 (3.5%)	1,653 (6.1%)	142 (0.5%)	2,755 (10.2%)	13,431	1,075 (8.0%)	3,830 (14.1%)
	Other[11]	147	11 (7.5%)	62 (42.2%)	19 (12.9%)	92 (62.6%)	27	14 (51.9%)	106 (72.1%)
Total		39,490	1,271 (3.2%)	2,328 (5.9%)	270 (0.7%)	3,869 (9.8%)	25,685	1,843 (7.2%)	5,712[15] (14.5%)

Table 2. Rates at which different types of polymorphisms are detected using primers designed using various strategies

Primer design strategy	Gel based					TGCE[5] based		Total
	No. primers	Polymorphic type			Subtotal	No. primers	Polymorphism	
		Size[2]	B+/M-[3]	B-/M+[4]				
3' UTRs	12,227	313 (2.6%[6])	658 (5.4%)	117 (1.0%)	1,088 (8.9%)	12,227	776 (6.3%)	1,864 (15.2%)
EE[1]	16,317	639 (3.9%)	873 (5.4%)	93 (0.6%)	1,605 (9.8%)	6,804	743 (10.9%)	2,348 (14.4%)
EB[1]	1,319	28 (2.1%)	49 (3.7%)	3 (0.2%)	80 (6.1%)	1,307	33 (2.5%)	113 (8.6%)
EO[1]	8,931	311 (3.5%)	770 (8.6%)	53 (0.6%)	1,134 (12.7%)	4,771	295 (6.2%)	1,429 (16.0%)
BO[1]	370	9 (2.6%)	41 (11.7%)	6 (1.7%)	56 (16.0%)	351	25 (7.1%)	81 (23.1%)
OO[1]	179	10 (5.6%)	41 (22.9%)	1 (0.6%)	52 (29.1%)	179	8 (4.5%)	60 (33.5%)
Total	39,324	1,312 (3.3%)	2,434 (6.2%)	273 (0.7%)	4,019 (10.2%)	25,639	1,880 (7.3%)	5,899 (15.0%)

[1] E, primer was completely contained within an exon; B, primer located on an exon-intron boundary; O, primer not located on known a exon or exon-intron boundary. For example, EB indicates that one primer is within exon region and the other one is on exon-intron boundary.
[2] Codominant size polymorphism
[3] B73 presence / Mo17 absence polymorphism
[4] B73 absence / Mo17 presence polymorphism
[5] Polymorphism detected by Temperature Gradient Capillary Electrophoresis

Table 3. Summary of marker types on each chromosome of the ISU-IBM Map7

	ISU markers[1]				MMP markers[2]				Falque et. al.	All			
Chr	SK[4]	MU[5]	UMI[6]	Subtotal	SK	MU	UMI[6]	Subtotal	UMI[6]	SK	MU	UMI[6]	Total
	525	401	39	965	84	213	37	334	219	609	614	295	1,518
1	5.6%[7]	4.3%	0.4%	10.4%	0.9%	2.3%	0.4%	3.6%	2.4%	6.5%	6.6%	3.2%	16.3%
	342	306	7	655	67	108	24	199	184	409	414	215	1,038
2	3.7%	3.3%	0.1%	7.0%	0.7%	1.2%	0.3%	2.1%	2.0%	4.4%	4.4%	2.3%	11.1%
	350	331	10	691	65	152	26	243	163	415	483	199	1,097
3	3.8%	3.6%	0.1%	7.4%	0.7%	1.6%	0.3%	2.6%	1.7%	4.5%	5.2%	2.1%	11.8%
	269	314	9	592	43	134	27	204	152	312	448	188	948
4	2.9%	3.4%	0.1%	6.4%	0.5%	1.4%	0.3%	2.2%	1.6%	3.3%	4.8%	2.0%	10.2%
	308	228	9	545	57	110	13	180	154	365	338	176	879
5	3.3%	2.4%	0.1%	5.8%	0.6%	1.2%	0.1%	1.9%	1.7%	3.9%	3.6%	1.9%	9.4%
	279	281	12	572	47	96	26	169	172	326	377	210	913
6	3.0%	3.0%	0.1%	6.1%	0.5%	1.0%	0.3%	1.8%	1.8%	3.5%	4.0%	2.3%	9.8%
	255	214	5	474	41	102	16	159	124	296	316	145	757
7	2.7%	2.3%	0.1%	5.1%	0.4%	1.1%	0.2%	1.7%	1.3%	3.2%	3.4%	1.6%	8.1%
	245	189	6	440	40	93	17	150	131	285	282	154	721
8	2.6%	2.0%	0.1%	4.7%	0.4%	1.0%	0.2%	1.6%	1.4%	3.1%	3.0%	1.7%	7.7%

[1] Markers generated by Iowa State University maize genetic mapping project
[2] Markers generated by Missouri Maize Mapping Project
[3] Markers generated by Falque et al. 2005
[4] Skeleton markers
[5] Muscle markers
[6] Markers linked to Skeleton/Muscle markers using the U-Map-It software
[7] All percentage values in parenthesis are based on the total number of markers, i.e., 7,458

Table 3. (continued)

	ISU markers				MMP markers				Falque et al.,	All			
Chr	SK	MU	UMI	Subtotal	SK	MU	UMI	Subtotal	UMI	SK	MU	UMI	Total
	280	173	6	459	50	107	14	171	120	330	280	140	750
9	3.0%	1.9%	0.1%	4.9%	0.5%	1.1%	0.2%	1.8%	1.3%	3.5%	3.0%	1.5%	8.0%
	229	200	7	436	36	94	24	154	108	265	294	139	698
10	2.5%	2.1%	0.1%	4.7%	0.4%	1.0%	0.3%	1.7%	1.2%	2.8%	3.2%	1.5%	7.5%
	3,082	2,637	110	5,829	530	1,209	224	1,963	1,527	3,612	3,846	1,861	9,319
Total	33.1%	28.3%	1.2%	62.5%	5.7%	13.0%	2.4%	21.1%	16.4%	38.8%	41.3%	20.0%	100.0%

Table 4. Comparisons between ISU-IBM Map7 and Map4

Chromosome	Chromosome length (cM)			Largest gap (cM)			Tail length of shared markers[1] (cM)					
							Map 7		Map4		Difference[2]	
	Map7	Map4	Difference[2]	Map7	Map4	Difference[2]	Left end	Right end	Left end	Right end	Left end	Right end
1	304	276	28	6.9	9	-2.1	2.3	3.5	0	0	2.3	3.5
2	202	196	6	5.3	8	-2.7	0	0.8	0	3.5	0	-2.7
3	226	210	16	7.7	6	1.7	0.5	0.3	0	0	0.5	0.3
4	187	185	2	6.8	8	-1.2	0	0.3	0	0	0	0.3
5	153	191	-38	7.6	13	-5.4	3.9	0	0	35.7	3.9	-35.7
6	132	129	3	5.9	6	-0.1	8.4	0	0	0	8.4	0
7	175	174	1	10	11	-1	1.8	0.8	0	15.7	1.8	-14.9
8	193	155	38	9.2	9	0.2	4	0	0	0	4	0
9	168	142	26	4.6	10	-5.4	0	1.8	0	0	0	1.8
10	144	130	14	5.8	9	-3.2	6.9	18.7	3.3	9	3.6	9.7
Total	1884	1788	96	69.8	89	-19.2	27.8	26.2	3.3	63.9	24.5	-37.7

[1] Indicates the genetic distance from the last marker on each chromosome end shared by Map7 and Map4 to the end of the corresponding chromosome.

[2] Difference between values of Map7 and Map4.

Table 5. The genetic, physical and rice synteny locations of gap flanking and gap filling markers

Chr	Marker source	Marker ID	Map4 location (cM)	ISU-IBM Map7			BAC/BAC contig			Rice locus[5]	Fill in the expected location?
				Chr	Marker type[3]	Location (cM)	Accession No.	Contig[4]	Anchored Chr		
1	Gap flanking[1]	IDP806	248	1	sk	271.8	-	-	-	Os03g58480	-
		IDP772	256.5	1	mu	281.5	-	-	-	Os03g60950	-
	Gap filling[2]	IDP7387	-[6]	1	mu	294.5	-	-	-	Os03g62740	Yes
		IDP7909	-	1	sk	299.1	AC186520	66	1	Os03g63280	Yes
		IDP7902	-	5	sk	2.1	-	-	-	Os03g62690	No
		IDP8017	-	7	mu	100.8	AC195981	326	8	Os03g62790	No
	Gap flanking	IDP626	274.3	1	sk	299.9	AC177870	66	1	Os03g63400	-
		IDP3920	274.3	1	sk	301.1	AC191423	66	1	Os03g63700	-

[1] Markers flanking the largest gaps on ISU-IBM Map4
[2] Markers designed to filling in the largest gaps on ISU-IBM Map4
[3] sk – skeleton marker; mu – muscle marker
[4] BAC contig assembled by AGI
[5] Physical position in The Institute for Genomic Research's (TIGR's) release 3.0 of the rice genome (http://www.tigr.org/tdb/e2k1/osa1/pseudomolecules)
[6] Data not available

Table 5. (continued)

Chr	Marker source	Marker ID	Map4 location (cM)	ISU-IBM Map7			BAC/BAC contig			Rice locus	Fill in the expected location?
				Chr	Marker type	Location (cM)	Accession No.	Contig	Anchored Chr		
5	Gap flanking	IDP233	152.7	5	mu	150.3	-	-	-	Os02g49330	-
		IDP2474	155.3	-	-	-	-	-	-	Os02g49840	-
	Gap filling	IDP7908	-	1	sk	72.6	-	-	-	Os02g51880	No
		IDP7907	-	3	mu	86.5	-	-	-	Os02g52780	No
		IDP7898	-	4	sk	113.9	AC185668	182	4	Os02g53520	No
		IDP7911	-	4	mu	115.3		-	-	Os02g52670	No
		IDP8018	-	4	sk	115.6	AC183914	182	4	Os02g52740	No
		IDP7912	-	4	sk	115.9	AC183914	182	4	Os02g52550	No
		IDP7899	-	4	sk	117.1	AC185627	182	4	Os02g52180	No
		IDP7504	-	4	sk	121.4	AC185478	182	4	Os02g51480	No
		IDP7901	-	4	sk	121.7	AC185478	182	4	Os02g51440	No
		IDP7900	-	8	mu	149.5	AC155590	253	5	Os02g52610	No
		IDP7905	-	8	mu	149.5	-	-	-	Os02g52850	No
	Gap flanking	IDP1491	171.4	-	-	-	-	-	-	Os02g54080	-
		IDP4002	175.3	-	-	-	-	-	-	Os02g54640	-
7	Gap flanking	IDP3822	121	7	sk	134.7	AC194977	323	7	Os07g38590	-
		IDP1981	122.5	7	mu	136.5	-	-	-	Os07g38960	-
	Gap filling	IDP7913	-	7	sk	137.7	-	-	-	Os07g39310	Yes
		IDP7252	-	7	sk	139.5	AC197343	323	7	Os07g39810	Yes
		IDP7184	-	2	sk	144.6	-	-	-	Os07g39980	No
	Gap	IDP1960	136.5	7	sk	148.1	-	-	-	Os07g4097	-

Table 5. (continued)

Chr	Marker source	Marker ID	Map4 location (cM)	ISU-IBM Map7			BAC/BAC contig			Rice locus	Fill in the expected location?
				Chr	Marker type	Location (cM)	Accession No.	Contig	Anchored Chr		
7	flanking	IDP657	158	7	sk	171.3	-	-	-	Os07g4418	-
9	Gap flanking	IDP63	94.1	9	sk	108.4	-	-	-	Os03g15050	-
		IDP3826	94.1	9	mu	108.4	-	-	-	Os03g14370	-
	Gap filling	IDP6028	-	9	sk	114.1	-	-	-	Os03g13550	Yes
		IDP8021	-	9	sk	121.9	-	-	-	Os03g12510	Yes
		IDP7904	-	1	sk	72.3	-	-	-	Os03g12630	No
		IDP7583	-	1	sk	72.3	-	-	-	Os03g12620	No
		IDP7238	-	1	mu	72.3	AC197594	9	1	Os03g12890	No
		IDP6029	-	1	sk	76.8	-	-	-	Os03g14260	No
	Gap flanking	IDP493	105.1	9	sk	121.9	-	-	-	Os03g12500	-
		IDP549	108.9	9	sk	127	-	-	-	Os03g11610	-

Table 6. Comparisons of genetic distances between one pair of markers per chromosomes in FIBC and IBM IRIL mapping populations

Chr	No. scored spots	No. recombined spots	Recombination rate (%)	Haldane distance in F_1BC	Genetic distance on map7
1	287	27	9.4	10	6.8
2	335	9	2.7	2.8	4
3	352	19	5.4	5.7	4.4
4	330	22	6.7	7.2	5.9
5	330	18	5.4	5.8	6.3
6	339	44	7.9	8.6	8
7	294	11	3.7	3.9	7.9
8	308	24	7.8	8.5	6.1
9	318	35	11	12.4	7.1
10	309	37	12	13.7	10.5

Table 7. Number of markers within QTL intervals on the IBM2 and ISU-IBM Map7 genetic maps and the numbers of sequenced BACs associated with the ISU-IBM Map7 intervals

QTL[1]	Flanking markers[1]	Chr	No. markers in QTL region		No. BACs[2]
			IBM2	Map7	
1	php20537-ufg33	1	3	-	-
2	umc1824-bnl2g277	2	7	66	28
3	mmp144-mmp36	3	3	35	20
4	bnlg1816-umc1920	3	13	72	28
5	mmp9-umc1449	3	3	23	5
6	umc1167-psr119a	3	5	42	18
7	lim446-php10025	4	3	60	23
8	umc1155-nbp35	5	3	18	15
9	bnlg1174-phi078	6	-	16	4
10	bnl5.09a-bnl14.28	9	5	-	-
11	umc1789-umc1675	9	5	11	4
12	psb527d-umc1053	10	-	30	6
13	psb365a-umc1993	10	4	26	10

[1] QTL intervals were reported by (HAZEN *et al*. 2003)
[2] Number of sequenced BACs linked to the QTL interval through ISU IDP markers

Table 8. Kolmogorov-Smirnov (K-S) tests on the distributions of strongly and weakly expressed genes

Chr	No. Low[1]	No. High[2]	P-value[3]
1	110	69	5.80E-06*
2	82	41	0.0391*
3	86	52	0.0237*
4	72	45	0.0390*
5	70	29	0.0711
6	72	46	0.0005*
7	48	44	3.78E-05*
8	53	18	0.9690
9	41	34	0.1263
10	60	50	0.0019*
Total	694	428	-

[1] Number of mapped genes in the lowest 25th percentile based on expression level.
[2] Number of mapped genes in the highest 25th percentile based on expression level.
[3] P-value from Kolmogorov-Smirnov (K-S) test; * indicates significant at the 0.05 level.

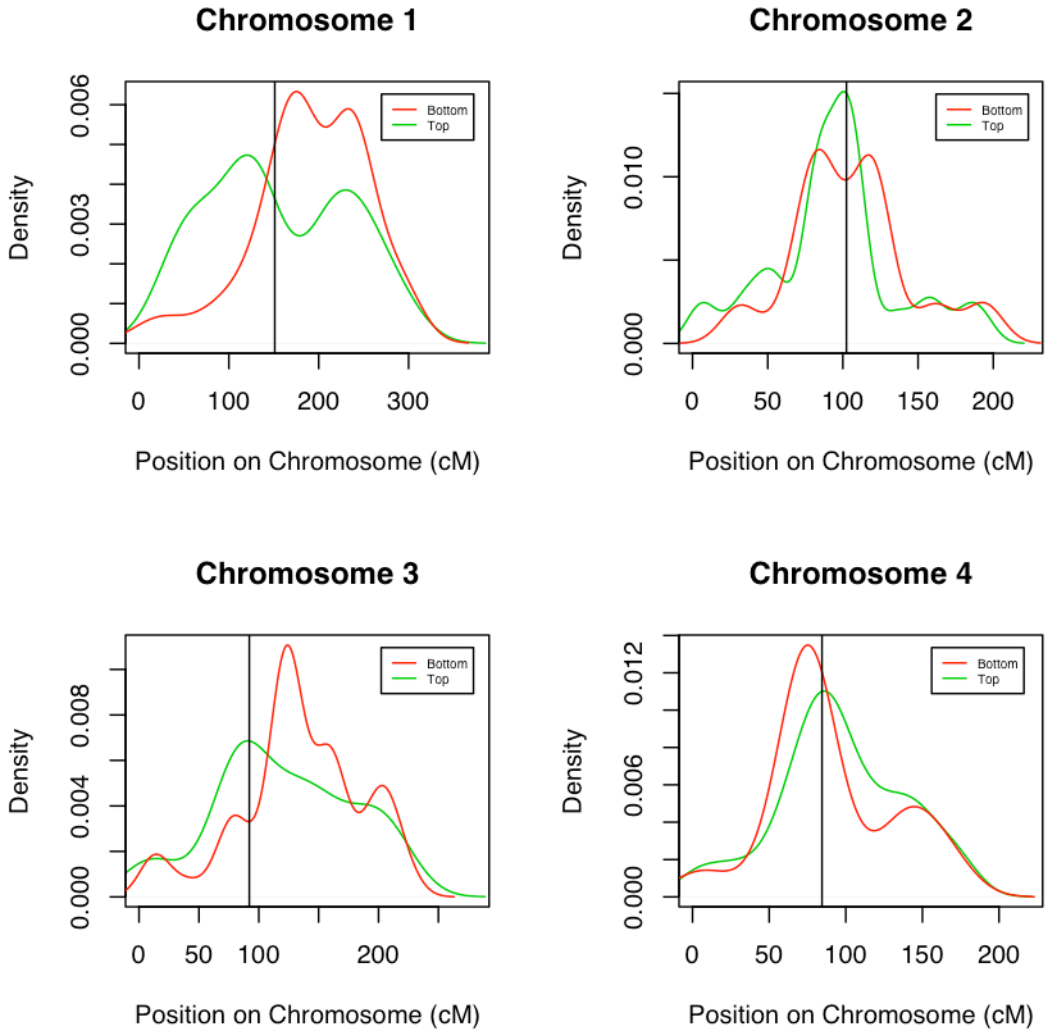

Figure 2. Density plots of strongly and weakly genes on chromosomes 1-10. Genes that are included in the bottom and top 25th percentiles are plotted in blue and green respectively. The numbers of genes plotted for each chromosome are presented in Table 8. Vertical line indicates the position of the centromere.

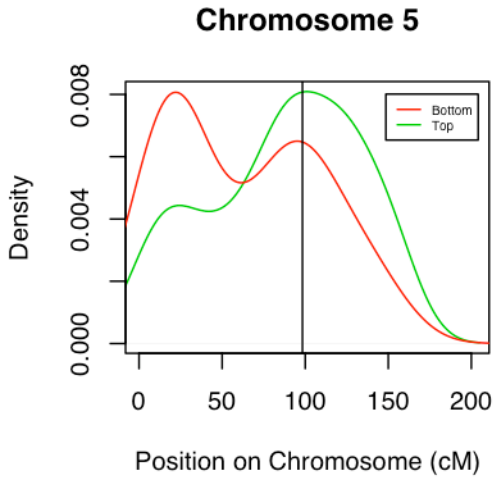
Chromosome 5
Density
0.000
0.004
0.008
Bottom
Top
0
50
100
150
200
Position on Chromosome (cM)

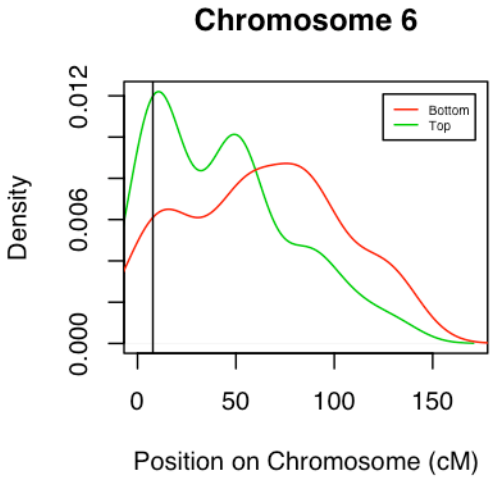
Chromosome 6
Density
0.000
0.006
0.012
Bottom
Top
0
50
100
150
Position on Chromosome (cM)

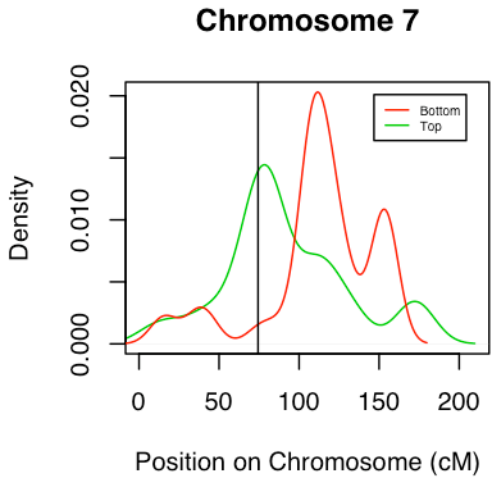
Chromosome 7
Density
0.000
0.010
0.020
Bottom
Top
0
50
100
150
200
Position on Chromosome (cM)

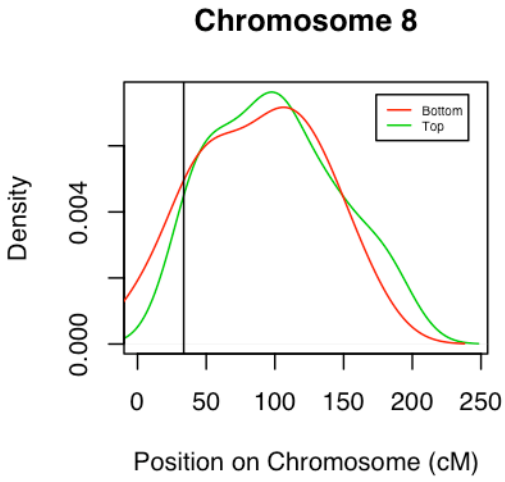
Chromosome 8
Density
0.000
0.004
Bottom
Top
0
50
100
150
200
250
Position on Chromosome (cM)

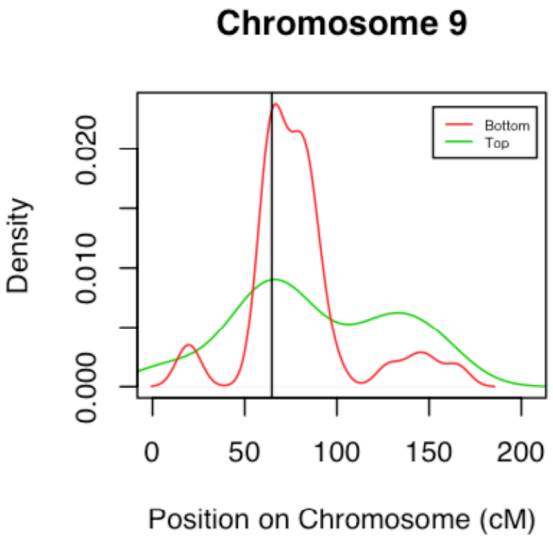
Chromosome 9
Density
0.000
0.010
0.020
Bottom
Top
0
50
100
150
200
Position on Chromosome (cM)

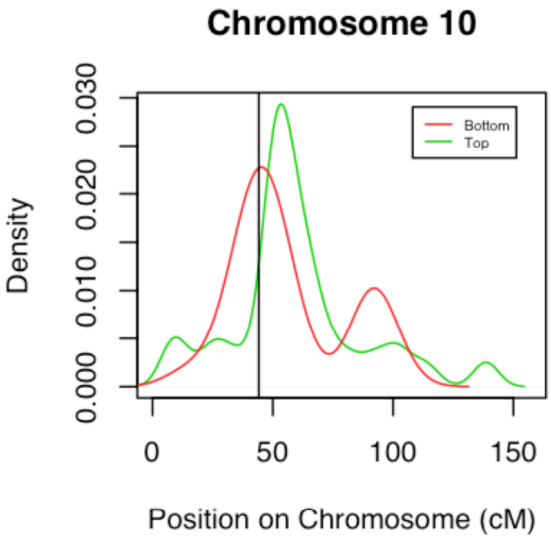
Chromosome 10
Density
0.000
0.010
0.020
0.030
Bottom
Top
0
50
100
150
Position on Chromosome (cM)

Supplementary Data

Table 1. Anchoring information for all BAC FPCs

Contig id	Chr[1]	Pos[2]	No. of markers[3]	Anchoring information[4]	Cate-gory[5]
Ctg1	1	0.6	4	Chr1:4:3-sk_ISU:1-mu_MMP	#4
Ctg2	1	3.8	9	Chr1:8:6-sk_ISU:2-sk_MMP Chr10:1:1-mu_ISU	#3
Ctg3	1	15.1	14	Chr1:14:10-sk_ISU:2-mu_ISU:2-mu_MMP	#4
Ctg4	1	29.4	34	Chr8:2:2-mu_ISU Chr1:32:15-sk_ISU:12-mu_ISU:2-sk_MMP:3-mu_MMP	#3
Ctg5	1	40.7	12	Chr1:6:5-sk_ISU:1-sk_MMP Chr3:3:2-sk_ISU:1-mu_ISU Chr7:1:1-sk_ISU Chr9:1:1-sk_ISU Chr2:1:1-sk_ISU	#3
Ctg6	1	47.8	4	Chr1:3:1-sk_ISU:1-mu_ISU:1-mu_MMP Chr9:1:1-mu_MMP	#3
Ctg7	-	-	2	Chr1:1:1-mu_ISU Chr9:1:1-sk_ISU	#2
Ctg8	1	54.2	12	Chr1:10:1-sk_ISU:6-mu_ISU:2-umapit_ISU:1-sk_MMP Chr3:1:1-sk_ISU Chr9:1:1-mu_ISU	#3
Ctg9	1	67.2	19	Chr1:15:7-sk_ISU:7-mu_ISU:1-sk_MMP Chr3:2:2-sk_ISU Chr9:2:1-sk_ISU:1-sk_MMP	#3
Ctg10	1	72.6	2	Chr1:2:2-mu_ISU	#4
Ctg11	1	88.3	20	Chr6:1:1-mu_ISU Chr1:17:11-sk_ISU:2-mu_ISU:2-sk_MMP:2-mu_MMP Chr9:1:1-sk_MMP Chr10:1:1-sk_ISU	#3
Ctg12	1	67.8	6	Chr1:6:2-sk_ISU:4-mu_ISU	#4
Ctg13	1	101.1	3	Chr1:3:3-sk_ISU	#4
Ctg14	1	104.4	11	Chr1:11:7-sk_ISU:3-mu_ISU:1-mu_MMP	#4

[1] Chromosome to which BAC contig is anchored.

[2] Anchored genetic position, which is the average of the genetic position of closely linked markers (≤ 30 cM).

[3] Number of markers linked to the BAC contig.

[4] The format of the anchoring information is chromosome number:number markers from this chromosome:number markers of each specific type. Marker types type of markers is consist of two parts linked by underscore. sk – skeleton marker, mu – muscle marker, umapit – markers linked to ISU-IBM Map7 using the U-Map-It software, ISU – markers identified by Iowa State University, MMP – markers identified by the Missouri Maize Mapping Project.

[5] Categories: #1 - BAC contig was hit by one marker; #2 – BAC contig hit by multiple non-closely linked and inconsistent markers; #3- BAC contig hit by multiple markers and majority of those markers were closely linked; #4 – BAC contig hit by multiple closely linked markers.

Table 1. (continued)

Contig id	Chr	Pos	No. of markers	Anchoring information	Cate-gory
Ctg15	1	140.6	4	Chr1:4:2-sk_ISU:2-mu_ISU	#4
Ctg17	-	-	1	Chr1:1:1-mu_ISU	#1
Ctg18	1	115.6	3	Chr1:3:1-sk_ISU:2-mu_ISU	#4
Ctg19	1	118.1	4	Chr1:4:2-sk_ISU:2-mu_ISU	#4
Ctg20	1	142.4	5	Chr1:4:2-sk_ISU:2-mu_ISU Chr2:1:1-mu_MMP	#3
Ctg21	1	122.5	5	Chr1:5:4-sk_ISU:1-mu_ISU	#4
Ctg22	1	122.9	3	Chr1:3:2-sk_ISU:1-mu_ISU	#4
Ctg23	1	124.7	9	Chr1:7:1-sk_ISU:5-mu_ISU:1-mu_MMP Chr4:1:1-mu_ISU Chr9:1:1-sk_ISU	#3
Ctg24	1	126.1	2	Chr1:2:2-sk_ISU	#4
Ctg25	1	125.1	2	Chr1:2:2-sk_ISU	#4
Ctg27	1	129.6	3	Chr1:2:2-mu_ISU Chr2:1:1-sk_ISU	#3
Ctg28	1	128.6	5	Chr6:1:1-mu_ISU Chr1:4:2-sk_ISU:2-mu_ISU	#3
Ctg29	1	129.8	3	Chr1:3:2-sk_ISU:1-sk_MMP	#4
Ctg30	1	145.8	9	Chr8:1:1-sk_ISU Chr1:5:2-sk_ISU:1-mu_ISU:1-sk_MMP:1-mu_MMP Chr10:1:1-mu_ISU Chr5:2:2-sk_ISU	#3
Ctg31	1	130.8	9	Chr1:6:4-sk_ISU:2-mu_ISU Chr9:3:2-sk_ISU:1-mu_ISU	#3
Ctg32	1	130.8	6	Chr1:6:6-mu_ISU	#4
Ctg33	1	132.6	1	Chr1:1:1-sk_ISU	#4
Ctg34	1	132.9	3	Chr1:3:2-umapit_ISU:1-umapit_MMP	#4
Ctg35	1	133.8	4	Chr1:4:1-mu_ISU:2-umapit_ISU:1-umapit_MMP	#4
Ctg36	1	135.9	11	Chr1:11:4-sk_ISU:2-mu_ISU:5-umapit_ISU	#4
Ctg37	1	139.6	18	Chr1:17:7-sk_ISU:8-mu_ISU:2-mu_MMP Chr4:1:1-sk_ISU	#3
Ctg38	1	150.4	7	Chr1:5:1-sk_ISU:2-mu_ISU:1-sk_MMP:1-mu_MMP Chr3:1:1-mu_MMP Chr2:1:1-sk_ISU	#3
Ctg39	1	154.8	5	Chr1:4:3-sk_ISU:1-umapit_MMP Chr10:1:1-mu_MMP	#3
Ctg41	1	164.5	19	Chr1:19:5-sk_ISU:11-mu_ISU:3-mu_MMP	#4

Table 1. (continued)

Contig id	Chr	Pos	No. of markers	Anchoring information	Cate-gory
Ctg42	1	179	4	Chr1:4:4-mu_ISU	#4
Ctg43	1	179.8	10	Chr1:10:8-sk_ISU:2-mu_ISU	#4
Ctg44	1	190.3	15	Chr1:15:8-sk_ISU:7-mu_ISU	#4
Ctg45	1	200.7	2	Chr1:2:1-sk_ISU:1-mu_MMP	#4
Ctg46	1	205.8	9	Chr1:9:3-sk_ISU:4-mu_ISU:1-sk_MMP:1-mu_MMP	#4
Ctg47	1	209.5	3	Chr1:2:1-sk_ISU:1-mu_ISU Chr4:1:1-mu_ISU	#3
Ctg48	1	183.1	5	Chr1:5:5-sk_ISU	#4
Ctg49	1	214.6	16	Chr6:1:1-sk_ISU Chr8:1:1-mu_ISU Chr1:13:6-sk_ISU:4-mu_ISU:1-umapit_ISU:2-mu_MMP Chr5:1:1-umapit_MMP	#3
Ctg50	1	221.4	7	Chr1:7:4-sk_ISU:2-mu_ISU:1-mu_MMP	#4
Ctg51	1	228	1	Chr1:1:1-sk_ISU	#4
Ctg52	1	225.8	6	Chr1:3:2-sk_ISU:1-mu_MMP Chr3:3:1-sk_ISU:1-mu_ISU:1-umapit_MMP	#3
Ctg53	2	98.3	4	Chr2:4:3-sk_ISU:1-mu_ISU	#4
Ctg54	1	234.1	3	Chr1:3:3-sk_ISU	#4
Ctg55	4	139.3	7	Chr4:4:2-sk_ISU:1-mu_ISU:1-mu_MMP Chr1:3:2-sk_ISU:1-mu_ISU	#3
Ctg56	1	235	5	Chr1:4:1-sk_ISU:3-mu_ISU Chr3:1:1-sk_ISU	#3
Ctg57	1	241.8	33	Chr6:2:2-mu_ISU Chr1:22:9-sk_ISU:8-mu_ISU:2-umapit_ISU:3-mu_MMP Chr3:6:4-sk_ISU:1-mu_ISU:1-mu_MMP Chr7:1:1-umapit_MMP Chr9:1:1-mu_ISU Chr2:1:1-umapit_MMP	#3
Ctg58	1	212.1	6	Chr1:4:1-sk_ISU:2-mu_ISU:1-umapit_ISU Chr5:2:2-sk_ISU	#3
Ctg59	1	254.5	6	Chr1:6:5-sk_ISU:1-mu_ISU	#4
Ctg60	1	256.5	4	Chr1:4:3-sk_ISU:1-mu_ISU	#4
Ctg61	1	260.8	5	Chr1:5:4-sk_ISU:1-mu_ISU	#4
Ctg62	1	267.7	3	Chr1:3:3-sk_ISU	#4
Ctg63	1	271.4	9	Chr1:9:4-sk_ISU:1-mu_ISU:1-sk_MMP:3-mu_MMP	#4

Table 1. (continued)

Contig id	Chr	Pos	No. of markers	Anchoring information	Cate-gory
Ctg64	1	273.9	7	Chr1:6:3-sk_ISU:2-mu_ISU:1-mu_MMP Chr2:1:1-sk_ISU	#3
Ctg65	1	290.7	7	Chr1:6:4-sk_ISU:1-mu_ISU:1-mu_MMP Chr5:1:1-mu_MMP	#3
Ctg66	1	300.3	14	Chr1:14:10-sk_ISU:1-mu_ISU:3-mu_MMP	#4
Ctg67	1	303.6	2	Chr1:2:1-sk_ISU:1-mu_ISU	#4
Ctg68	2	6.4	20	Chr1:1:1-mu_ISU Chr3:1:1-mu_ISU Chr10:1:1-mu_MMP Chr2:17:13-sk_ISU:2-mu_ISU:1-mu_MMP:1-umapit_MMP	#3
Ctg69	2	21.1	11	Chr2:11:3-sk_ISU:5-mu_ISU:2-mu_MMP:1-umapit_MMP	#4
Ctg70	2	31.5	23	Chr10:1:1-sk_ISU Chr2:22:6-sk_ISU:13-mu_ISU:3-mu_MMP	#3
Ctg71	2	52.8	13	Chr8:1:1-mu_ISU Chr2:12:7-sk_ISU:4-mu_ISU:1-sk_MMP	#3
Ctg72	2	52.5	6	Chr2:6:4-sk_ISU:1-mu_ISU:1-sk_MMP	#4
Ctg73	2	55.5	7	Chr10:1:1-mu_MMP Chr2:6:3-sk_ISU:3-mu_ISU	#3
Ctg74	2	75.2	18	Chr10:3:2-sk_ISU:1-mu_ISU Chr2:15:9-sk_ISU:5-mu_ISU:1-mu_MMP	#3
Ctg75	2	79.2	2	Chr2:2:2-mu_ISU	#4
Ctg76	2	81.8	14	Chr10:3:1-mu_ISU:2-umapit_MMP Chr2:11:3-sk_ISU:4-mu_ISU:1-sk_MMP:2-mu_MMP:1-umapit_MMP	#3
Ctg77	2	84.2	6	Chr2:6:4-sk_ISU:1-mu_ISU:1-sk_MMP	#4
Ctg78	2	88.6	14	Chr1:2:2-sk_ISU Chr2:12:6-sk_ISU:5-mu_ISU:1-mu_MMP	#3
Ctg79	2	96.1	10	Chr6:1:1-mu_ISU Chr2:9:1-sk_ISU:7-mu_ISU:1-mu_MMP	#3
Ctg80	2	100.1	2	Chr2:2:1-sk_ISU:1-mu_MMP	#4
Ctg82	2	97.8	8	Chr6:1:1-mu_ISU Chr3:1:1-sk_ISU Chr10:1:1-sk_ISU Chr9:1:1-mu_ISU Chr2:4:1-sk_ISU:2-mu_ISU:1-sk_MMP	#3

Table 1. (continued)

Contig id	Chr	Pos	No. of markers	Anchoring information	Cate-gory
Ctg84	10	43.7	6	Chr10:5:3-sk_ISU:2-mu_ISU Chr2:1:1-sk_ISU	#3
Ctg85	2	102.4	3	Chr2:3:1-sk_ISU:2-mu_ISU	#4
Ctg86	2	102.5	13	Chr1:2:1-sk_ISU:1-sk_MMP Chr2:11:2-sk_ISU:8-mu_ISU:1-sk_MMP	#3
Ctg87	-	-	2	Chr4:1:1-sk_ISU Chr2:1:1-mu_ISU	#2
Ctg88	-	-	2	Chr8:1:1-mu_ISU Chr2:1:1-mu_ISU	#2
Ctg89	2	104.6	9	Chr1:1:1-mu_MMP Chr2:7:4-sk_ISU:2-mu_ISU:1-mu_MMP Chr5:1:1-sk_ISU	#3
Ctg90	2	105.3	5	Chr4:1:1-sk_ISU Chr2:4:1-sk_ISU:3-mu_ISU	#3
Ctg91	2	109.6	11	Chr7:2:1-mu_MMP:1-umapit_MMP Chr2:9:3-sk_ISU:5-mu_ISU:1-umapit_ISU	#3
Ctg92	2	112.6	7	Chr1:1:1-mu_MMP Chr2:6:3-mu_ISU:3-sk_MMP	#3
Ctg93	-	-	1	Chr2:1:1-sk_ISU	#1
Ctg94	2	112.5	2	Chr2:2:2-sk_ISU	#4
Ctg95	-	-	1	Chr2:1:1-sk_ISU	#1
Ctg96	2	112.9	2	Chr2:2:1-sk_ISU:1-mu_ISU	#4
Ctg97	-	-	1	Chr4:1:1-mu_ISU	#1
Ctg98	2	118.7	13	Chr2:13:8-sk_ISU:5-mu_ISU	#4
Ctg99	2	120.9	3	Chr2:3:3-mu_ISU	#4
Ctg100	2	123.4	2	Chr2:2:1-sk_ISU:1-mu_ISU	#4
Ctg101	-	-	1	Chr2:1:1-sk_ISU	#1
Ctg102	2	128.8	5	Chr2:5:1-sk_ISU:4-mu_ISU	#4
Ctg103	2	134.6	20	Chr8:1:1-sk_ISU Chr1:2:1-mu_ISU:1-mu_MMP Chr3:1:1-mu_ISU Chr7:1:1-mu_ISU	#3
Ctg104	2	151.4	10	Chr1:1:1-sk_ISU Chr2:9:4-sk_ISU:4-mu_ISU:1-umapit_MMP	#3
Ctg105	2	160.9	6	Chr2:6:2-sk_ISU:4-mu_ISU	#4
Ctg106	9	65.2	4	Chr9:4:4-mu_ISU	#4
Ctg107	2	166.7	4	Chr2:4:3-sk_ISU:1-sk_MMP	#4
Ctg108	2	172	14	Chr2:14:13-sk_ISU:1-mu_ISU	#4

Table 1. (continued)

Contig id	Chr	Pos	No. of markers	Anchoring information	Cate-gory
Ctg109	2	191.5	6	Chr3:1:1-sk_ISU Chr2:5:2-sk_ISU:3-mu_ISU	#3
Ctg110	2	199.4	4	Chr7:1:1-mu_MMP Chr10:1:1-mu_ISU Chr2:2:2-sk_ISU	#3
Ctg111	3	17.3	25	Chr6:3:2-sk_ISU:1-mu_ISU Chr3:22:9-sk_ISU:5-mu_ISU:1-umapit_ISU:2-sk_MMP:5-mu_MMP	#3
Ctg112	3	45.4	3	Chr3:3:3-sk_ISU	#4
Ctg114	3	65.7	5	Chr3:5:1-sk_ISU:1-mu_ISU:1-sk_MMP:2-mu_MMP	#4
Ctg115	3	72.4	11	Chr1:1:1-sk_ISU Chr3:10:5-sk_ISU:3-mu_ISU:2-mu_MMP	#3
Ctg116	3	74.6	5	Chr3:5:3-sk_ISU:1-sk_MMP:1-mu_MMP	#4
Ctg117	3	77.8	32	Chr8:2:1-sk_ISU:1-sk_MMP Chr3:30:14-sk_ISU:13-mu_ISU:1-sk_MMP:1-mu_MMP:1-umapit_MMP	#3
Ctg118	3	80.3	23	Chr1:5:5-mu_ISU Chr4:2:2-mu_ISU Chr3:9:2-sk_ISU:6-mu_ISU:1-mu_MMP Chr7:1:1-mu_ISU Chr10:4:3-sk_ISU:1-mu_ISU Chr5:2:1-sk_ISU:1-mu_ISU	#3
Ctg119	3	82.2	7	Chr3:6:4-mu_ISU:1-umapit_ISU:1-mu_MMP Chr9:1:1-mu_MMP	#3
Ctg120	3	82.4	2	Chr3:2:2-mu_ISU	#4
Ctg121	3	84.4	10	Chr1:2:1-sk_ISU:1-mu_MMP Chr3:7:4-sk_ISU:3-mu_ISU Chr10:1:1-sk_ISU	#3
Ctg122	-	-	1	Chr1:1:1-sk_MMP	#1
Ctg123	3	85.9	10	Chr3:9:2-sk_ISU:6-mu_ISU:1-mu_MMP Chr7:1:1-sk_ISU	#3
Ctg124	3	90.6	18	Chr1:1:1-sk_ISU Chr3:12:4-sk_ISU:8-mu_ISU Chr10:1:1-mu_MMP Chr2:4:1-sk_ISU:3-mu_ISU	#3
Ctg125	3	92.5	4	Chr3:4:1-sk_ISU:3-mu_ISU	#4
Ctg126	3	96.1	4	Chr3:4:4-sk_ISU	#4
Ctg127	4	141	4	Chr4:4:1-sk_ISU:3-mu_ISU	#4

Table 1. (continued)

Contig id	Chr	Pos	No. of markers	Anchoring information	Cate-gory
Ctg128	3	97.4	9	Chr3:8:3-sk_ISU:3-mu_ISU:1-mu_MMP:1-umapit_MMP Chr2:1:1-sk_ISU	#3
Ctg129	3	101.6	1	Chr3:1:1-mu_ISU	#4
Ctg131	3	106.5	4	Chr3:4:2-sk_ISU:2-mu_ISU	#4
Ctg132	3	114.7	17	Chr8:1:1-sk_ISU Chr3:16:4-sk_ISU:6-mu_ISU:5-mu_MMP:1-umapit_MMP	#3
Ctg134	3	123.7	6	Chr3:6:3-sk_ISU:3-mu_ISU	#4
Ctg135	3	88.5	2	Chr3:2:1-sk_ISU:1-umapit_ISU	#4
Ctg136	3	133.3	8	Chr3:8:4-sk_ISU:3-mu_ISU:1-mu_MMP	#4
Ctg137	3	133.3	5	Chr1:1:1-mu_ISU Chr3:4:2-sk_ISU:2-mu_ISU	#3
Ctg138	3	147.3	13	Chr3:12:5-sk_ISU:4-mu_ISU:3-mu_MMP Chr9:1:1-sk_ISU	#3
Ctg139	3	152.8	6	Chr1:1:1-sk_ISU Chr3:5:4-mu_ISU:1-mu_MMP	#3
Ctg140	3	152.8	2	Chr3:2:1-sk_ISU:1-mu_ISU	#4
Ctg141	3	153.6	7	Chr3:7:4-sk_ISU:1-mu_ISU:1-sk_MMP:1-mu_MMP	#4
Ctg142	3	160.7	10	Chr8:1:1-mu_ISU Chr3:9:2-sk_ISU:4-mu_ISU:1-sk_MMP:1-mu_MMP:1-umapit_MMP	#3
Ctg143	3	165.3	3	Chr3:3:3-sk_ISU	#4
Ctg144	-	-	1	Chr3:1:1-sk_ISU	#1
Ctg145	3	173.7	7	Chr3:6:4-sk_ISU:2-mu_ISU Chr10:1:1-sk_ISU	#3
Ctg146	3	186.9	7	Chr3:7:5-sk_ISU:1-sk_MMP:1-mu_MMP	#4
Ctg147	3	190.8	2	Chr3:2:1-sk_ISU:1-mu_ISU	#4
Ctg148	3	191.8	10	Chr1:1:1-mu_ISU Chr3:9:7-sk_ISU:2-mu_ISU	#3
Ctg149	3	199.5	11	Chr3:11:3-sk_ISU:5-mu_ISU:3-mu_MMP	#4
Ctg150	3	208.5	14	Chr6:1:1-mu_ISU Chr3:13:7-sk_ISU:6-mu_ISU	#3
Ctg151	3	221.5	23	Chr8:1:1-sk_ISU Chr3:21:13-sk_ISU:8-mu_ISU Chr2:1:1-mu_ISU	#3
Ctg152	-	-	1	Chr3:1:1-mu_ISU	#1

Table 1. (continued)

Contig id	Chr	Pos	No. of markers	Anchoring information	Cate-gory
Ctg153	3	226.1	3	Chr3:3:2-sk_ISU:1-sk_MMP	#4
Ctg154	4	0.4	3	Chr4:3:2-sk_ISU:1-mu_MMP	#4
Ctg155	4	10.5	11	Chr4:9:2-sk_ISU:7-mu_ISU Chr10:2:2-mu_ISU	#3
Ctg156	4	20.3	4	Chr4:4:2-sk_ISU:2-mu_ISU	#4
Ctg157	4	38.3	3	Chr4:3:1-sk_ISU:2-mu_ISU	#4
Ctg158	4	51.4	6	Chr4:6:3-sk_ISU:1-mu_ISU:2-mu_MMP	#4
Ctg159	4	57.6	3	Chr4:3:2-mu_ISU:1-mu_MMP	#4
Ctg160	4	63.4	11	Chr4:10:3-sk_ISU:7-mu_ISU Chr5:1:1-sk_ISU	#3
Ctg161	-	-	1	Chr3:1:1-mu_ISU	#1
Ctg162	4	73.1	8	Chr8:1:1-sk_ISU Chr4:7:2-sk_ISU:4-mu_ISU:1-mu_MMP	#3
Ctg163	4	74.6	9	Chr4:7:7-mu_ISU Chr10:2:1-sk_ISU:1-sk_MMP	#3
Ctg164	4	76.5	26	Chr6:2:2-mu_ISU Chr1:2:1-mu_ISU:1-sk_MMP Chr4:19:6-sk_ISU:13-mu_ISU Chr3:1:1-mu_ISU Chr7:1:1-mu_ISU Chr5:1:1-sk_ISU	#3
Ctg165	4	82.7	2	Chr4:2:2-mu_ISU	#4
Ctg166	4	82.5	4	Chr4:3:1-mu_ISU:2-mu_MMP Chr3:1:1-sk_ISU	#3
Ctg168	4	84.3	4	Chr4:3:2-sk_ISU:1-mu_ISU Chr1:1:1-sk_ISU	#3
Ctg170	4	84.5	2	Chr4:2:2-mu_ISU	#4
Ctg171	-	-	2	Chr4:1:1-mu_ISU Chr5:1:1-sk_ISU	#2
Ctg172	4	83.4	7	Chr4:6:3-sk_ISU:3-mu_ISU Chr9:1:1-sk_ISU	#3
Ctg173	-	-	1	Chr4:1:1-sk_ISU	#1
Ctg174	-	-	1	Chr9:1:1-mu_ISU	#1
Ctg176	4	84.5	9	Chr4:9:2-sk_ISU:7-mu_ISU	#4
Ctg179	4	87.2	8	Chr4:8:1-sk_ISU:7-mu_ISU	#4
Ctg181	4	95.3	20	Chr4:16:9-sk_ISU:6-mu_ISU:1-mu_MMP Chr10:1:1-sk_ISU Chr5:3:1-sk_ISU:1-sk_MMP:1-mu_MMP	#3

Table 1. (continued)

Contig id	Chr	Pos	No. of markers	Anchoring information	Cate-gory
Ctg182	4	110.5	53	Chr4:43:25-sk_ISU:14-mu_ISU:1-umapit_ISU:2-mu_MMP:1-umapit_MMP Chr1:2:1-sk_ISU:1-mu_ISU Chr3:1:1-sk_ISU Chr9:1:1-mu_ISU Chr5:6:1-sk_ISU:2-mu_ISU:1-umapit_ISU:1-sk_MMP:1-mu_MMP	#3
Ctg184	4	127.7	6	Chr6:1:1-mu_ISU Chr4:5:3-sk_ISU:1-mu_ISU:1-mu_MMP	#3
Ctg185	-	-	1	Chr4:1:1-sk_ISU	#1
Ctg186	4	128	1	Chr4:1:1-sk_ISU	#4
Ctg187	-	-	1	Chr4:1:1-sk_ISU	#1
Ctg188	4	134.1	10	Chr4:9:4-sk_ISU:3-mu_ISU:1-mu_MMP:1-umapit_MMP Chr2:1:1-sk_ISU	#3
Ctg189	4	141.9	3	Chr4:3:3-mu_ISU	#4
Ctg190	4	80	4	Chr4:4:4-mu_ISU	#4
Ctg191	4	135.7	5	Chr4:5:4-mu_ISU:1-mu_MMP	#4
Ctg192	-	-	1	Chr4:1:1-mu_ISU	#1
Ctg193	4	138.4	5	Chr8:1:1-mu_ISU Chr4:3:1-sk_ISU:1-mu_ISU:1-sk_MMP Chr9:1:1-sk_ISU	#3
Ctg194	4	135.9	4	Chr4:4:2-sk_ISU:2-mu_ISU	#4
Ctg195	4	139.4	1	Chr4:1:1-sk_ISU	#4
Ctg197	9	65.2	4	Chr4:1:1-mu_ISU Chr9:3:2-sk_ISU:1-mu_ISU	#3
Ctg198	4	149.5	6	Chr4:6:1-sk_ISU:3-mu_ISU:1-sk_MMP:1-mu_MMP	#4
Ctg199	4	146.4	7	Chr4:6:5-sk_ISU:1-mu_ISU Chr5:1:1-mu_MMP	#3
Ctg200	4	152.1	7	Chr4:7:6-sk_ISU:1-mu_ISU	#4
Ctg201	4	169.2	18	Chr4:17:5-sk_ISU:10-mu_ISU:1-sk_MMP:1-mu_MMP Chr3:1:1-mu_ISU	#3
Ctg202	4	180.8	9	Chr4:9:5-sk_ISU:2-mu_ISU:2-mu_MMP	#4
Ctg203	4	186.7	2	Chr4:2:1-sk_ISU:1-mu_ISU	#4
Ctg204	5	9.6	48	Chr1:1:1-mu_MMP Chr10:1:1-mu_MMP Chr5:46:19-sk_ISU:18-mu_ISU:3-	#3
Ctg205	5	24.7	5	Chr5:5:2-sk_ISU:3-mu_ISU	#4

Table 1. (continued)

Contig id	Chr	Pos	No. of markers	Anchoring information	Cate-gory
Ctg206	5	36	9	Chr1:1:1-sk_MMP Chr5:8:5-sk_ISU:3-mu_ISU	#3
Ctg207	5	44.3	2	Chr5:2:2-sk_ISU	#4
Ctg208	5	45.9	4	Chr5:4:3-sk_ISU:1-sk_MMP	#4
Ctg209	5	57.3	8	Chr5:8:6-sk_ISU:2-mu_ISU	#4
Ctg210	5	61.8	6	Chr5:6:5-sk_ISU:1-mu_ISU	#4
Ctg211	5	71	10	Chr5:10:5-sk_ISU:4-mu_ISU:1-sk_MMP	#4
Ctg212	5	73.2	5	Chr5:5:3-sk_ISU:2-mu_ISU	#4
Ctg213	5	75.1	1	Chr5:1:1-mu_ISU	#4
Ctg215	5	76.9	6	Chr5:6:2-sk_ISU:3-mu_ISU:1-umapit_MMP	#4
Ctg216	5	77.1	7	Chr5:7:1-sk_ISU:6-mu_ISU	#4
Ctg217	5	79	10	Chr6:2:2-sk_ISU Chr1:1:1-mu_MMP Chr5:7:4-sk_ISU:1-mu_ISU:1-mu_MMP:1-umapit_MMP	#3
Ctg218	5	80	4	Chr1:1:1-sk_ISU Chr5:3:2-mu_ISU:1-sk_MMP	#3
Ctg219	5	82.7	6	Chr6:1:1-sk_MMP Chr5:5:3-mu_ISU:2-mu_MMP	#3
Ctg220	5	85.6	17	Chr5:17:7-sk_ISU:9-mu_ISU:1-mu_MMP	#4
Ctg221	-	-	1	Chr5:1:1-sk_ISU	#1
Ctg223	5	88.1	4	Chr5:4:3-sk_ISU:1-umapit_MMP	#4
Ctg224	5	88.8	3	Chr5:3:2-sk_ISU:1-mu_ISU	#4
Ctg225	5	92.1	4	Chr5:4:3-sk_ISU:1-mu_ISU	#4
Ctg229	-	-	1	Chr5:1:1-mu_ISU	#1
Ctg231	-	-	2	Chr1:1:1-sk_ISU Chr3:1:1-mu_ISU	#2
Ctg232	-	-	1	Chr5:1:1-sk_ISU	#1
Ctg233	3	76.1	4	Chr3:3:2-sk_ISU:1-mu_ISU Chr5:1:1-sk_MMP	#3
Ctg234	3	79.5	2	Chr3:1:1-sk_ISU Chr5:1:1-mu_MMP	#3
Ctg235	5	96.2	5	Chr5:5:2-sk_ISU:2-mu_ISU:1-mu_MMP	#4
Ctg236	5	98.3	3	Chr5:3:2-sk_ISU:1-mu_ISU	#4
Ctg237	5	101.6	2	Chr5:2:1-mu_ISU:1-mu_MMP	#4
Ctg238	5	107.3	5	Chr5:5:4-sk_ISU:1-mu_ISU	#4
Ctg239	5	112.1	4	Chr2:1:1-sk_ISU Chr5:3:2-sk	#3

Table 1. (continued)

Contig id	Chr	Pos	No. of markers	Anchoring information	Cate-gory
Ctg240	5	115.3	3	Chr5:3:1-sk_ISU:1-mu_ISU:1-mu_MMP	#4
Ctg241	-	-	1	Chr5:1:1-mu_ISU	#1
Ctg242	5	119.2	16	Chr5:16:14-sk_ISU:2-mu_ISU	#4
Ctg243	5	120.6	3	Chr5:3:1-sk_ISU:2-mu_ISU	#4
Ctg244	5	121	2	Chr5:2:2-sk_ISU	#4
Ctg245	5	126.2	8	Chr4:1:1-mu_MMP Chr2:1:1-mu_ISU Chr5:6:5-sk_ISU:1-mu_ISU	#3
Ctg246	-	-	1	Chr4:1:1-mu_ISU	#1
Ctg247	5	130.1	2	Chr5:2:2-sk_ISU	#4
Ctg248	5	137.8	2	Chr5:2:1-mu_ISU:1-mu_MMP	#4
Ctg250	5	145.7	16	Chr1:1:1-mu_MMP Chr10:1:1-sk_ISU Chr5:14:12-sk_ISU:1-mu_ISU:1-mu_MMP	#3
Ctg251	4	119.1	3	Chr4:2:1-mu_ISU:1-sk_MMP Chr5:1:1-mu_ISU	#3
Ctg252	5	152.6	3	Chr5:3:2-sk_ISU:1-umapit_ISU	#4
Ctg253	6	108.8	10	Chr6:4:3-mu_ISU:1-umapit_ISU Chr8:2:2-mu_ISU Chr4:1:1-mu_MMP Chr1:2:1-sk_ISU:1-mu_ISU Chr7:1:1-mu_ISU	#3
Ctg255	3	82.7	5	Chr6:1:1-umapit_ISU Chr3:4:3-sk_ISU:1-mu_ISU	#3
Ctg256	-	-	1	Chr6:1:1-mu_ISU	#1
Ctg257	6	4	3	Chr6:3:3-mu_ISU	#4
Ctg259	-	-	1	Chr9:1:1-sk_ISU	#1
Ctg260	6	2.6	6	Chr6:5:4-mu_ISU:1-sk_MMP Chr8:1:1-mu_MMP	#3
Ctg261	6	4.8	3	Chr6:3:3-mu_ISU	#4
Ctg262	6	7.4	6	Chr6:4:4-mu_ISU Chr8:1:1-sk_ISU Chr2:1:1-sk_ISU	#3
Ctg263	6	3.7	13	Chr6:12:2-sk_ISU:10-mu_ISU Chr10:1:1-mu_MMP	#3
Ctg265	6	8.4	7	Chr6:7:4-sk_ISU:2-mu_ISU:1-mu_MMP	#4
Ctg267	6	8.4	4	Chr6:2:1-sk_ISU:1-mu_ISU Chr4:1:1-sk_ISU Chr10:1:1-sk_ISU	#3
Ctg268	-	-	1	Chr6:1:1-sk_ISU	#1
Ctg269	6	8.4	6	Chr6:6:5-sk_ISU:1-sk_MMP	#4

Table 1. (continued)

Contig id	Chr	Pos	No. of markers	Anchoring information	Cate-gory
Ctg270	6	8.7	5	Chr6:3:1-sk_ISU:2-mu_ISU Chr2:2:1-sk_ISU:1-umapit_MMP	#3
Ctg271	6	13.6	6	Chr6:6:3-sk_ISU:1-mu_ISU:1-umapit_ISU:1-sk_MMP	#4
Ctg272	-	-	1	Chr6:1:1-sk_ISU	#1
Ctg273	6	19.5	5	Chr6:5:4-sk_ISU:1-mu_ISU	#4
Ctg274	6	21.4	6	Chr6:6:1-sk_ISU:5-mu_ISU	#4
Ctg275	6	24.8	3	Chr6:3:1-sk_ISU:2-mu_ISU	#4
Ctg276	6	28.4	7	Chr6:7:2-sk_ISU:2-mu_ISU:2-mu_MMP:1-umapit_MMP	#4
Ctg277	-	-	1	Chr6:1:1-sk_ISU	#1
Ctg280	6	35.7	3	Chr6:2:1-sk_ISU:1-mu_ISU Chr1:1:1-mu_MMP	#3
Ctg281	6	44.6	21	Chr6:20:11-sk_ISU:7-mu_ISU:1-sk_MMP:1-mu_MMP Chr10:1:1-mu_ISU	#3
Ctg282	6	51.5	7	Chr6:6:2-sk_ISU:3-mu_ISU:1-umapit_ISU Chr5:1:1-mu_ISU	#3
Ctg283	6	53.5	9	Chr6:8:3-sk_ISU:3-mu_ISU:1-sk_MMP:1-umapit_MMP Chr8:1:1-mu_MMP	#3
Ctg285	6	61.5	9	Chr6:8:4-sk_ISU:3-mu_ISU:1-mu_MMP Chr8:1:1-sk_ISU	#3
Ctg287	6	81.8	12	Chr6:12:8-sk_ISU:3-mu_ISU:1-sk_MMP	#4
Ctg288	6	101.4	20	Chr6:18:7-sk_ISU:7-mu_ISU:1-umapit_ISU:1-sk_MMP:2-mu_MMP Chr8:1:1-mu_MMP Chr5:1:1-mu	#3
Ctg289	6	121.5	6	Chr8:1:1-mu_MMP Chr6:4:1-sk_ISU:3-mu_ISU Chr4:1:1-mu_ISU	#3
Ctg290	6	128.4	8	Chr6:7:4-sk_ISU:2-mu_ISU:1-mu_MMP Chr1:1:1-sk_ISU	#3
Ctg291	-	-	3	Chr6:1:1-sk_MMP Chr8:1:1-mu_ISU Chr1:1:1-mu_ISU	#2
Ctg293	7	8.2	7	Chr7:7:3-sk_ISU:2-mu_ISU:1-mu_MMP:1-umapit_MMP	#4
Ctg294	7	42	8	Chr7:8:4-sk_ISU:3-mu_ISU:1-mu_MMP	#4
Ctg296	7	60.1	9	Chr7:9:3-sk_ISU:6-mu_ISU	#4

Table 1. (continued)

Contig id	Chr	Pos	No. of markers	Anchoring information	Cate-gory
Ctg298	7	73.6	4	Chr7:4:2-sk_ISU:2-mu_ISU	#4
Ctg299	7	75.4	5	Chr7:5:4-sk_ISU:1-mu_ISU	#4
Ctg300	7	75.9	8	Chr7:8:8-mu_ISU	#4
Ctg301	7	89	8	Chr3:2:1-mu_ISU:1-mu_MMP Chr7:6:1-sk_ISU:4-mu_ISU:1-mu_MMP	#3
Ctg304	3	209.8	4	Chr4:1:1-mu_ISU Chr3:3:3-sk_ISU	#3
Ctg305	-	-	1	Chr7:1:1-mu_ISU	#1
Ctg306	-	-	1	Chr7:1:1-mu_ISU	#1
Ctg307	7	78.4	4	Chr7:4:4-sk_ISU	#4
Ctg309	7	80.9	4	Chr7:3:3-sk_ISU Chr2:1:1-mu_ISU	#3
Ctg310	7	83.3	6	Chr7:5:2-sk_ISU:2-mu_MMP:1-umapit_MMP Chr2:1:1-mu_ISU	#3
Ctg313	7	86.1	5	Chr7:5:3-sk_ISU:2-mu_ISU	#4
Ctg314	7	86.9	2	Chr7:2:1-sk_ISU:1-mu_MMP	#4
Ctg315	-	-	2	Chr8:1:1-mu_ISU Chr7:1:1-sk_ISU	#2
Ctg316	-	-	1	Chr7:1:1-mu_ISU	#1
Ctg317	7	91.9	4	Chr7:4:2-sk_ISU:2-mu_ISU	#4
Ctg318	7	101.7	13	Chr4:1:1-mu_MMP Chr7:12:5-sk_ISU:7-mu_ISU	#3
Ctg320	7	110.6	17	Chr6:1:1-mu_ISU Chr7:16:5-sk_ISU:9-mu_ISU:2-mu_MMP	#3
Ctg321	7	113.6	4	Chr7:4:2-sk_ISU:2-mu_ISU	#4
Ctg322	7	117.8	13	Chr7:13:9-sk_ISU:2-mu_ISU:2-sk_MMP	#4
Ctg323	7	131.5	20	Chr7:20:12-sk_ISU:6-mu_ISU:1-sk_MMP:1-mu_MMP	#4
Ctg324	-	-	1	Chr7:1:1-sk_ISU	#1
Ctg325	7	162.7	25	Chr6:2:2-sk_ISU Chr4:1:1-mu_ISU Chr7:20:9-sk_ISU:7-mu_ISU:1-sk_MMP:3-mu_MMP Chr2:1:1-mu_ISU Chr5:1:1-mu_ISU	#3

Table 1. (continued)

Contig id	Chr	Pos	No. of markers	Anchoring information	Cate-gory
Ctg326	8	29.5	44	Chr8:40:25-sk_ISU:10-mu_ISU:2-sk_MMP:2-mu_MMP:1-umapit_MMP Chr4:2:1-mu_ISU:1-mu_MMP Chr1:1:1-mu_ISU Chr7:1:1-mu_ISU	#3
Ctg327	8	52.3	3	Chr8:3:1-sk_ISU:1-mu_ISU:1-sk_MMP	#4
Ctg328	8	55.8	3	Chr8:3:1-sk_ISU:2-mu_ISU	#4
Ctg329	8	64.3	13	Chr8:12:8-sk_ISU:4-mu_ISU Chr6:1:1-mu_ISU	#3
Ctg331	8	76.5	2	Chr8:2:1-sk_ISU:1-mu_ISU	#4
Ctg332	-	-	1	Chr8:1:1-mu_ISU	#1
Ctg333	-	-	1	Chr8:1:1-sk_ISU	#1
Ctg334	8	80.1	5	Chr8:5:5-mu_ISU	#4
Ctg336	-	-	1	Chr6:1:1-sk_MMP	#1
Ctg337	8	86.2	1	Chr8:1:1-mu_ISU	#4
Ctg338	-	-	1	Chr8:1:1-sk_ISU	#1
Ctg339	8	82.8	2	Chr8:2:1-sk_ISU:1-mu_ISU	#4
Ctg340	8	87.1	6	Chr8:6:3-sk_ISU:2-mu_ISU:1-mu_MMP	#4
Ctg341	-	-	1	Chr8:1:1-mu_ISU	#1
Ctg345	-	-	2	Chr8:1:1-sk_ISU Chr7:1:1-mu	#2
Ctg347	-	-	1	Chr8:1:1-sk_ISU	#1
Ctg348	8	94.9	4	Chr8:4:3-sk_ISU:1-mu_ISU	#4
Ctg349	8	95.7	8	Chr8:7:2-sk_ISU:3-mu_ISU:1-umapit_ISU:1-umapit_MMP Chr10:1:1-mu_ISU	#3
Ctg350	-	-	1	Chr8:1:1-mu_ISU	#1
Ctg351	8	100.2	10	Chr8:10:5-sk_ISU:4-mu_ISU:1-mu_MMP	#4
Ctg353	8	107.1	6	Chr8:6:4-mu_ISU:2-umapit_ISU	#4
Ctg354	8	110	19	Chr8:17:3-sk_ISU:11-mu_ISU:3-mu_MMP Chr3:2:2-mu_MMP	#3
Ctg355	8	112.3	3	Chr8:3:2-mu_ISU:1-mu_MMP	#4
Ctg357	8	114.2	3	Chr8:3:2-sk_ISU:1-mu_ISU	#4
Ctg358	3	191.9	2	Chr3:2:2-mu_ISU	#4
Ctg360	4	40.3	3	Chr4:1:1-sk_ISU Chr3:1:1-sk_ISU Chr7:1:1-sk_ISU	#3
Ctg361	8	124.2	6	Chr8:6:2-mu_ISU:1-sk_MMP:3-mu_MMP	#4

Table 1. (continued)

Contig id	Chr	Pos	No. of markers	Anchoring information	Cate-gory
Ctg362	8	129	22	Chr8:21:10-sk_ISU:10-mu_ISU:1-mu_MMP Chr4:1:1-mu_ISU	#3
Ctg363	8	153.3	6	Chr8:5:2-sk_ISU:3-mu_ISU Chr4:1:1-mu_ISU	#3
Ctg364	8	164.7	10	Chr8:10:5-sk_ISU:1-mu_ISU:1-sk_MMP:3-mu_MMP	#4
Ctg365	8	172.6	5	Chr8:5:4-sk_ISU:1-umapit_MMP	#4
Ctg366	8	175.7	4	Chr8:4:2-sk_ISU:1-mu_ISU:1-mu_MMP	#4
Ctg367	9	65.2	6	Chr9:6:3-sk_ISU:3-mu_ISU	#4
Ctg368	-	-	3	Chr6:1:1-sk_MMP Chr9:2:2-sk_ISU	#2
Ctg370	9	28.1	4	Chr9:4:1-sk_ISU:3-mu_ISU	#4
Ctg371	6	51.6	7	Chr6:4:2-mu_ISU:1-mu_MMP:1-umapit_MMP Chr9:2:1-sk_ISU:1-mu_MMP Chr2:1:1-mu_MMP	#3
Ctg372	-	-	1	Chr9:1:1-mu_ISU	#1
Ctg373	9	54.8	20	Chr9:19:11-sk_ISU:3-mu_ISU:3-mu_MMP:2-umapit_MMP Chr5:1:1-sk_ISU	#3
Ctg374	-	-	1	Chr9:1:1-mu_ISU	#1
Ctg375	9	65.2	2	Chr9:2:1-sk_ISU:1-mu_ISU	#4
Ctg376	9	65.8	13	Chr6:1:1-sk_ISU Chr4:1:1-sk_ISU Chr1:3:1-sk_ISU:2-mu_ISU Chr9:8:3-sk_ISU:2-mu_ISU:3-mu_MMP	#3
Ctg377	-	-	1	Chr9:1:1-mu_ISU	#1
Ctg378	-	-	1	Chr9:1:1-mu_ISU	#1
Ctg380	9	72.1	1	Chr9:1:1-sk_ISU	#4
Ctg381	-	-	1	Chr9:1:1-sk_ISU	#1
Ctg382	1	170.4	2	Chr1:2:2-sk_ISU	#4

Table 1. (continued)

Contig id	Chr	Pos	No. of markers	Anchoring information	Cate-gory
Ctg383	9	77.6	4	Chr9:4:3-sk_ISU:1-mu_ISU	#4
Ctg384	9	79.6	4	Chr9:4:2-mu_ISU:2-sk_MMP	#4
Ctg385	9	83.8	8	Chr1:1:1-sk_ISU Chr9:6:4-sk_ISU:1-mu_ISU:1-mu_MMP Chr5:1:1-mu_ISU	#3
Ctg387	9	93.9	9	Chr4:1:1-sk_ISU Chr9:8:6-sk_ISU:1-mu_ISU:1-sk_MMP	#3
Ctg388	9	101.4	2	Chr9:2:2-sk_ISU	#4
Ctg389	9	115.8	7	Chr9:7:3-sk_ISU:3-mu_ISU:1-sk	#4
Ctg390	9	130	10	Chr1:1:1-sk_MMP Chr9:7:4-sk_ISU:1-mu_ISU:1-mu_MMP:1-umapit_MMP Chr5:2:1-sk_ISU:1-mu_ISU	#3
Ctg391	9	154	70	Chr1:4:2-sk_ISU:1-mu_ISU:1-mu_MMP Chr9:64:37-sk_ISU:17-mu_ISU:5-sk_MMP:4-mu_MMP:1-umapit_MMP Chr10:1:1-sk_ISU Chr5:1:1-sk_ISU	#3
Ctg392	10	11.3	14	Chr3:1:1-mu_ISU Chr10:13:8-sk_ISU:3-mu_ISU:1-mu_MMP:1-umapit_MMP	#3
Ctg393	10	34.5	9	Chr4:1:1-umapit_MMP Chr10:8:3-sk_ISU:4-mu_ISU:1-umapit_ISU	#3
Ctg394	10	38.8	4	Chr10:4:2-sk_ISU:2-mu_ISU	#4
Ctg395	-	-	1	Chr10:1:1-mu_ISU	#1
Ctg397	-	-	1	Chr10:1:1-mu_ISU	#1
Ctg398	-	-	1	Chr10:1:1-mu_ISU	#1
Ctg399	10	43.5	6	Chr4:1:1-mu_MMP Chr10:5:2-sk_ISU:2-mu_ISU:1-mu_MMP	#3
Ctg400	-	-	1	Chr10:1:1-mu_MMP	#1
Ctg401	10	46	4	Chr10:4:3-sk_ISU:1-mu_ISU	#4
Ctg403	10	48.5	8	Chr10:7:4-sk_ISU:3-mu_ISU Chr2:1:1-sk_ISU	#3
Ctg404	10	49.4	4	Chr10:4:2-sk_ISU:1-mu_ISU:1-mu_MMP	#4
Ctg405	10	50	2	Chr10:2:2-mu_ISU	#4
Ctg406	10	50	6	Chr10:6:3-mu_ISU:3-mu_MMP	#4
Ctg407	10	50.5	5	Chr10:5:2-sk_ISU:1-mu_ISU:2-mu_MMP	#4
Ctg408	-	-	1	Chr3:1:1-mu_ISU	#1

Table 1. (continued)

Contig id	Chr	Pos	No. of markers	Anchoring information	Cate-gory
Ctg409	10	52.5	5	Chr10:5:1-sk_ISU:3-mu_ISU:1-mu_MMP	#4
Ctg411	10	53.9	4	Chr10:4:2-sk_ISU:2-mu_ISU	#4
Ctg412	10	56	6	Chr10:6:1-sk_ISU:3-mu_ISU:2-mu_MMP	#4
Ctg413	10	60.4	20	Chr10:19:8-sk_ISU:11-mu_ISU Chr2:1:1-mu_MMP	#3
Ctg414	10	69.7	4	Chr10:4:2-sk_ISU:1-mu_ISU:1-mu_MMP	#4
Ctg415	10	75.6	12	Chr10:11:5-sk_ISU:5-mu_ISU:1-mu_MMP Chr2:1:1-mu_ISU	#3
Ctg416	10	85.3	6	Chr10:5:4-sk_ISU:1-mu_ISU Chr2:1:1-mu_MMP	#3
Ctg417	10	96.3	13	Chr6:1:1-mu_MMP Chr1:1:1-mu_ISU Chr4:1:1-sk_ISU Chr10:8:4-sk_ISU:1-mu_ISU:1-umapit_ISU:1-mu_MMP:1-umapit_MMP Chr2:2:2-mu_ISU	#3
Ctg418	10	102.5	4	Chr10:4:2-sk_ISU:1-mu_ISU:1-mu_MMP	#4
Ctg419	10	120.4	10	Chr10:8:6-sk_ISU:1-mu_ISU:1-mu_MMP Chr2:2:2-sk_ISU	#3
Ctg420	-	-	1	Chr9:1:1-sk_ISU	#1
Ctg421	-	-	2	Chr8:1:1-sk_ISU Chr2:1:1-sk_ISU	#2
Ctg423	-	-	1	Chr10:1:1-mu_ISU	#1
Ctg426	-	-	1	Chr2:1:1-mu_ISU	#1
Ctg428	8	80.5	1	Chr8:1:1-umapit_ISU	#1
Ctg430	7	77	2	Chr7:2:2-sk_ISU	#4
Ctg432	-	-	2	Chr6:1:1-mu_ISU Chr9:1:1-mu_ISU	#2
Ctg434	8	69.5	1	Chr8:1:1-mu_MMP	#1
Ctg435	-	-	1	Chr7:1:1-sk_ISU	#1
Ctg438	-	-	1	Chr6:1:1-mu_ISU	#1
Ctg440	-	-	1	Chr6:1:1-sk_ISU	#1
Ctg441	9	0.8	2	Chr1:1:1-sk_ISU Chr9:1:1-mu	#3
Ctg442	6	8.4	1	Chr6:1:1-sk_ISU	#1
Ctg445	1	109.8	1	Chr1:1:1-sk_ISU	#1
Ctg448	9	65.2	1	Chr9:1:1-mu_ISU	#1
Ctg449	-	-	1	Chr2:1:1-mu_ISU	#1
Ctg451	-	-	1	Chr7:1:1-sk_ISU	#1

Table 1. (continued)

Contig id	Chr	Pos	No. of markers	Anchoring information	Cate-gory
Ctg452	7	106.8	2	Chr7:2:2-mu_ISU	#4
Ctg453	9	65.2	2	Chr9:2:1-sk_ISU:1-mu_ISU	#4
Ctg454	1	146.3	4	Chr1:4:3-sk_ISU:1-mu_ISU	#4
Ctg456	7	77	1	Chr7:1:1-sk_ISU	#1
Ctg457	-	-	1	Chr8:1:1-mu_ISU	#1
Ctg461	-	-	1	Chr9:1:1-sk_ISU	#1
Ctg466	-	-	1	Chr10:1:1-sk_ISU	#1
Ctg469	4	138.9	2	Chr4:2:1-sk_ISU:1-mu_ISU	#4
Ctg474	-	-	1	Chr1:1:1-sk_ISU	#1
Ctg476	-	-	1	Chr6:1:1-sk_ISU	#1
Ctg477	6	35.7	2	Chr6:2:1-mu_ISU:1-umapit_ISU	#4
Ctg480	-	-	1	Chr1:1:1-mu_ISU	#1
Ctg482	4	143.6	2	Chr4:2:2-mu_ISU	#4
Ctg484	-	-	1	Chr9:1:1-sk_ISU	#1
Ctg485	-	-	1	Chr2:1:1-sk_ISU	#1
Ctg486	5	82.5	3	Chr5:3:2-sk_ISU:1-mu_ISU	#4
Ctg487	7	43.1	3	Chr7:3:3-mu_ISU	#4
Ctg488	3	82.4	2	Chr3:2:2-mu_ISU	#4
Ctg490	-	-	1	Chr4:1:1-mu_ISU	#1
Ctg492	1	200.4	3	Chr4:1:1-sk_ISU Chr1:2:2-sk	#3
Ctg498	-	-	1	Chr3:1:1-mu_ISU	#1
Ctg500	-	-	1	Chr5:1:1-sk_MMP	#1
Ctg508	1	130.8	3	Chr1:3:2-sk_ISU:1-mu_ISU	#4
Ctg518	-	-	1	Chr8:1:1-sk_ISU	#1
Ctg528	-	-	1	Chr8:1:1-mu_ISU	#1
Ctg531	4	70.5	3	Chr4:3:1-sk_ISU:2-mu_ISU	#4
Ctg536	-	-	1	Chr7:1:1-mu_ISU	#1
Ctg654	4	185.6	2	Chr4:2:2-sk_ISU	#4
Ctg677	-	-	1	Chr3:1:1-sk_ISU	#1
Ctg700	7	77.3	2	Chr7:2:2-sk_ISU	#4
Ctg713	-	-	1	Chr1:1:1-mu_ISU	#1
Ctg715	5	123	2	Chr5:2:2-sk_ISU	#4
Ctg720	-	-	2	Chr8:1:1-sk_ISU Chr1:1:1-mu	#2
Ctg721	-	-	1	Chr10:1:1-sk_ISU	#1
Ctg725	6	3.6	2	Chr6:2:1-sk_ISU:1-mu_ISU	#4
Ctg726	6	77.6	16	Chr6:6:2-sk_ISU:1-sk_MMP:3-mu_MMP Chr1:4:1-sk_MMP:3-mu_MMP Chr4:2:1-sk_MMP:1-mu_MMP Chr9:2:1-mu_MMP:1-umapit_MMP Chr5:1:1-sk_MMP	#3

CHAPTER 4. GENERAL CONCLUSOINS

In this dissertation, we showed how bioinformatics would help us to better reveal interesting biology information from the enormous amount of biological data. The new clustering algorithm – K-means multiclustering algorithm can help biologists organize the microarray data by group genes with similar expression pattern into one group. Multiclustering algorithm exhibits the ability to reveal the real date structure of the synthetics microarray with high accuracy that is comparable to the model-based clustering on datasets generated in a manner consistent with the hypothesis of model based clustering. In this paper we discussed the utilization of tree to display the data structure instead of giving just one clustering result. Because of the ambiguity of the definition of cluster, the tree generated by multiclustering algorithm shows the clusters in different levels of cut off values, which reveals the real data structure and give biology the right to choose what is the right decision based on their biological judgments. The graphic display of the tree is also a good way to present the data. However , the graphic tool we used to display the tree still need some improvements, like display the length of branches proportion to the cut off values and show the cut off value at each internal nodes. The second paper indicates how the combination of biological experiments and computational support work together to construct the high-density genetic map. From primer design, polymorphism screen, mapping score collection and map construction, and the management and storage of the information generated by the project, bioinformatics play an important role in all the steps. After the construction of map, the integration of genetic and physical map and genetic map to microarray all conducted in a

computational way. This two papers just some examples that show the roles of bioinformatics plays in maize genome research.

ACKNOWLEDGEMENTS

I would like to give my special thanks to my mother, Long-Bai Wang, even though she cannot hear it or see it, for giving me a life full of many precious gifts, love, trust, encouragement, patient, brave …

I would express my gratitude and appreciate to my two major professors for their guidance, encouragement, and support during my graduate studies. I also thank the members of my Program of Study Committee, Dr. Hui-Hsien Chou, Dr. Heike Hofmann, and Dr. Steven A. Whitham for serving on my committee and for their helpful advises on my thesis. I thank Cheng-Ting "Eddy" Yeh for computational support, and the members in Schnable lab for their kindness, friendship, and encouragement.

I'm sincerely grateful for having Jeanne and Rod Rogert as part of my family, for their years of continuous love, caring and support. I would thank my father, Zhugang Guo, and parent in-law, Ruiqi Zhang and Yanping Zhao, for their unconditional love and sacrifice. The last but not least, my thanks go to my family, my husband, Bin Zhang, and my two sons, Travis and Tyler, for their love and making my life richer and meaningful.